

The Texas Medical Center Library

DigitalCommons@TMC

The University of Texas MD Anderson Cancer
Center UTHealth Graduate School of
Biomedical Sciences Dissertations and Theses
(Open Access)

The University of Texas MD Anderson Cancer
Center UTHealth Graduate School of
Biomedical Sciences

8-2011

Upregulation of Reactive Oxygen Species During the Retrovirus Life Cycle and Their Roles in a Mutant of Moloney Murine Leukemia Virus, ts1-Mediated Neurodegeneration

SOO JIN KIM

Follow this and additional works at: https://digitalcommons.library.tmc.edu/utgsbs_dissertations



Part of the [Biology Commons](#), [Molecular and Cellular Neuroscience Commons](#), [Nervous System Diseases Commons](#), [Other Immunology and Infectious Disease Commons](#), [Virology Commons](#), and the [Virus Diseases Commons](#)

Recommended Citation

KIM, SOO JIN, "Upregulation of Reactive Oxygen Species During the Retrovirus Life Cycle and Their Roles in a Mutant of Moloney Murine Leukemia Virus, ts1-Mediated Neurodegeneration" (2011). *The University of Texas MD Anderson Cancer Center UTHealth Graduate School of Biomedical Sciences Dissertations and Theses (Open Access)*. 170.

https://digitalcommons.library.tmc.edu/utgsbs_dissertations/170

This Dissertation (PhD) is brought to you for free and open access by the The University of Texas MD Anderson Cancer Center UTHealth Graduate School of Biomedical Sciences at DigitalCommons@TMC. It has been accepted for inclusion in The University of Texas MD Anderson Cancer Center UTHealth Graduate School of Biomedical Sciences Dissertations and Theses (Open Access) by an authorized administrator of DigitalCommons@TMC. For more information, please contact digitalcommons@library.tmc.edu.

The
TMC LIBRARY
Health Sciences Resource Center

**UPREGULATION OF REACTIVE OXYGEN SPECIES
DURING THE RETROVIRUS LIFE CYCLE AND
THEIR ROLES IN A MUTANT OF MOLONEY MURINE LEUKEMIA VIRUS, *ts1*-
MEDIATED NEURODEGENERATION**

By

SOO JIN KIM, M.A., M.S.

APPROVED:

Supervisory Professor, Paul K.Y. Wong, Ph.D

David Johnson, Ph.D

Dean Tang, M.D., Ph.D

Feng Wang-Johanning, M.D., Ph.D

Mark Bedford, Ph.D

APPROVED:

Dean, The University of Texas

Graduate School of Biomedical Science at Houston

**UPREGULATION OF REACTIVE OXYGEN SPECIES
DURING THE RETROVIRUS LIFE CYCLE AND
THEIR ROLES IN A MUTANT OF MOLONEY MURINE LEUKEMIA VIRUS, *ts1*-
MEDIATED NEURODEGENERATION**

**A
DISSERTATION**

**Presented to the Faculty of
The University of Texas
Health Science Center at Houston**

and

**The University of Texas
M.D.Anderson Cancer Center
Graduate School of Biomedical Sciences
in Partial Fulfillment
of the Requirements
for the Degree of**

DOCTOR OF PHILOSOPHY

By

**SOO JIN KIM, M.S., M.A.
Houston, Texas
August, 2011**

DEDICATION

I dedicate this dissertation to my families who have always stood by my side and inspired me, believed in diligence at work, instilled the importance of higher education, and, above all, believed in me.

ACKNOWLEDGEMENTS

I would like to thank all of those people who helped make this dissertation possible. I thank Dr. Paul Wong for persevering with me as my advisor through out the time to complete this study and dissertation. This thesis would not have been possible without his generous time and support. I also wish to thank Dr. Martin Poenie for his inspiration for doing the research. I am grateful as well to my committee members Dr. David Johnson, Dr. Dean Tang, Dr. Mark Bedford, and Dr. Feng Wang-Johanning for their insights, comments and suggestions. Especially I am grateful to Dr. David Johnson to provide $p53^{+/-}$ FVB/N mice. I also would like to acknowledge Lifang Zhang, Jeusun Kim, Mingshan Yan, Virginia Scofield, and Xianghong Kuang who assisted, advised and supported my research. Their friendship, hospitality and knowledge have supported through the years. I thank Molecular Biology Core for genotyping of p53 mice and RT-PCR, Kevin Lin for helping statistical analysis, Christine Brown for preparing the figures and Lifang Zhang for providing invaluable technical assistance.

**UPREGULATION OF REACTIVE OXYGEN SPECIES
DURING THE RETROVIRUS LIFE CYCLE AND
THEIR ROLES IN A MUTANT OF MOLONEY MURINE LEUKEMIA VIRUS, *ts1*-
MEDIATED NEURODEGENERATION**

ABSTRACT

Viral invasion of the central nervous system (CNS) and development of neurological symptoms is a characteristic of many retroviruses. The mechanism by which retrovirus infection causes neurological dysfunction has yet to be fully elucidated. Given the complexity of the retrovirus-mediated neuropathogenesis, studies using small animal models are extremely valuable. Our laboratory has used a mutant moloney murine leukemia retrovirus, *ts1*-mediated neurodegeneration. We hypothesize that astrocytes play an important role in *ts1*-induced neurodegeneration since they are retroviral reservoirs and supporting cells for neurons. It has been shown that *ts1* is able to infect astrocytes *in vivo* and *in vitro*. Astrocytes, the dominant cell population in the CNS, extend their end feet to endothelial cells and neuronal synapse to provide neuronal support. Signs of oxidative stress in the *ts1*-infected CNS have been well-documented from previous studies.

After viral infection, retroviral DNA is generated from its RNA genome and integrated into the host genome. In this study, we identified the life cycle of *ts1* in the infected astrocytes. During the infection, we observed reactive oxygen species (ROS) upregulations: one at low levels during the early infection phase and another at high levels during the late infection phase. Initially we hypothesized that p53 might play an important role in *ts1*-mediated astrocytic cell death. Subsequently, we found that p53 is unlikely to be involved in the *ts1*-mediated astrocytic cell death. Instead, p53 phosphorylation was increased by the early ROS upregulation via ATM, the protein encoded by the ataxia-telangiectasia (A-T) mutated gene. The early upregulation of p53 delayed viral gene expression by suppressing

expression of the catalytic subunit of NADPH oxidase (NOX). We further demonstrated that the ROS upregulation induced by NOX activation plays an important role in establishing retroviral genome into the host. Inhibition of NOX decreased viral replication and delayed the onset of pathological symptoms in *ts1*-infected mice. These observations lead us to conclude that suppression of NOX not only prevents the establishment of the retrovirus but also decreases oxidative stress in the CNS. This study provides us with new perspectives on the retrovirus-host cell interaction and sheds light on retrovirus-induced neurodegeneration as a result of the astrocyte-neuron interaction.

TABLE OF CONTENTS

Approval page	i
Title page	ii
Dedication	iii
Acknowledgement	iv
Abstract	v
Table of contents	vii
List of illustrations	xi
List of table	xiii
 Chapter 1. Introduction	 1
1.1. Background and Significance	1
1.2. General features of retrovirus and a neuropathogenic mutant of moloney murine leukemia virus (MoMuLV), <i>ts1</i>	2
1.2.1. General features of retroviruses	2
1.2.2. Infection, replication and neuropathogenesis of retrovirus	7
1.2.3. The <i>ts1</i> mouse model, a model of retrovirus-induced neurodegenerative diseases	9
1.3. Current perspectives on intracellular ROS regulation and oxidative challenge in <i>ts1</i> -infected astrocytes	12
1.3.1. ROS, a constant challenge in homeostasis of cellular environment	12
1.3.2. ROS as messenger molecules in cells	16
1.3.3. ROS may play important roles in life cycle of retrovirus	19
1.4. Astrocytes may play important roles in retrovirus-mediated neuropathogenesis	23
1.4.1 Cell types in the CNS infected by retroviruses	23

1.4.2. Astrocytes may play an important role in <i>ts1</i> -mediated-neuropathogenesis.....	28
1.5. Project overview.....	28

Chapter 2. ROS upregulation in the early phase of retrovirus infection and the role of p53 as an oxidative stress modulator.....31

2.1. Introduction.....	31
2.2. Materials and methods.....	33
2.2.1. Mice.....	33
2.2.2. Virus.....	33
2.2.3. Cell culture and <i>ts1</i> infection for cultured astrocytes.....	34
2.2.4. ROS measurement.....	35
2.2.5. mRNA extraction and real-time PCR.....	35
2.2.6. Western blot analysis and subcellular protein fractionation.....	36
2.3. Results.....	37
2.3.1. The early phase of infection in <i>ts1</i> life cycle.....	37
2.3.2. ROS upregulation in the early phase of infection.....	41
2.3.3. p53 does not play an important role in <i>ts1</i> -induced astrocytic apoptosis.....	46
2.3.4. p53 is activated by ROS upregulation in the early phase of infection.....	50
2.3.5. ATM phosphorylates p53 in response to ROS upregulation.....	53
2.3.6. p53 as an intracellular ROS modulator.....	56
2.4. Discussion.....	61

Chapter 3. *ts1* infection activates NOX in the early phase of virus life

cycle.....	67
3.1. Introduction.....	67
3.1.1. NOX in <i>ts1</i> -mediated neurodegeneration.....	67
3.2. Materials and Methods.....	70
3.2.1. NOX activity assay.....	70
3.2.2. Apocynin treatment to <i>ts1</i> -infected mice.....	71
3.2.3. Tissue virus titer assay.....	72
3.2.4. Immunohistochemistry and immunocytochemistry.....	72
3.2.5. Genomic DNA preparation and quantitative PCR.....	73
3.3. Results.....	73
3.3.1. Cellular distribution of NOX subunits in astrocytes.....	73
3.3.2. NOX is activated in <i>ts1</i> -infected astrocytes.....	76
3.3.3. NOX activation occurs in the early phase of infection.....	79
3.3.4. O_2^- upregulation by NOX activation may enhance viral gene integration into host genome.....	84
3.3.5. O_2^- production increased in the <i>ts1</i> -infected mouse brain stem.....	88
3.3.6. Inhibition of NOX prevented <i>ts1</i> -mediated cell death and prolonged the life span of <i>ts1</i> -infected mice.....	97
3.4. Discussion.....	102
3.4.1. Subcellular localization of NOX subunits may determine its local activation using different subunits.....	104
3.4.2. NOX isoforms may have distinct functions in different subcellular location.....	105
3.4.3. The complex relationship of <i>ts1</i> infection, O_2^- , and neuronal death..	106

Chapter 4. Conclusion and future studies.....108

 4.1. Conclusion.....108

 4.2. Proposed models and future studies.....112

Bibliography.....115

Vita.....137

LIST OF ILLUSTRATIONS

Chapter 1

Figure 1.1. Diagram of retrovirus genome, its gene products, and virus particle.....	4
Figure 1.2. <i>ts1</i> envelope protein from biosynthesis, folding, trimerization and transport to the Golgi apparatus.	11
Figure 1.3. Cellular ROS resources.....	15
Figure 1.4. Different levels of intracellular ROS and cell fates.	17
Figure 1.5. Retrovirus life cycle.....	21
Figure 1.6. Astrocytic neuronal support in the CNS	27

Chapter 2

Figure 2.1. Viral gene transcription in <i>ts1</i> -infected astrocytes.....	39
Figure 2.2. Subcellular locations of viral proteins in <i>ts1</i> -infected astrocytes.....	40
Figure 2.3. Intracellular H ₂ O ₂ measurement in <i>ts1</i> -infected astrocytes.....	43
Figure 2.4. Mitochondrial O ₂ ⁻ measurement in <i>ts1</i> -infected astrocytes.....	44
Figure 2.5. Cellular apoptosis in <i>ts1</i> -infected astrocytes.....	45
Figure 2.6. The life span of <i>ts1</i> -infected p53 ^{+/+} and p53 ^{-/-} mice.....	47
Figure 2.7. Viable cell count assay of <i>ts1</i> -infected PACs from p53 ^{+/+} and p53 ^{-/-} mouse brains.....	48
Figure 2.8. <i>ts1</i> -mediated apoptosis in PACs from p53 ^{-/-} and p53 ^{-/-} mouse brains.....	49
Figure 2.9. Upregulation of intracellular ROS increases p53 phosphorylation.....	51
Figure 2.10. p53 phosphorylation in <i>ts1</i> -infected astrocytes.....	52
Figure 2.11. ATM activation in <i>ts1</i> -infected astrocytes and H ₂ O ₂ -treated astrocytes.....	54
Figure 2.12. Suppression of p53 phosphorylation by inhibiting ATM activation.....	55
Figure 2.13. Intracellular ROS levels in PACs from p53 ^{+/+} and p53 ^{-/-} mouse brains.....	57
Figure 2.14. Expression of viral proteins in <i>ts1</i> -infected PACs.....	58

Figure 2.15. Expression of NOX subunits in <i>ts1</i> infected PACs.....	60
Figure 2.16. The life cycle of <i>ts1</i> and distinct ROS upregulations in C1 astrocytes.....	62

Chapter 3

Figure 3.1. The current model of NOX complex activation in phagocytes.....	69
Figure 3.2. Cellular distribution of NOX subunits in C1 astrocytes.....	75
Figure 3.3. NOX activation in <i>ts1</i> -infected astrocytes.....	78
Figure 3.4. Measurement of intracellular NADPH levels during <i>ts1</i> life cycle.....	80
Figure 3.5. Measurement of extracellular O ₂ ⁻ production during <i>ts1</i> life cycle.....	81
Figure 3.6. SOD upregulation in the early phase of <i>ts1</i> infection.....	82
Figure 3.7. Redistribution of SOD during the early phase of <i>ts1</i> infection.....	83
Figure 3.8. Inhibition of NOX decreased viral establishment into the host genome.....	85
Figure 3.9. <i>ts1</i> viral titer assay in the apocynin-treated mouse CNS.....	87
Figure 3.10. O ₂ ⁻ upregulation and reactive gliosis in the <i>ts1</i> -infected CNS.....	90
Figure 3.11. The subcellular O ₂ ⁻ upregulation in the perinuclear area of the CNS cells.....	91
Figure 3.12. Intimate locations of astrocytes and neurons in the CNS.....	92
Figure 3.13. Astrocytes are infected by <i>ts1</i> in the CNS.....	93
Figure 3.14. Inhibition of NOX decreased O ₂ ⁻ levels in the <i>ts1</i> -infected CNS.....	95
Figure 3.15. Inhibition of NOX decreased O ₂ ⁻ levels in neurons of the <i>ts1</i> -infected CNS....	96
Figure 3.16. Inhibition of NOX prevented <i>ts1</i> -mediated astrocytic cell death.....	99
Figure 3.17. Inhibition of NOX suppressed <i>ts1</i> -mediated apoptosis but not the ER stress.....	100
Figure 3.18. Inhibition of NOX extended the life span of <i>ts1</i> -infected mice.....	101

LIST OF TABLE

Table 1. Classification of retrovirus.....	6
--	---

Chapter I. Introduction

1.1. Background and Significance

The retrovirus is a specific class of virus, which poses a major health hazard due to its ability to cause persistent infection of the host system through integration into the host genome. Overwhelming evidence has demonstrated that retroviral infection is associated with pathogenic diseases in many animal species including humans (1). Recent HIV studies emphasize retrovirus-mediated diseases, yet the role of retroviruses in disease progression is still unclear. More importantly, retroviruses act not only as oncogenic or cytopathic agents but also as highly conserved endogenous genes in the DNA of many different species (1). This suggests that retroviruses are multifaceted agents with the ability to modulate cellular signaling pathways in the host cell.

Many morphological characteristics and many pathological and biological features of retroviruses are shared across subfamilies. Studies with human retroviruses are very limited due to the lack of appropriate tissue models, resulting in relatively slow progress. Instead, a considerable amount of information about the biological features of retroviruses has become available from animal models of retroviruses. In particular, murine retroviruses provide useful models for neuropathology of retroviruses because variation in virus strains as well as the age and strain of mouse models studied provide significant insights into the pathogenic mechanisms of the virus (2). Virus-host cell interaction can lead to various biological manifestations depending on host cell type and characteristics of the retrovirus. We believe that the most promising, rapid, and relatively safe approach toward acquiring knowledge of human disease associated with retroviruses would be obtained by the study of neuropathogenic retroviruses in murine models. We also believe that research on retrovirus-induced diseases should be broadened from a basic understanding of virus-host

cell interaction toward a better understanding of cellular communication in a tissue-specific manner. Together, knowledge about the interaction of virus, host cells, and infected neighboring cells will provide perspective on pathogenic mechanisms and physiological disease progression *in vivo*. Throughout our study on the murine retrovirus-associated neurological disease, we have utilized a murine model infected with *ts1*, a neurovirulent mutant of moloney murine leukemia (MoMuLV), isolated from nonneurovirulent parental wild type MoMuLV-TB (3). *ts1* infection of astrocytes and the events that follow play crucial roles in the *ts1*-induced neuropathogenesis (4). This Chapter is divided into four parts. The first part will illustrate general features of retrovirus and our model of *ts1*. *ts1* infection has been shown to be associated with the dysregulation of cellular ROS homeostasis (5). The second part will be devoted to current perspectives on intracellular ROS regulation and the challenge of oxidative stress in *ts1*-infected cells. Our study is focused on astrocytes because redox environment in the CNS is regulated by astrocytes (6). In the third part, the influence of *ts1*-infected astrocytes on neighboring neurons will be discussed. The final part will give a brief overview of the project.

1. 2. General features of retrovirus and a neuropathogenic mutant of MoMuLV, *ts1*

1.2.1. General features of retroviruses

In order to understand the biological features of retroviruses, it is essential to acquire knowledge of their structure and life cycle. Shortly after the discovery of Rous sarcoma virus (RSV), the RNA virus was established as one of the etiological causes of the tumor (7). However, the early years of molecular biology presumed the “central dogma” in the viral replication process, which represents irreversible flow of genetic information from DNA to RNA to protein. In 1970, Howard Temin hypothesized that RNA tumor virus might have the ability to generate DNA from its RNA genome (8). The discovery of reverse transcriptase

(RNA-dependent DNA polymerase) added a new paradigm in replicating genomic materials (9). The RNA tumor virus was then renamed to retrovirus. Reverse transcriptase allows single strand retroviral RNA genome to be reverse transcribed into double strand DNA, which integrates into the host chromosome. All retroviruses have a central core containing a diploid single strand RNA genome composed of three major open reading frames that encode polyproteins, Gag, Pol and Env, which are cleaved proteolytically to generate the functional viron components. Gag proteins are cleaved to form the internal viron protein components including the matrix, the capsid, and nucleoprotein. The Pol polyproteins are cleaved into reverse transcriptase, integrase, RNAase H and protease, and Env precursor polyproteins are processed into surface proteins and transmembrane proteins composed of viral envelope (Figure 1.1).

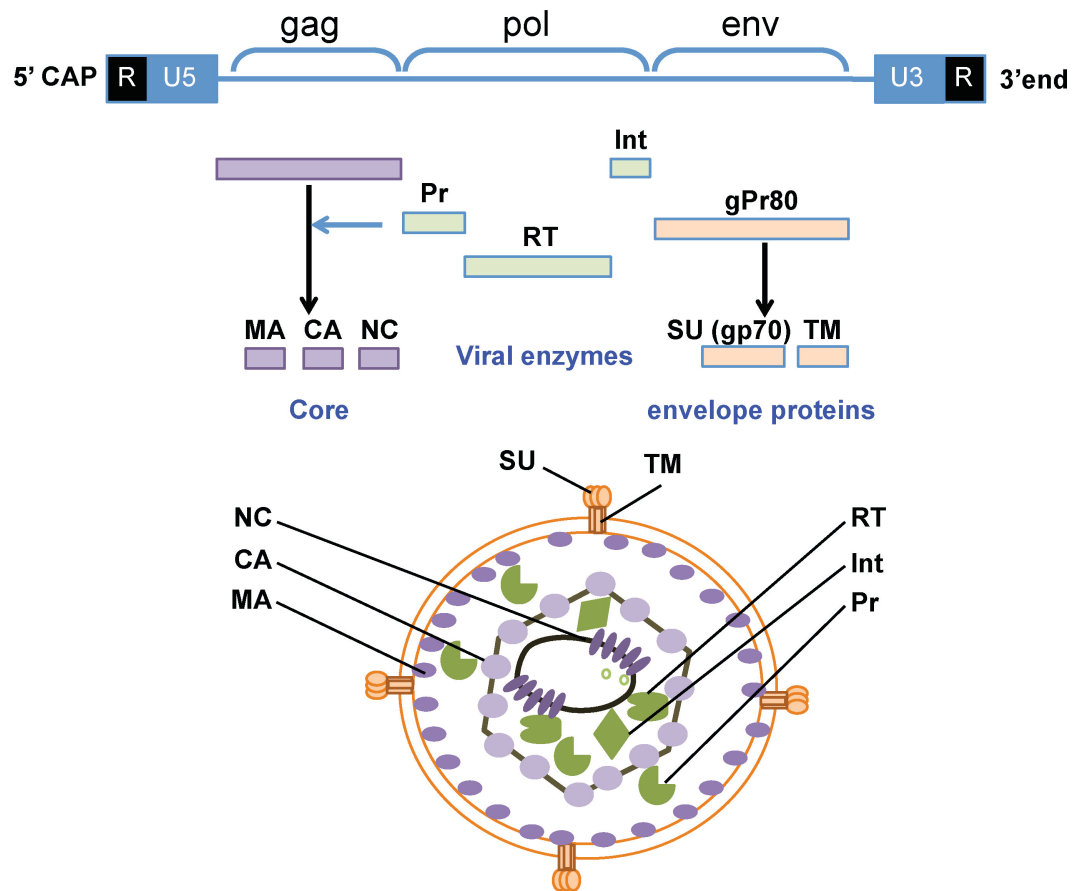


Figure 1.1 Diagram of retrovirus genome, gene products (polyproteins), and virus particle. MA-matrix, CA-capsid, NC-nuclear capsid, Pr-protease, RT-reverse transcriptase, SU-surface protein, TM-transmembrane protein, Int-Integrase.

In the early years of retrovirus investigation, retroviruses were divided into three subfamilies: 1) oncoretrovirus, including all the oncogenic members and many closely related nononcogenic viruses; 2) lentivirus, the 'slow' replicating viruses, such as visna virus and human immunodeficiency virus; and 3) spumaviruse, the foamy viruses that induces cell death without any clinical diseases (1). Current knowledge has now been expanded into seven genera: alpha-beta-, gamma-, delta-, epsilon-retrovirus, lentivirus and spumavirus. Retroviruses are categorized into these groups by distinctive biological features including morphology, site of assembly of the core, and presence of accessory genes, as well as degree of nucleotide sequence similarity in reverse transcriptases (Table 1) (10). Simple retroviruses (alpha-, beta-, gamma-, delta-, epsilon-retrovirus) usually carry only this elementary information, whereas complex retroviruses (lentiviruses and spumaviruses) code for additional regulatory nonvirion proteins by producing alternative spliced products (11).

Subfamilia	Genus	Genome	Distinctive features	Example
Orthoretrovirinae	Alpha-retrovirus	Simple	Smaller genome (<8kb), wide spread in avian species, round morphology assembly at the plasma membrane	Avian leukosis virus, RSV
	Beta-retrovirus (B or D type)	Simple	Intracytoplasmic assembly, after budding, core maturation occurs	Mouse mammary tumor virus Mason-Pfizer monkey virus
	Gamma-retrovirus	Simple	Most oncornaviruses, Assembly at the plasma membrane	MoLuLV
	Delta-retrovirus (c-type)	Complex	Assembly at the plasma membrane, contain genes tax and rex	Human T-cell leukemia virus,
	Epsilon-retrovirus	Simple	Contains orfs, A, B, and C. orfA is a viral homolog of cyclin D	Walley dermal sarcoma virus
	Lentiviruses	Complex	Long latency, Infectable non-dividing cells, Contain auxillary genes	HIV, Visna-maedi,
Spumaretrovirinae	Spumaviruses	Complex	Prominent spikes on the surface, contain tas and bel gene forms large vacuoles in the host cells, no apparent disease association	Human foamy virus

Table 1. Classification of retrovirus. Retrovirus familia is composed of seven genera, alpha-, beta, gamma, delta, epsilon-retrovirus, lentivirus, and spumavirus. Their distinctive features and some examples are listed.

1.2.2. Infection, replication, and neuropathogenesis of retrovirus

Retrovirus infection in host cells affects the entire spectrum of cell fate from proliferation to cell death. The relationship between the status of target cells and retroviral replication has important implications, not only for the basic life cycle of retroviruses in the infected host cells, but also for our understanding of systemic pathogenesis caused by retrovirus-infected cells directly or indirectly. Most retroviruses in the host cells rarely induce cytopathic effects. These cells can serve as productive factories of virus progeny. After infection virus remains present in the cell, but often its expression of RNA or protein is undetectably low or suppressed. This enables the virus-infected cells to escape immunosurveillance. This latency is a particular characteristic of lentivirus and spumavirus infections (1). It has been shown that productive retroviral replication is determined by intracellular milieu of the host cells. For instance, the mouse ectropic virus introduced into human cells via the xenotropic virus envelope replicates much less than it does in mouse cells (12). The dependence of retroviral replication on host cell proliferation or differentiation is also a commonality, although some retroviruses are able to infect non-dividing cells at greatly reduced efficiencies (13). Infection by some retroviruses, however, can lead to cell death. This is a particularly important element of lentiviral infections. Both direct and indirect cytopathic effects from the viral proteins have been proposed. Virions in the host cells may hijack host resources to replicate themselves. As a result, depletion of cellular resources may induce host cell death. Viral proteins at the host surface may also elicit cell-mediated destruction of the infected cells by the host's own immunological response. However, the etiology of the retrovirus-mediated pathogenesis *in vivo* system appears to be more complex. For example, direct CD4-T cell death predominates when immortalized T cell lines are infected with laboratory-adapted human immunodeficiency virus -1 strains in culture (14). Conversely, *in vivo* physiological systems, infection of lymphoid tissue with HIV-1, the majority of dying cells appear to be uninfected "bystander" T cells (14, 15, 16), suggesting

that cytopathic effects of the virus are not necessarily limited to the infected cells. Viral infection may affect cell-to-cell communication leading to disruption of normal cellular functions (17). As a consequence, either infected cells or nearby cells may die. This bystander effect appears as a main cause of neuronal cell death in retrovirus-induced neurological diseases (18).

A number of retroviruses are associated with neurological and systemic disorders. Viral invasion of the nervous system and the development of neurological symptoms are characteristics of many retroviruses, including the murine leukemia viruses (MuLV), and HIV-1 (19), as well as human endogenous retroviruses (20). A recently identified retrovirus, called xenotropic MuLV-related virus, is also linked to chronic fatigue syndrome in humans, but this remains controversial (21). With the appearance of HIV, which can also cause disease in the nervous system, investigation of the pathogenesis of neurological problems induced by retroviruses has become highlighted. In spite of many years of study, much is still poorly understood about the mechanisms that underlie retrovirus-induced neuropathogenesis. Retrovirus-mediated neurodegeneration in the CNS possibly evolved in two separate events: Invasion of retrovirus in the CNS cells, and exerting cytopathic effects on neurons. Neurovirulent retrovirus must penetrate the blood brain barrier (BBB) either as free virus or within infected cells to gain access into the nervous system. Some neurotropic viruses, like herpes simplex and rabies virus, enter the CNS by retrograde axonal transport following peripheral infection of nerve endings. Lentiviruses penetrate the CNS via infected immune cells or endothelial cells. Although there have been more intensive studies focusing on HIV-infected immune cells as a virus carrier to the CNS, some immunohistochemical studies have demonstrated HIV infection of capillary endothelial cells in the brain (22), which may produce progeny virus into abluminal space. It is also noteworthy that infection of endothelial cells typically occurs in the absence of morphologic or functional defect (23). The area with infected CNS endothelial cell does not necessarily

determine the site of neuropathology, which occurs in a later period in the course of the disease (24). The relationship between viral load and disease progression in the CNS is much less clear. Although HIV is detectable in the CNS, the viral load does not necessarily reflect the incidence of HIV-mediated neuronal death because retroviruses do not replicate in neurons. The most perplexing and intriguing question in retrovirus-mediated neuropathogenesis is which cell type plays a crucial role in neuronal death. Highly neuroactive antiretroviral therapies (HAART), which target replicating virus, offer only partial clinical benefit to patients with HIV associated dementia, suggesting that neuronal death in retrovirus-infected CNS may not directly associated with productive viral replication (2, 25).

1.2.3. The *ts1* mouse model, a model of retrovirus-induced neurodegenerative diseases.

Some mutant murine retroviruses, including *ts1* and FrCas^{NC} (derived from the CasBrE retrovirus) cause spongiform encephalopathy in infected mice whereas their parental wild type retroviruses do not cause neurovirulent pathogenesis (26, 27). For many years, our research has focused on a murine model of retroviral-induced CNS disorders. Our model utilized several temperature-sensitive mutants of MoMuLV. One of these mutants, designated *ts1*, has been studied most extensively (28). Although *ts1* was isolated originally from spontaneous temperature-sensitive mutants (29), temperature sensitivity per se is not necessarily an essential property for neurologic disease induction (30). The neurovirulent symptoms of *ts1* infection in mice compared to nonneurovirulent parental virus appear to be caused by misfolded viral envelope proteins (3). The newly synthesized envelope precursor polyprotein gPr80^{env} begins to process soon after biosynthesis and forms trimers in the endoplasmic reticulum (ER) (31). At the restrictive temperature (39°C), the gPr80^{env} is unable to fold properly due to a single amino acid substitution Val-25->Ile in gPr80^{env}, and accumulated in the ER instead of trafficking to the Golgi apparatus and plasma membrane

by chaperones (Figure 1.2) (32). As a consequence, gPr80^{env} is inefficiently processed into gp70 (surface protein) and Prp15E (precursor of transmembrane protein). Since the neurovirulent mutants are derived from known, nonparalytogenic parental viruses, the exact gene or gene sequence that confers the ability to induce paralysis can be elucidated. The neurovirulent property of the gene sequences of the mutants should help to gain insight into the molecular mechanisms of the pathogenesis of neurologic diseases. Another benefit of the *ts1* system is that *ts1*-inoculation of susceptible strain of mice (FVB/N) show a predictable histopathologic profile. FVB/N mice infected with *ts1* shortly after birth develop lesions and a mild, generalized body tremor appearing about 20 days post inoculation. This progresses to hind-limb paralysis within 25-30 days. The mice also exhibit severe retardation in growth, body wasting, and thymic atrophy that correlates with depletion of circulating T cells (33). The latency period depends on the relative amount of virus and the age of mice when the virus is inoculated (30). Induction of the disease is correlated with the appearance of a spongiform encephalomyelopathy with no inflammatory response by peripheral immune cells. The severe spongiform lesions and reactive gliosis manifest in the brain stem and lumbar spinal cord. Vacuolization is observed in neurons and neighboring glial cells in the brain stem, and ventral horns of the spinal cord. Histological findings confirmed that the neurologic signs of paralysis were caused by lower motor neuron degeneration in *ts1*-infected mice. Lateral and vertical funiculi had generalized symmetric spongiform changes and in some instances, lesions appeared in the gray and white matter as well as at the gray/white matter junction. The distribution of spongiform changes in the CNS of *ts1*-infected mice suggest that major involvement of upper motor neurons of the extrapyramidal system also occurred in addition to involvement of lower motor neurons (34).

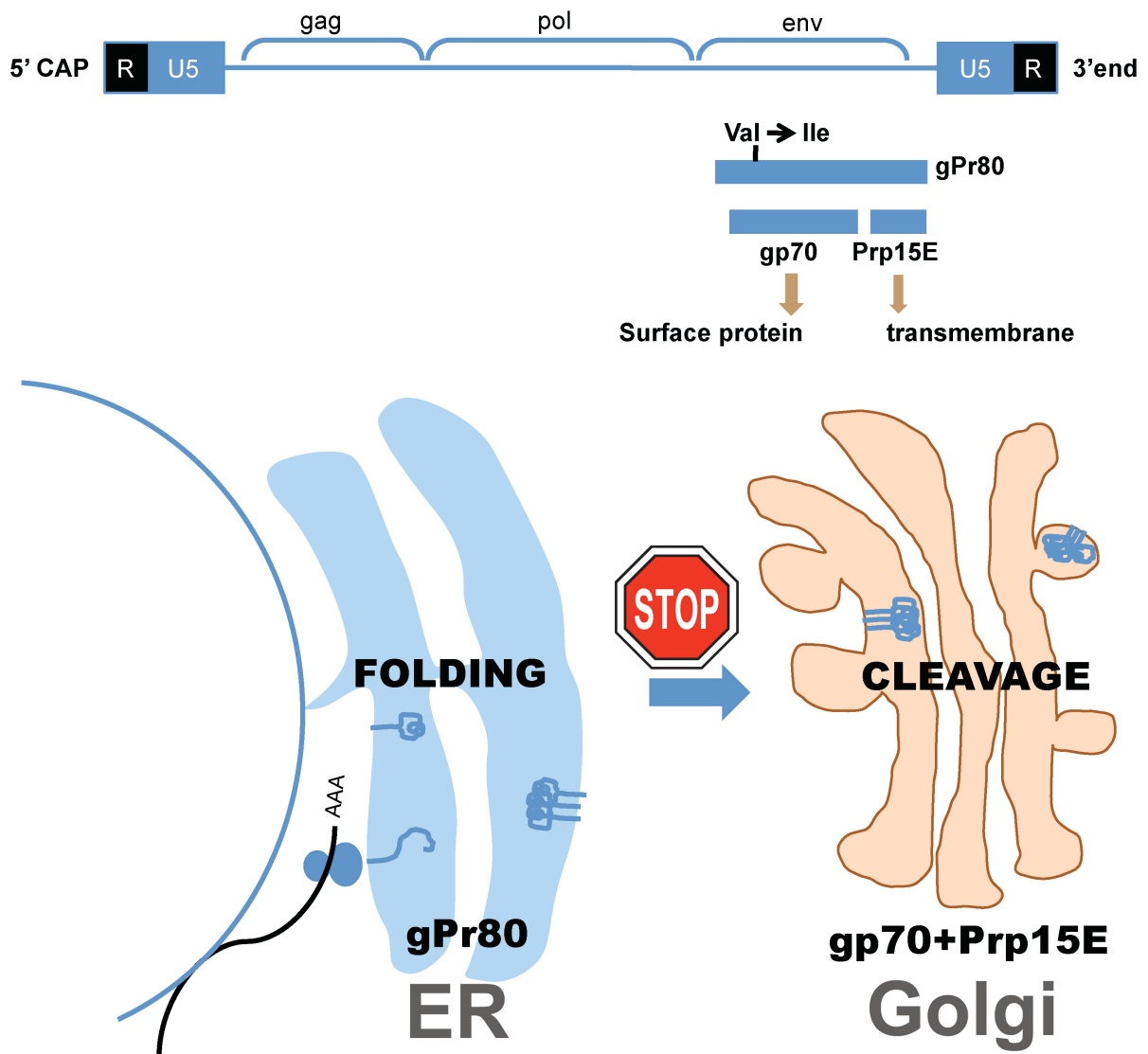


Figure 1.2. *ts1* envelope protein processing from biosynthesis, folding, trimerization and transport to the Golgi apparatus. The single amino acid substitution of Val25→Ile does not prevent oligomerization of monomers. However, due to improper folding, the structure of the oligomer renders it defective in transport from the ER to the Golgi apparatus. As a consequence, gPr80^{env} accumulates in the ER.

ts1 has cell type-specific cytopathic effects, by which it causes neurodegeneration and immunodeficiency through infection of the cells in the CNS and in T-lineage lymphoid cells (30). The result is a disease that resembles HIV infection in several important ways (19, 35). The characteristic features of both HIV- and *ts1*-induced diseases are T cell depletion (35, 36), and cell death in astrocytes and neurons in the CNS (19, 37, 38, 39, 40). T cells and macrophages are primary peripheral targets for both HIV and *ts1* (33, 41). In the CNS, both HIV and *ts1* infect microglia, astrocytes, and endothelial cells, but not neurons (33, 42, 43, 44, 45). *ts1*-induced neurodegenerative disease (ND) is possibly recapitulating many clinical and pathological features of HAD, suggesting that important similarities exist between *ts1*-induced ND and HAD. Moreover, one of the phenomenal advantages of using *ts1* to study retrovirus-mediated ND is that the progression of pathogenesis is highly reproducible. There is little variation within the visually detectable stages of pathogenesis and a high mortality in *ts1*-infected mice. The relatively short and predictable time period to produce neuropathogenic symptoms makes the *ts1* model an excellent tool to identify many aspects of pathogenesis in retrovirus-induced ND.

1.3. Current perspectives on intracellular ROS regulation and oxidative challenge in *ts1*-infected astrocytes

1.3.1. ROS, a constant challenge in homeostasis of cellular environment

ROS are a class of oxygen containing molecules that react with cellular macromolecules, including proteins, lipids, and nucleic acids. Understandably, ROS levels are tightly regulated to avoid dysregulation of signaling pathways and damage in cells. Depending on its concentration, location, and context, ROS may be either beneficial or detrimental to cells. For a long time, mitochondria have been considered as the major source of intracellular ROS. The electrons from nicotinamide adenine dinucleotide

phosphate (NADPH) and 1,5-dihydro-flavin adenin dinucleotide (FADH₂) transfer to oxygen (O₂) via serial electron transfer chains in mitochondria to generate cellular energy, adenosine triphosphate (ATP). However, the stepwise respiratory chains are not thermodynamically perfect machines. Some electrons escape from the electron transfer chain and react with O₂ producing superoxide (O₂⁻) as a consequence (46). In quiescent cells quantal burst of O₂⁻ production has been reported. This O₂⁻ burst is observed in a wide range of cell types including neurons and muscles at different frequencies (47). The other possible depository for intracellular ROS is the ER. Newly synthesized proteins need to fold properly in order to be delivered to the destined intracellular location. The ER provides an oxidative environment that is conducive for disulfide bond formation. During disulfide bond formation in nascent protein, oxidants are produced as a result of electron transport from SH-groups in the cysteine residues of the protein. Reduced (GSH) and oxidized glutathione (GSSG) in the ER lumen participate in catalysis of protein disulfide isomerase (PDI) and ER oxidoreductase 1(Ero1) redox (Figure 1.3). In this context, it is not surprising that inappropriate disulfide bond formation or breakage occurs when thiol redox potentials are disturbed. These conditions cause protein misfolding and exacerbate oxidative stress in the cell, leading to release of Ca²⁺ from ER stores. The excess Ca²⁺ is taken up into the inner membranes of the mitochondria, thereby disrupting the electron transport chain. This diverts the electrons off-course and allows their release from the mitochondria and reaction with O₂ in the cytoplasm, producing ROS. The ROS produced during these events can cause further Ca²⁺ release from the ER, resulting in amplified accumulation of ROS, at toxic levels leading to cell death (48, 49). Thus, oxidative stress, ER stress and mitochondrial impairment are intimately linked (50, 51). It is noteworthy that pathogenesis in neurodegenerative diseases share common mechanisms involving oxidative stress although they may have diverse causes. Retrovirus-mediated oxidative stress may involve all these sources of ROS. Another O₂⁻-generating source is respiratory bursts in

phagocytes. NADPH oxidase (NOX) in phagocytic cells transfers singlet electrons to O_2 to produce O_2^- (52). NOX was first studied in phagocytic cells but recent studies have shown that NOX subunits are also present in non-phagocytic cells including neurons and astrocytes (53, 54).

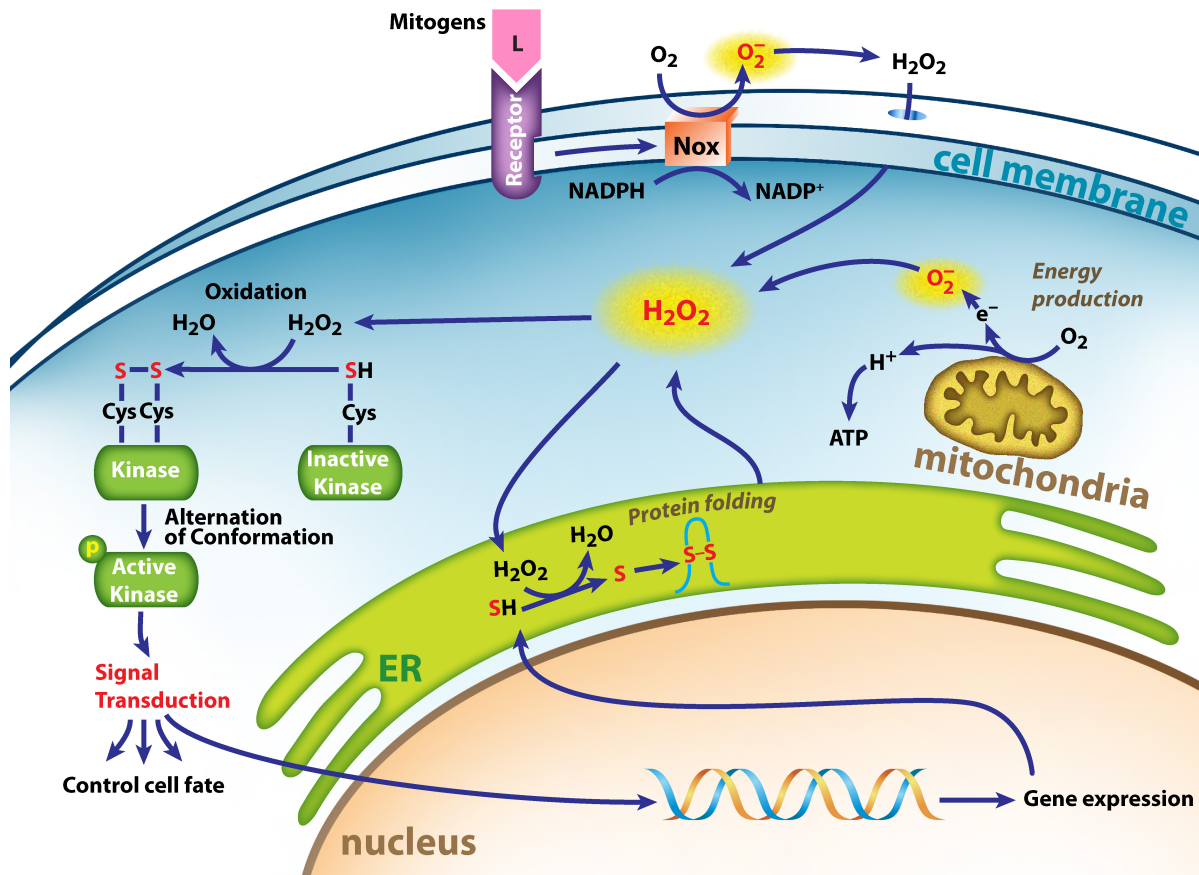


Figure 1.3. Cellular ROS sources. Mitochondria. Some electrons escape from the electron transfer chain in the mitochondria and produce $O_2^{\cdot -}$. ER. Oxidative environment in the ER produces oxidants during formation and correction of disulfide bond. NOX. NOX located on the membrane transfer an electron to O_2 generating $O_2^{\cdot -}$. Short-live $O_2^{\cdot -}$ is a precursor to other ROS and is dismutated to H_2O_2 . $O_2^{\cdot -}$ can react with limited chemical targets as an oxidant whereas H_2O_2 acts as a more prevalent oxidant targeting cysteine residues in enzyme active sites.

As mentioned above, ROS are constantly produced during normal metabolism. It is natural that cells engage in a variety of ways to regulate or modulate ROS levels to maintain intracellular redox balance to control cell fate. One good example is the antioxidant defense system involving p53. While p53 is linked to pro-apoptotic processes, expression of p53 drives a number of antioxidant responses that can limit accumulation of ROS. p53 induces antioxidant genes including glutathione peroxidase 1 (GPX1), manganese superoxide dismutase (MnSOD), and aldehyde dehydrogenase 4 family (ALDH4) (55). The diversion of glucose-6-phosphate into the oxidative pentose phosphate pathway (PPP) by a p53-dependent factor, TP53-induced glycolysis and apoptosis regulator (TIGAR), produces NADPH that reduces GSSG to GSH (56). p53-dependent glutaminase 2 (GLS2) expression upregulates the production of the GSH precursor glutamate (57, 58). The sestrins, a family of stress-responsive proteins involved in the regulation of ROS, are also induced by p53 (59). The importance of antioxidant activity of p53 is further supported by antioxidant treatment of p53 knockout mice. The absence of p53 leads to imbalance of cellular metabolism that has lower mitochondrial oxidative phosphorylation. p53 knockout mice often develop spontaneous lymphoma, which is prevented by antioxidant treatment (55).

1.3.2. ROS as messenger molecules in cells

ROS can elicit a wide range of cellular responses (Figure 1.4). For many years, ROS have been viewed as harmful molecules that damage cellular macromolecules. Recent studies showed that low levels of ROS often modulate normal intracellular signaling pathways. Interestingly, ROS produced in non-immune tissues oxidize a more limited spectrum of target molecules, and these specific oxidations can be used for particular biological functions rather than producing widespread molecular damage (56, 60).

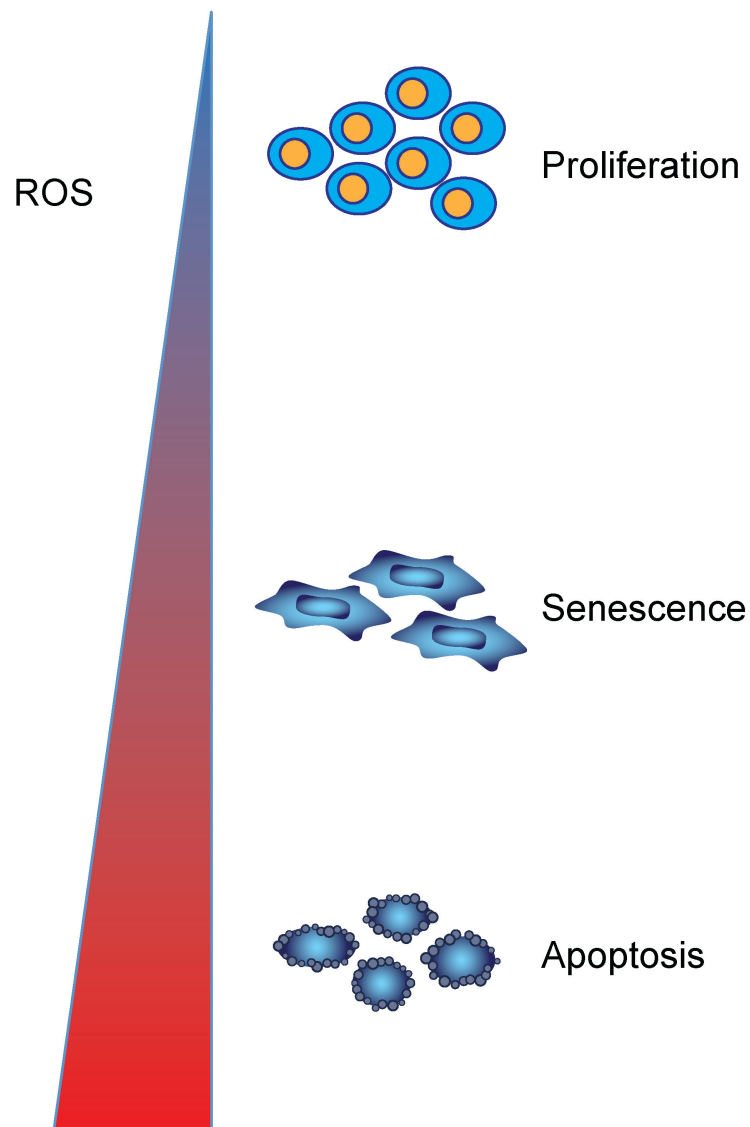


Figure 1.4. Different levels of intracellular ROS and cell fates. Low levels of ROS can induce cell proliferation. Moderate levels of ROS cause temporary or permanent growth arrest, resulting in cellular differentiation or senescence. High levels of ROS can cause cellular apoptosis.

As noted before, ROS generated by normal cellular processes in the mitochondria and ER are unintentional byproducts. However, cells also produce ROS intentionally. Phagocytic cells engulf foreign microorganisms and produce O_2^- by NOX to destroy them. The reactivity of individual ROS differs greatly. O_2^- is a precursor to other ROS and is dismutated to hydrogen peroxide (H_2O_2) either by superoxide dismutase (SOD) or spontaneously in low pH. O_2^- can react with limited chemical targets as an oxidant whereas H_2O_2 acts as a more prevalent oxidant targeting cysteine residues in enzyme active sites (61). H_2O_2 is further decomposed into innocuous H_2O and gaseous O_2 by catalase. H_2O_2 is also involved in the oxidation of cysteine residues on proteins, which may affect enzyme activity (62). Upon cell attachment to the extracellular matrix or receptor binding to its ligand, the tyrosine kinase becomes oxidized by H_2O_2 at cysteine residues and thus activated. On the other hand, tyrosine phosphatase becomes inactivated when it is oxidized by H_2O_2 at cysteine residues (63). In this case, ROS, mainly H_2O_2 , serve as a messenger molecule for the modification of signaling proteins. The concentration and location of ROS must be carefully controlled by specific ROS detoxifying enzymes in the cells. Given the reactivity of ROS, spatial and temporal regulatory strategies must be present to ensure that a specific kind of ROS upregulation occurs only where it is desirable and that the ROS signal is terminated in a timely manner. Whereas catalase is confined to the peroxisome, several peroxiredoxin isoforms exist in the cytoplasm (64). H_2O_2 must be sheltered from destruction by peroxiredoxin in selected contexts. The advantage of intracellular vesicles is that they can have distinct ROS levels separate from the cytoplasm. Indeed, they have very different and highly specialized functions. For example, a subgroup of early endosomes contains NOX (65, 66). These vesicles, termed “signaling endosomes” (66) or “redoxosomes” (67), function in the processing of endocytosed proteins. O_2 from the extracellular space is secluded in the lumen of early endosomes and converted into O_2^- by the NOX accepting electron from NADPH. The primary function of endosomes may be to

provide the limited area for signaling process mediated by ROS upregulation. It is also possible that NOX-dependent generation of ROS in endosomes may also be relevant to other subcellular locations in which the NOX is activated (68). The highly reactive environment of the endosome lumen may play an important role in the activation of the pre-integration complex of invaded retroviruses (69). After fusion of the viral envelope with the plasma membrane, the viral preintegration complex is released into the cytoplasm. At this point, the viral reverse transcriptase has to be activated. It is possible that ROS in early endosomes may catalyze viral protein activation. The relevant oxidation targets for viral activation that are presumably enriched in these microenvironments must be identified.

1.3.3. ROS may play important roles in life cycle of retrovirus

The life cycle of the retrovirus can be generally divided into two distinct phases. An early phase refers to the binding of virions to the cell surface through the integration of viral DNA into the host genome (pre-integration phase). A late phase includes the transcription and translation of the provirus through the assembly of all viral components at the plasma membrane and release of progeny virions, followed by a maturation process of the virus outside of the cell (post-integration phase) (70) (Figure 1.5). ROS may play important roles in both phases of retrovirus life cycle. In the early phase, viral pre-integration complex reinforces reverse transcriptase activity to generate viral DNA from genomic RNA and transport the viral DNA into the host nucleus. During this early phase, low levels of ROS upregulation may activate the host cells either to enhance viral DNA synthesis (71) or the DNA integration process to establish a viral gene in the host cells. In the late phase, after viral establishment in the host genome, viral replication, initiated by transcription and translation of viral genes, appears to be more favorable if the cells are in a more proliferative state. For example, following the entry of the retrovirus, the vast majority of the viruses may not successfully establish themselves as an integrated provirus (70).

Moreover, the integrated provirus may have limited opportunity to replicate depending on the microenvironmental status of the cell. The intracellular environment plays an important role in retrovirus replication (72). Retrovirus-infected cells can produce progeny virus productively or restrictedly (73, 74). Productively infected cells support viral replication and participate in the transmission of the infection. Astrocyte infection by HIV-1 in the CNS is generally known to have restricted viral replication (74). In these restrictive cells, efficient viral replication might be blocked at different phases of the life cycle of retrovirus, including reverse transcription, viral gene integration in the cells, expression of the provirus and assembly, as well as release of progeny viral particles. These cells are able to restrict viral replication and survive. However, they may act as a virus reservoir in which a replication-competent viral genome persists. For instance, cells are permissive to infection by retrovirus and they could be refractory to efficient viral expression. Virus production in chronically infected cells can be transiently activated by cytokines (75, 76). In the same context, the quiescent environment of the CNS may pose an obstacle in retrovirus replication and ROS may play an important role in promoting productive viral replication.

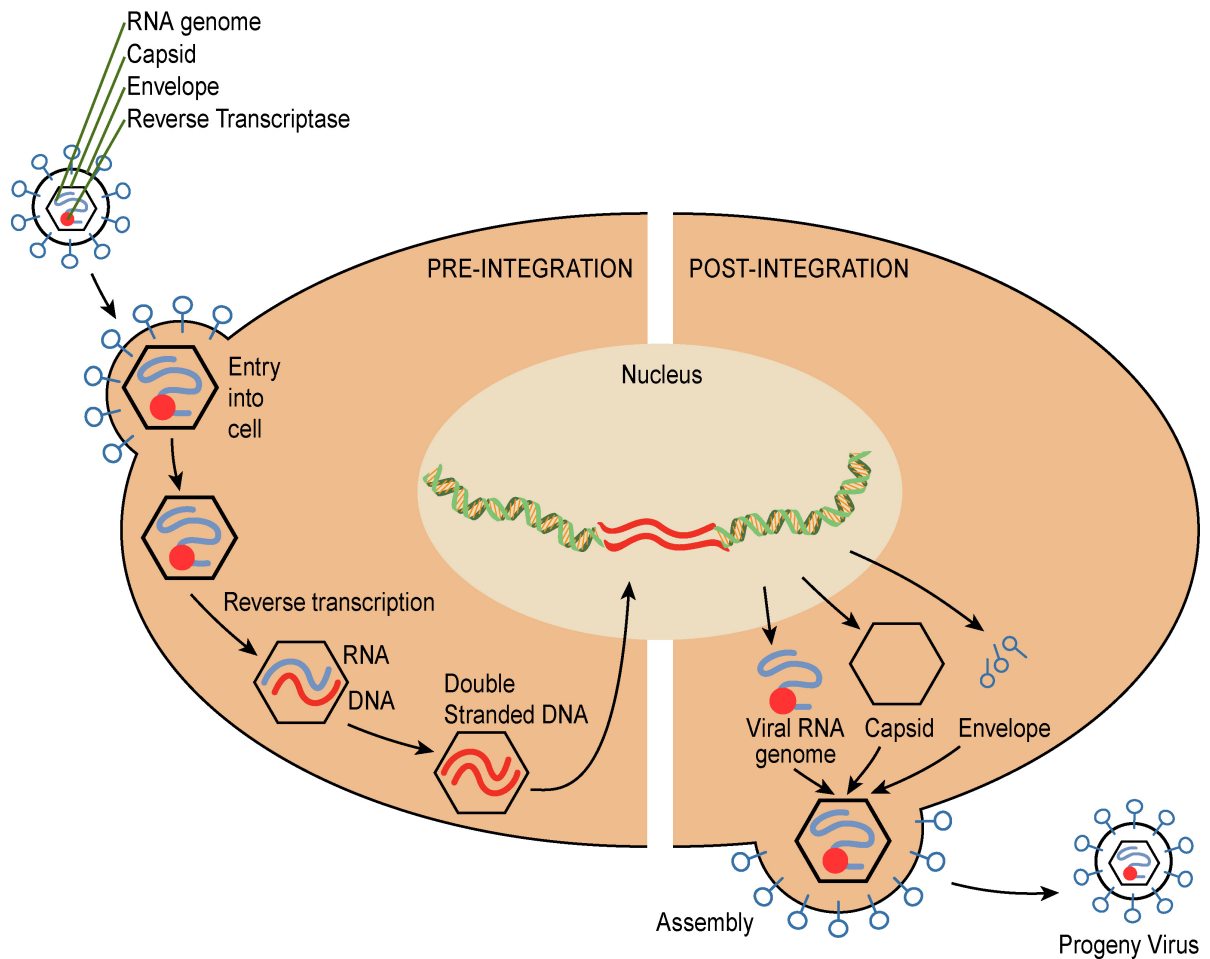


Figure 1.5. Retrovirus life cycle. The life cycle of the retrovirus is arbitrarily divided into two phases: the pre-integration and post-integration phases. The pre-integration phase involved from binding of virions to the cell surface through the integration of viral DNA into the host genome. The post-integration phase consist of the transcription and translation of the provirus through the assembly of viral components at the plasma membrane and release of progeny virons. A maturation process of MoMuLV occurs outside of the cell.

ROS generated in some nonphagocytic cells are involved in mitogenic signaling. As mentioned above, ROS and its signaling effects at low physiologic levels play a role in mitogenic effect in many cells types (77). Many cancer cells show increased production of ROS (78), while normal cells exposed to H₂O₂ show increased proliferation (79) and express growth related genes (80). ROS producing enzymes, such as NOX, have been described to be activated by mitogenic stimuli (81). ROS have been shown to induce and maintain G1 phase cyclin D1 expression in mouse lung epithelial cells (82). Similarly, Havens et al have shown that ROS levels are increased in a cell cycle–dependent manner and oscillated with every cell division in human T98G glioblastoma cells, human leukemic T cells, and NIH 3T3 cells (83). Although they did not identify the source of ROS in these cells, ROS upregulation appears to play an important role in cell cycle because the proliferative cells undergo transient arrest and fail to progress from G1 to S phase during treatment with various antioxidants (84, 85, 86). Although many of the mechanisms of cyclins in entrance and progression of G1 phase have been widely explored, ROS have been more recently shown to be important for the expression of G1 phase cyclins (82, 83, 86, 87, 88). Consequently, the commitment of the cell to division is critical to achieve retrovirus replication (89). This notion is supported by a number of studies showing that productive retroviral infection requires cell activation (90). For instance, cell cycle progression and viral replication in cells may be efficiently suppressed with the use of cyclin-dependent kinase inhibitors (91). However, up until this point it had not been established whether the entry of retroviruses into the cell could promote action of the proliferative signaling pathway. It has been reported that HIV-1 gene expression is markedly increased by progression of the cell cycle beyond the G1-S phase checkpoint (92). Low levels of ROS upregulation by viral infection may promote productive virus infection. It is noteworthy that not all *ts1*-infected astrocytes die. Previously Qiang et al have investigated surviving cells from chronic *ts1*-infection. To determine how these resistant

cells survive *ts1* infection in culture, they established and characterized a subline of these cells (C1-*ts1*-S). C1-*ts1*-S cells proliferate slower and produce fewer viruses than C1 cells. This is associated with their antioxidant defense responses. For example, they show lower levels of H₂O₂, increased uptake of cystine, and higher levels of GSH and cysteine, compared to those in acutely infected cells or to those in uninfected cells (93). This suggests that C1-*ts1*-S cells upregulate their thiol defenses in order to survive, and by doing so, virus replication in C1-*ts1*-S decreased.

A previous study in our laboratory has also shown ROS upregulation in *ts1*-infected astrocytes and that antioxidant treatment significantly delays *ts1*-induced neurodegeneration. It also demonstrated that enhanced antioxidant defense does not remove the retrovirus, yet it does significantly decrease viral replication significantly in the infected host by delayed antioxidant treatment in *ts1*-infected mice (94). Taken together, ROS upregulation appears to be involved in two separate steps in retrovirus-infected cells. First, ROS upregulation increases viral replication in the host cells. The notion that ROS may play a role in cell proliferation is supported by the proliferative characteristics of cancer cells coinciding with higher ROS levels (55). To promote viral replication, the retrovirus may possess a mechanism to increase intracellular ROS levels. In particular, *ts1* may have to change the quiescent microenvironment of the CNS to a more proliferative environment to replicate progeny virion productively by upregulating ROS. At 30 days post-infection, neurovirulent *ts1* titer in brain tissues is higher than non-neurovirulent WT virus. Second, excess ROS upregulation can induce cell death by causing oxidative stress, which has been well documented previously (95).

1.4. Astrocytes may play important roles in retrovirus-mediated neuropathogenesis

1.4.1. Cell types in the CNS infected by retroviruses.

Some retroviruses are known to cause neurological diseases, but the pathogenic mechanisms remain poorly understood. Although the viral envelope protein has been shown to be crucial in the pathogenesis of these NDs, the mechanisms underlying neuronal death in these diseases are unclear. Neuropathological features show no detectable peripheral inflammatory cell infiltration in the brain of *ts1*-infected mice. The most controversial question is whether neuronal cell death is the direct result of viral infection or the indirect result of glial cell infection. Despite the fact that the loss of motor neurons is the cause of MuLV-mediated neurologic diseases, replication of MuLV is known to occur only in mitotic cells (90). Capillary endothelial cells and pericytes are the most conspicuously infected cell type by all the neuropathogenic MuLVs. In spite of the observation that endothelial cells are highly supportive of neuropathogenic MuLV replication, infected endothelial cells are not likely to be directly associated with neuronal cell death. Endothelial cell infection is widespread and not restricted to the location of spongiform lesions (42). Furthermore, morphological or functional changes are not observed from the capillary endothelial cells in the PVC-211-infected CNS (96). The CNS is composed of neurons and glial cells. Neurons are the main cell type involved in motor and cognitive function, and glial cells support the neurons. Glial cells can be divided into four different cell types: ependymal cells, microglia, oligodendrocytes, and astrocytes (97). Ependymal cells line the cerebrospinal fluid (CSF)-filled ventricles in the brain and central canal of spinal cord. These cells possess microvilli, which is believed to be involved in the directional movement of CSF. The fact that the location of ependymal cells correspond to the fourth ventricle area with high *ts1* titer may indicate that retrovirus may gain access to the CNS via CSF (98). However, whether ependymal cells are infected by retrovirus is not known. Microglia are derived from macrophages, which migrate to the CNS during development (99). This is another cell type that expresses neuropathogenic MuLVs in infected mouse CNS. However, whether microglia are infected by neuropathogenic MuLVs is in debate because CasBrE-

virus antigens are not detected in the infected microglia in the CNS (100). Although the presence of neuropathic MuLV particles was detected in microglia in the CNS, this may reflect phagocytosis of virus-infected cells and virions in the infected regions of the CNS. Oligodendrocytes produce a myelin membrane that surrounds axon to promote axonal conduction. Due to the difficulty in identifying oligodendrocytes in the CNS, the ability of MuLVs to infect oligodendrocytes is ambiguous. Although *ts1* was found at the surface of oligodendrocytes (98), whether their infection actively participates in neuronal death also remains unclear. Astrocytes provide a functional and physical link between endothelial cells to neurons by transporting nutrients and maintaining the integrity of Blood-brain-barrier (BBB) (Figure 1.6). *In vivo* studies suggest that perivascular astrocytes foot processes are the first structures to exhibit vacuolar changes. Vacuolization is the prominent histopathologic feature shared by neuropathologic MuLVs. As the disease progresses, vacuoles increase in size and number in the areas of the spongiform lesion. Several reports also indicated that HIV can directly infect and replicate in cultured astrocytes (101, 102, 103, 104). The expression of HIV-1 gp120 in astrocytes induces neuropathologic alteration in the mouse CNS (98, 105). In the CNS, astrocytes comprise more than 50% of total cells (106) and they have crucial homeostatic and redox regulatory functions that maintain neuron integrity (107). Extracellular GSH is metabolized into gamma glutamyl-dipeptide amino acid and cysteinylglycine, which are then broken down to cysteine and glycine. Cysteine is used for neuronal GSH synthesis after transported by the EAAC1 transporter (108). The intimate association between astrocytes and neurons and the role of astrocytes in regulating the neuronal environment suggests that neuronal degeneration appears as a secondary effect of retrovirus-infected astrocytes (30). It is also possible that a functional interplay between macrophages, endothelial cells and astrocytes might contribute to retrovirus-induced neuropathogenesis. Proteomic modeling of HIV-1 infected cells, in a

study of astrocyte-microglia interactions, has shown that astrocytes have a profound effect on protein expression in HIV-infected microglia (109).

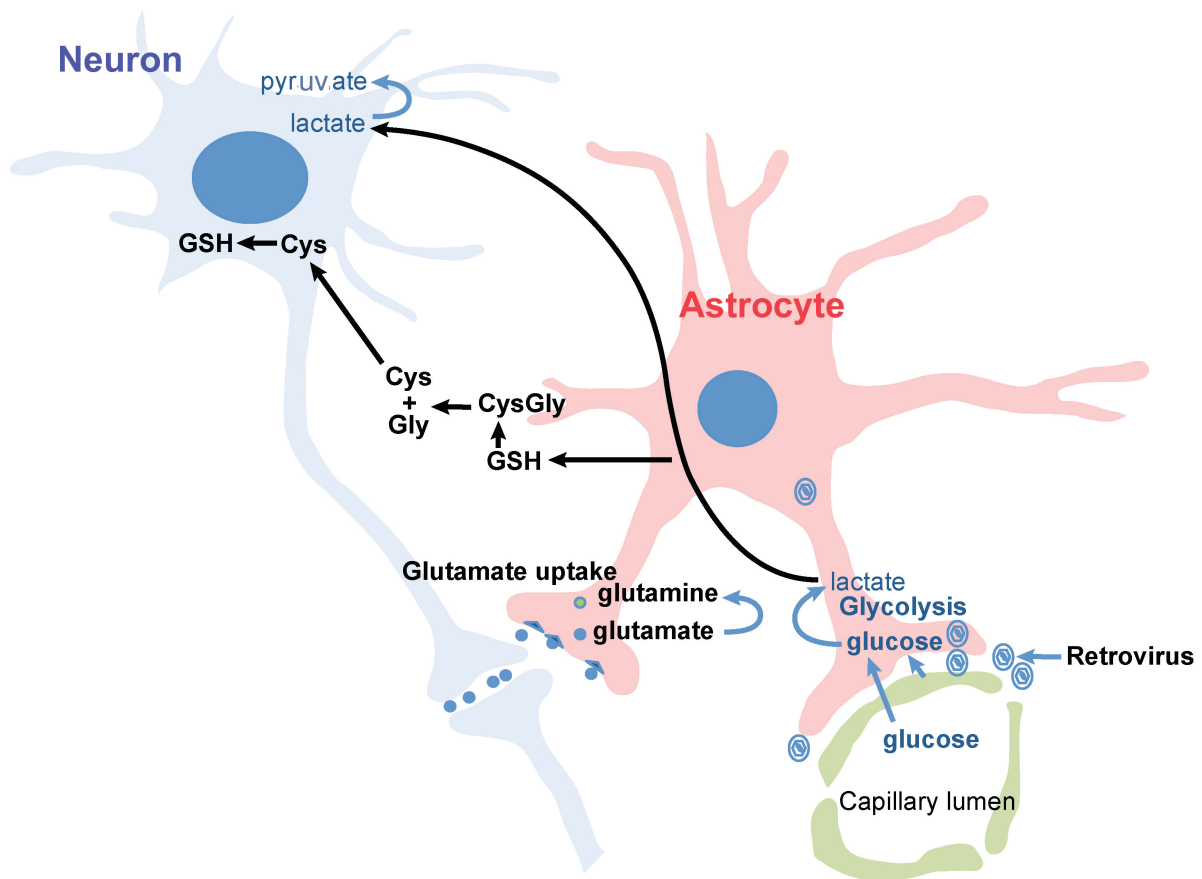


Figure 1.6. Astrocytic neuronal support in the CNS

Astrocytes play an important role in maintaining the microenvironment of neurons. Delivery of nutrients from capillary endothelial cells to neurons as well as maintenance of the integrity of BBB is a responsibility of astrocytes. Astrocytes also are crucial in providing a homeostatic environment by supplying cysteine and recycling neurotransmitters. Astrocytes supply the GSH precursor, cysteine. Glutamate, when released during synaptic transmission, is quickly reabsorbed and converted to glutamine by astrocytes and delivered back to the presynaptic neurons.

1.4.2. Astrocytes may play an important role in *ts1*-mediated neuropathogenesis

One puzzling aspect of *ts1*-mediated ND is the consequence of cell type-specific response after *ts1* infection. We speculate that the etiology of *ts1*-induced neurodegeneration underlies this cell type-specific response. *ts1* seems to infect all cell types in the CNS except neurons. The cell type that replicates *ts1* most productively within the *ts1*-infected CNS appears to be the endothelial cell type (42). However, *ts1* replication in capillary endothelial cells does not lead to morphological changes whereas astrocytes at the infected region show intracellular vacuolization. Progeny *ts1* produced by endothelial cells may penetrate into astrocytes due to their physical location. *ts1* infects astrocytes in the mouse CNS although the astrocytes may not replicate progeny viruses productively in the CNS. In Chapter 2, we demonstrate that ROS upregulation occurs before productive virus replication. ROS upregulation in *ts1*-infected astrocytes can cause thiol deficiency in neurons. Infected astrocytes may fail to provide GSH as antioxidative defense to their adjacent neurons. ROS upregulation in *ts1*-infected astrocytes may affect a wide range of other functions as well. For instance, ROS upregulation by *ts1*-infection can decrease glutamine synthase (GS) in the astrocytes (110). This results in failure of glutamate absorption by glial cells in close proximity, leading to neuronal death. Production of extracellular ROS from *ts1*-infected astrocytes may also induce oxidative stress in neurons and damage macromolecules of neurons. The subsequent release of viral proteins or toxic metabolites from *ts1*-infected astrocytes may then be harmful to neurons and result in amplification of neurodegenerative mechanisms as assumed in HIV-associated dementia (HAD) (111). As the disease progresses, apoptotic changes are seen in astrocytes and the adjacent neurons. These results indicate that neuronal loss induced by *ts1* may not be due directly from the productive viral infection of neurons, but rather indirectly from the infected astrocytes.

1.5. Project overview

The causes of ND are complex, but recent studies demonstrate that oxidative stress plays an important role in these conditions (53, 112, 113). Previous studies in our laboratory have shown that ROS are upregulated in cultured *ts1*-infected astrocytes, and that antioxidant treatment delays neurodegeneration in *ts1*-infected mice (5, 94). However, despite the great potential benefit of antioxidant treatment as shown in several animal models, many of the antioxidant therapies tested to treat retrovirus-mediated neurodegenerative diseases in humans thus far have not been effective (114). This is primarily because they are not inhibiting a validated therapeutic target or specific pathway. In this study using *ts1*-infected astrocyte model, we attempt to identify the interactions between retroviruses and the host cells in ROS regulation during the retrovirus life cycle. Throughout this study, we seek to define the early and late phases of *ts1* life cycle in astrocytes within the context of fluctuating ROS levels. We hypothesize that ROS upregulation during the early phase of *ts1* infection may activate astrocytes to replicate virion progeny productively. In Chapter 2, we demonstrate that *ts1* infection of astrocytes increases levels of intracellular ROS in the early stage of infection, and that this upregulation is distinct from ROS upregulation during the later apoptotic phase. We provide evidence to support antioxidant activity of p53 in the early phase of *ts1* infection. Although we initially hypothesize that p53 plays an important role in *ts1*-induced cellular apoptosis, we observe that the absence of p53 did not prevent either cell death in cell culture or the neuropathological symptoms in mice after *ts1* infection. Instead, the early ROS upregulation appears to activate p53 via protein kinase ATM. Because the absence of p53 expression increases intracellular ROS levels, we speculate that p53 plays an important role in suppressing *ts1*-induced ROS upregulation. In addition, the expression of viral proteins after *ts1* infection occurs earlier in $p53^{-/-}$ astrocytes than in $p53^{+/+}$ cells, suggesting that retroviruses utilize the lack of p53-mediated antioxidants as a tool to facilitate early viral

establishment. We also observe that p53 downregulate the expression of a catalytic subunit of O_2^- producing enzyme NOX in *ts1*-infected primary astrocytes. From these observations, we conclude that p53 is unlikely to play a direct role in anti-viral defense. Rather, p53 upregulation seems to provide an indirect cellular defense mechanism against the virus by modulating ROS levels.

Based on the observation that p53 downregulates NOX in *ts1*-infected astrocytes, we further hypothesize that NOX may play an important role in ROS upregulation in the early phase of *ts1* infection. In Chapter 3, we show that NOX is activated in cultured *ts1*-infected astrocytes as well as in the CNS. The activation of NOX occurs during retroviral establishment in host cells, but not during cell death. These results suggest that NOX plays an important role in the enhancement of viral gene integration into host genome, but is not involved in the unfolded protein response caused by misfolded viral *env* protein. As expected, the inhibition of NOX decreased viral replication, prevented *ts1*-induced cell death, and therefore, delayed onset of pathological symptoms in *ts1*-infected mice. These observations led us to conclude that the suppression of NOX in the early phase of viral life cycle can prevent the establishment of the retrovirus. Therefore, it helps host cells to win the battle against the virus instead of suppressing viral replication after viral establishment. The influence of retrovirus-infected astrocytes on the onset and progression of retrovirus-induced ND gives us a new perspective on the importance of CNS astrocyte-neuron interactions and on further understanding of the pathogenic mechanisms underlying retrovirus-induced ND.

Chapter 2. ROS upregulation in the early phase of retrovirus infection and the role of p53 as an oxidative stress modulator

2.1. Introduction

Oxidative stress occurs in cells when production of ROS exceeds antioxidant defenses (115). Cellular defense responses to oxidative stress occur in a controlled sequence. The first level of defense involves upregulation of SOD and catalase to counter ROS buildup. Uptake of cysteine is the rate-limiting step for intracellular GSH generation, suggesting that cysteine levels are important in cell proliferation. In an oxidative environment, extracellular cystine, which is formed by the oxidation of two cysteines, is imported into astrocytes in exchange for glutamate via cystine-glutamate antiporter (xCT), in turn reduced to cysteine. If ROS overload causes significant depletion of cysteine and GSH, the second line of defense is deployed via activation and nuclear translocation of the transcription factor NF-E2 related factor 2, or Nrf2 (116). In the nucleus, Nrf2 binds to antioxidant-responsive elements (117), resulting in upregulation of the xCT to reduce cystine to cysteine. Once sufficient cysteine is present in the cellular environment, the modulatory subunit of glutamyl cysteine ligase inhibits GSH production via a negative feedback mechanism. Previous studies in our laboratory have reported that *ts1*-infected astrocytes exhibit signs of oxidative stress, including lower intra- and extracellular cysteine and GSH levels compared to both uninfected and parental MoMuLV-TB WT-infected astrocytes. We suspected that the cell death process initiated by the accumulation of misfolded gPr80^{env} might increase intracellular ROS levels (32). Viral titer of *ts1* progeny virus was lower than that of MoMuLV-WT at 24 hours post infection (hpi) in astrocytic culture (5). However, *ts1* titer became higher than WT titer at 48 hpi. Coinciding with *in vitro* results, *ts1* also had a higher titer than WT virus in mouse CNS at 20-30 days following inoculation, although the titer of

ts1 and WT were initially similar (5, 43). One explanation for this late increase in *ts1* titer is that overwhelming ROS upregulation induces cell death in *ts1*-infected astrocytes and facilitates the breakdown of cell membrane. This allows the progeny virus to be quickly released from the host cells thereby disseminating viral progeny to nearby uninfected cells. Therefore, preventing *ts1*-mediated apoptosis process would be an important step in prevention of further virus propagation. We initially hypothesized that *ts1*-induced cell death may be mediated by p53. p53 induces ROS generation, which then causes disruption of mitochondrial membrane potential (118). p53 is a well-known transcription factor that induces pro-apoptotic gene expression. Elevated p53 immunoreactivity has been detected in the animal brains of human neurodegenerative disease models and from patients with HAD (119, 120, 121). Similarly upregulation of p53, bax and p21 in the CNS has been shown in *ts1*-infected mice compared to uninfected mice (122). However, it is noteworthy that p53 immunoreactive astrocytes in the CNS lesions do not have the characteristic morphology of apoptotic cells seen in *ts1*-infected mice despite p53 upregulation (122). This observation suggests that *ts1*-mediated p53 upregulation in astrocytes may not necessarily lead to apoptosis. This prompted us to further investigate whether p53 plays a critical role in *ts1*-mediated cell death. Although p53's role in apoptosis has been well-established, recent evidence indicates that p53 can sense a multitude of cellular stresses and orchestrate cellular signaling pathways. p53 may function as a survival factor by regulating intracellular ROS levels. In steady state conditions, cells maintain low levels of p53 that are sufficient for the cell-protective transcription of antioxidant genes to protect cells (55). p53 expression levels are more closely related to defend intracellular environment than to cause suicide as a consequence of cellular stress. For example, p53 protects DNA oxidation by regulating levels of cellular anti-oxidant factors, such as GSH or NADPH (56, 57, 58). Cells that express higher p53 level show a higher resistance to cell death caused by oxidative damage. Alternatively, suppression of p53 expression makes cells susceptible to H₂O₂ –

mediated damage. Disruption of cellular ROS homeostasis in p53-depleted cells was also detected by increased intracellular H₂O₂ (123).

In this chapter, we demonstrate that *ts1* infection causes two separate ROS upregulation events in host cells. The first occurs during early viral establishment in host cells and the second ROS increase occurs during the apoptotic process. We examined whether p53 plays a crucial role in the initiation of apoptosis or in protection against oxidative stress in *ts1*-infected astrocytes. p53 functions as a modulator of intracellular ROS followed by the early phase of ROS upregulation in *ts1*-infected astrocytes. However, *ts1*-mediated astrocytic apoptosis regulation is p53-independent.

2.2. Materials and methods

2.2.1. Mice

p53^{+/-} FVB/N mice were given as generous gifts from Dr. David Johnson (The University of Texas M.D. Anderson Cancer Center). Offsprings were genotyped by polymerase chain reaction (PCR)-based assays of mouse tail DNA. For *ts1* infection 2-day-old mice were inoculated intraperitoneally with 0.1ml of vehicle (uninfected control) or with 0.1ml of *ts1* virus suspension containing 2 x 10⁷ infectious units (IU)/ml. For mice given this dose of *ts1*, early stages of paralysis were evident by approximately 30 dpi. We differentiated disease progression into four stages (stage I, hindlimb drop; stage II, tremor; stage III, loss of mobility; stage IV, paralysis), and sacrificed mice at stage IV. The time of sacrifice was used as a measurement of the total number of survival days. Animal care was in accordance with The University of Texas M.D. Anderson Cancer Center guidelines for animal experiments.

2.2.2. Virus

ts1, a spontaneous temperature-sensitive mutant of MoMuLV-TB WT, propagates in TB cells as a thymus-bone marrow cell line. Virus titers were determined by a modified direct focus-forming assay in TB-derived 15F cell line, a murine untransformed, sarcoma virus-positive, leukemia negative cell line, as described previously (43).

2.2.3. Cell culture and *ts1* infection for cultured astrocytes

15F cells and immortalized murine C1 astrocytes were maintained in Dulbecco's modified Eagle's medium (DMEM) supplemented with 10% fetal bovine serum, 100 units/ml penicillin, 100µg/ml streptomycin in a 37°C incubator with 5% CO₂ in air. These cells were passaged biweekly and used for experiments while in the exponential growth phase. Primary astrocytes were isolated from 1 to 2 day-old newborn mouse pups by a method described previously (124). In brief, whole brains of each newborn mouse were removed and minced separately in ice-cold DMEM/F12 medium. Cell suspension was obtained by passing the minced tissue through a 70 mm nylon mesh cell strainer, and plated onto poly-L-lysine coated 100mm petri dish, and grown in DMEM/F12 medium, supplemented with 10%FBS, 5 units/ml penicillin, 5 µg/ml streptomycin and 2.5g/ml Fugizone for 4 days in an incubator with 5% CO₂, atmosphere at 37°C until reaching confluence. At this point, more than 99% of the cells in cultures were positive for the astrocyte-specific glial fibrillary acid protein (GFAP) marker (125). As noted above, pup genotypes (p53^{+/+} or p53^{-/-}) were identified using standard genotyping PCR on tissue samples and used to label the respective primary cultured cells. For infection, 10⁵ cells of C1 or primary cultured astrocytes were seeded into 100mm petri dishes. On the second day of culture, all cells are treated for overnight with 3µg/ml polybrene and 1% FBS in DMEM for C1 cells or DMEM/F12 for primary astrocyte culture (PAC). Cells were then trypsinized and counted. *ts1* virus was diluted in the same medium and added to the cells at a multiplicity of infection

(117) of 5 for C1 cells or 20 for PAC for 40 minutes. The cells were washed and incubated with normal cell medium containing 10% FBS (94).

2.2.4. ROS measurement

Intracellular levels of H_2O_2 in living cells were measured with 5-(and -6)-chloromethyl-2',7'-dichlorodihydrofluorescein diacetate acetyl ester (CM-H₂DCFDA)(Molecular Probes, Eugene, OR) as described previously (126). DCFDA is deacetylated by endogenous esterases to DCF, which reacts with H_2O_2 to generate fluorescence. In brief, cells were loaded with 20 μ M CM-H₂DCFDA and incubated at 37°C for 30 minutes. The dye-loaded cells are then washed with PBS and the levels of intracellular H_2O_2 is determined using a fluorescent plate reader (Synergy HT, BioTek) at excitation/emission maxima of 488/520nm. To determine the levels of O_2^- production at the mitochondrial membrane in living cells, MitoSOX Red (Molecular Probes, Eugene, OR) was used. MitoSOX Red reagent is selectively targeted to mitochondria and rapidly oxidized by O_2^- , but not by other ROS. Cells were loaded with 5 μ M MitoSOX Red and incubated at 37°C for 5 minutes and washed with PBS. Levels of the mitochondrial O_2^- are determined using a fluorescent plate reader (Synergy HT, BioTek) at excitation/emission maxima of 530/590nm.

2.2.5. mRNA extraction and real-time PCR

C1 astrocytes were infected with *ts1* at the multiplicity of infection (117) of 5. mRNA was extracted using RNeasy Extraction Kit and Oligotex followed the manufacturer's instruction (Quiagen, Valencia, CA). High Capacity cDNA Archive Kit (Applied Biosystems, Foster City, CA) was used to synthesize cDNA by reverse transcription polymerase chain reaction (RT PCR) and real-time quantitative polymerase chain reaction (qPCR) subsequently performed on the ABI 7900HT Fast Real Time PCR system with primers specific to *ts1* gPr80^{env} using SYBR Green master mix (BioRad, Inc. Hercules, CA). RNA

levels were normalized with the endogenous house-keeping gene, Glyceraldehyde 3-phosphate dehydrogenase (GAPDH). The experimental cycle threshold (127) was calibrated against the GAPDH control product and *delta delta* Ct (ddCt) method was used to determine the amount PCR product relative to that of RNA purified from uninfected cells.

2.2.6. Western blot analysis and subcellular protein fractionation

C1 or primary astrocytes were washed with PBS and lysed in RIPA buffer as previously described (94). Protein concentrations were determined using Bio-Rad D^o protein assay reagent (Bio-Rad Laboratories, Hercules, CA). The proteins were separated on SDS-PAGE gels, transferred to PVDF membrane, and then immunoblotted with indicated primary antibodies. The antibodies used were rabbit anti-phosphorylated p53 (serine15)(Cell Signaling, Danvers, MA), mouse anti-phospho ATM (serine 1981), mouse anti-ATM (Novus Biological Inc., Littleton, CO), rabbit anti-cleaved caspase 3 (Cell Signaling, Danvers, MA), rabbit anti-PUMA (Cell Signaling, Danvers, MA), goat anti-gp70^{env}, rabbit anti-p30^{capsid}, goat anti-gp91^{phox} (Santa Cruz Biotechnology, Santa Cruz, CA), and mouse anti-β actin (Sigma Aldrich). After *ts1* infection, C1 cells were harvested for fractionations and the cell lysates were separated into 5 subcellular fractions (cytoplasmic, membrane, nuclear soluble, chromatin-bound and cytoskeletal protein extracts) in accordance with manufacture's protocol (Thermo Scientific, Rockford IL). In brief, cytoplasmic fractions were collected after plasma membrane permeabilization. Membrane compartments (plasma membrane and organelle membranes) were then dissolved in the membrane fraction. After recovering intact nuclei by centrifugation, the agent yielded soluble nuclear extract, and then chromatin-bound nuclear proteins were extracted by incubation with nuclease. To verify fractionation, 25μl of each extract was analyzed by western blots, using specific antibodies against proteins from various cellular compartments including for anti-HSP90 (cytoplasmic)(Stratagene), calreticulin (membrane) (Cell Signaling, Danvers, MA), histone3

(chromatin bound) (Cell Signaling, Danvers, MA), and Bmi-1 (nuclear soluble) (Cell Signaling, Danvers, MA) antibodies (data not shown).

2.3. Results

2.3.1. The early phase of infection in *ts1* life cycle

As noted in Chapter 1, the life cycle of retroviruses during viral establishment in the host cells can be divided into two distinct phases: the pre-integration phase and post-integration. The pre-integration phase refers to the progression of infection from viral entry into the host cells to the integration of the viral DNA into the host cell genome. The post-integration phase denotes the expression of viral genes and continues through to the assembly, release, and maturation of progeny virions (70, 128) (Figure 1.5). To investigate *ts1* life cycle of viral gene integration into the host cell genome and the process of viral replications of viral progeny, we purified mRNA from 2, 4, 8, and 24 hpi, and performed RT PCR using viral *env* gene primers. To quantify RT PCR products, qPCR was performed. As shown Figure 2.1, we detected initiation of viral mRNA transcription at 8 hpi. From this result, we speculate that the viral proteins detected before 8 hours were most likely protein carried by the initial infected viral particles. We then investigated viral protein distribution in different subcellular fractions during the pre-integration phase. As shown in Figure 2.2, after *ts1* infection, viral Env protein detected by anti-gp70^{Env} antibody was mostly found in the membrane fraction at 2 and 4 hpi in very similar levels. Because we did not detect any viral gene transcription at 2 and 4 hpi, the envelope protein we observed were therefore from the initial viruses fused to the C1 cells. At 4 hpi, more p30^{capsid} was translocated to the nuclear membrane as compared to the levels seen at 2 hpi. In studies of HIV, p24^{capsid} penetrates the plasma membrane and delivers viral pre-integrated complex to the host nucleus. Interestingly, the number of intra-nuclear PICs reached its highest level at 6 hpi (129). As

seen in our study, *ts1* DNA established in the host genome starts transcription at 8 hpi, suggesting that between 4-8 hpi might be relevant to the pre-integration phase in the single life cycle of retrovirus-infection *in vitro*.

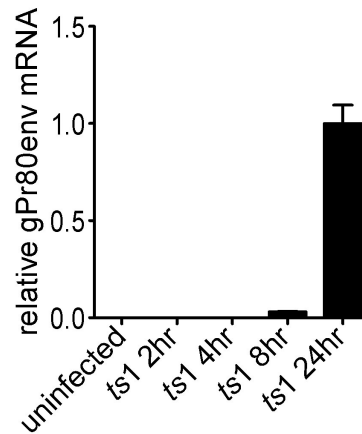


Figure 2.1. Viral gene transcription in *ts1*-infected astrocytes.

C1 astrocytes were infected with the *ts1* virus at a MOI of 5. We then harvested cells at 4, 8, 12, and 24 hpi and purified mRNA. Real time RT-PCR was performed and the relative amount of mRNA of viral *env* is presented after normalization to GAPDH.

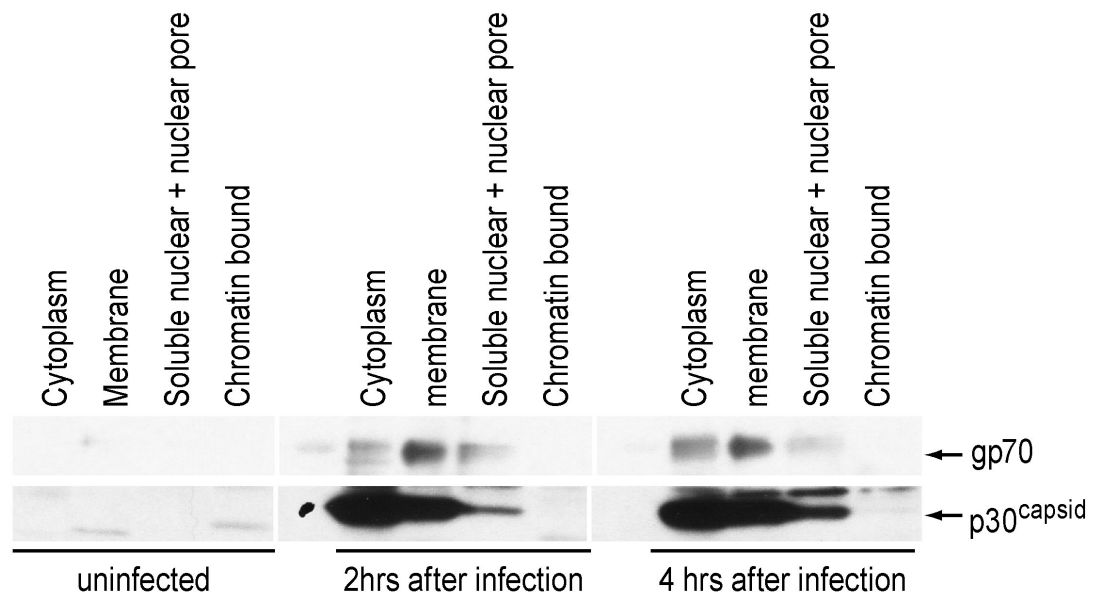


Figure 2.2. Subcellular locations of viral proteins in *ts1*-infected astrocytes.

At 2 and 4 hpi, C1 cell lysates were isolated into 5 subcellular fractions (cytosolic, membrane, soluble nuclear, chromatin-bound, and cytoskeletal fractions). To identify the location of viral proteins in the cell, the fractioned samples were probed for anti-gp70^{env}/gPr80^{env} and anti-p30^{capsid} antibodies.

2.3.2. ROS upregulation in the early phase of infection

Retrovirus replication requires host cell proliferation because retroviruses depend on host resources for replication (43, 130). To access those resources, retroviruses may possess mechanisms to activate the host cells. For example, mouse mammalian tumor virus (MMTV) activates B cells polyclonally and transiently during the first few hours following viral infection, which is independent from T cell mediated activation in the later phase (130). HIV virus infectious factor (Vif) mediates G1 to S phase progression for viral nucleotides replication (92). We have previously proposed that retroviral infection in the quiescent environment of the CNS might act to promote host cell proliferation in order to replicate the virus (94). Despite the fact that upregulation of intracellular ROS levels in retrovirus-infected cells and tissues has been well-documented (127, 131, 132, 133, 134, 135, 136, 137), most of these studies assume that ROS upregulation mediated by retrovirus infection is associated with cellular apoptosis. Recent studies suggest that intracellular ROS levels may have various cellular consequences. For example, high levels of ROS induce cell death and growth arrest whereas low levels of ROS mediate cell proliferation (Figure 1.4). Therefore, it is important to understand the mechanism by which retrovirus-infected cells channel ROS into particular signaling pathways spatially or temporally to accomplish desired outcomes (62, 95). In particular, the question of how the induction of intracellular ROS production contributes to the establishment of a retrovirus in the host cells remains underexplored. To investigate the life cycle of *ts1* in the context of ROS upregulation, we examined intracellular ROS levels after *ts1* infection using two different fluorescent probes: CM-H₂DCFDA to measure intracellular H₂O₂ levels and MitoSOX Red to selectively detect mitochondrial O₂⁻. *ts1*-infected astrocytes at the indicated times (4, 8, 24, and 48 hpi) were incubated with CM-H₂DCFDA for 30 minutes, and then DCF fluorescence was measured to determine intracellular H₂O₂ levels. Infected cells were shown to have higher H₂O₂ levels as compared to uninfected cells between 4-8 hours and at 48 hours, but not during 24-48 hpi

(Figure 2.3). When we treated cells with anti-oxidant NAC, *ts1*-mediated ROS upregulation disappeared, suggesting that DCF fluorescent signals represent intracellular H_2O_2 levels. As stated above, ROS upregulation has been assumed to come from mitochondria. To detect O_2^- from the mitochondria, we incubated *ts1*-infected cells with MitoSOX Red. As shown in Figure 2.4, O_2^- released from the mitochondria was detected at 48 hpi, but not at 4 or 24 hpi. This suggests that H_2O_2 upregulation in the early phase of infection is not originated from the mitochondria during the late phase of infection. Furthermore, we observed activated caspase 3 levels during cell death at 48 hpi, suggesting the ROS upregulation during the late phase of viral infection may be associated with cell death (Figure 2.5). These results provide strong evidence for at least two separate periods of H_2O_2 upregulation. The first with a relatively low H_2O_2 increase occurs during 4-8 hpi whereas the second with a relatively high H_2O_2 increase appears at 48 hpi.

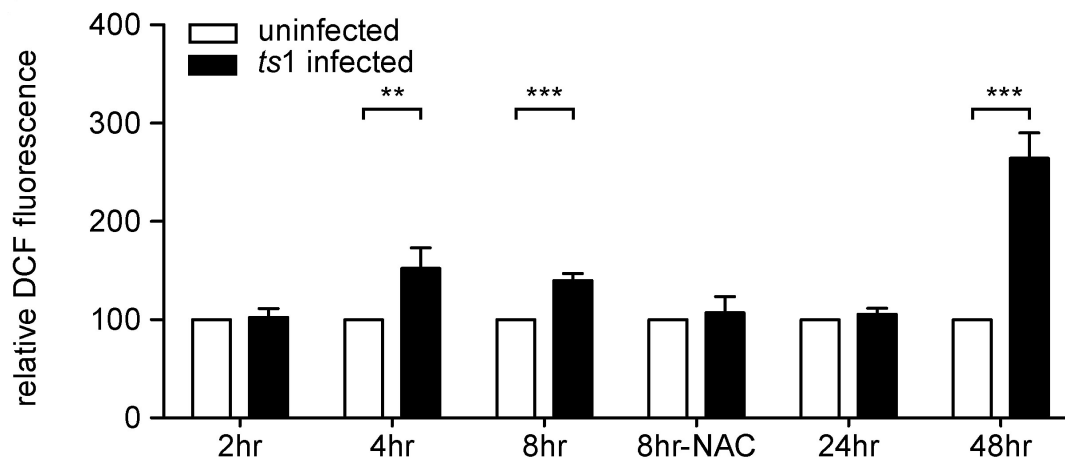


Figure 2.3. Intracellular H₂O₂ measurement in *ts1*-infected astrocytes

C1 cells were infected with *ts1*. To measure relative intracellular H₂O₂ levels, cells were loaded with CM-H₂DCFDA followed by measurement of the relative intensity of fluorescent signal. ** $p < 0.01$; *** $p < 0.001$ when compared with uninfected cells. H₂O₂ levels at 4, 8, and 48 hpi were increased in *ts1*-infected astrocytes as compared to in uninfected astrocytes. Lower intracellular H₂O₂ levels are present in *ts1*-infected, NAC-treated cells.

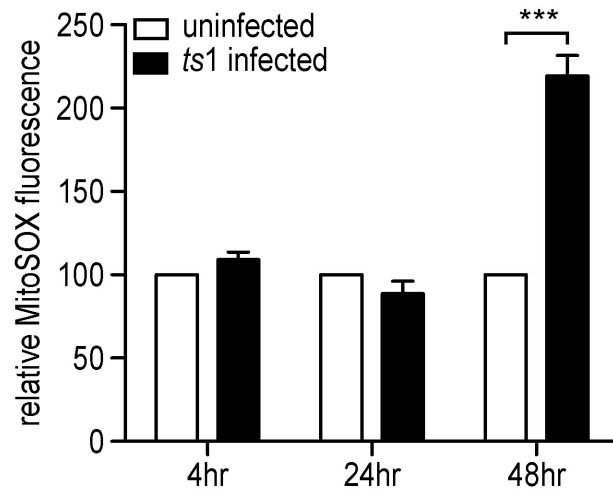


Figure 2.4. Mitochondrial O_2^- measurement in *ts1*-infected astrocytes.

C1 cells were infected with *ts1* and relative O_2^- levels were detected by loading with MitoSOX-Red and measuring the relative intensity of fluorescent signal. *** $p < 0.001$ when compared with uninfected cells.

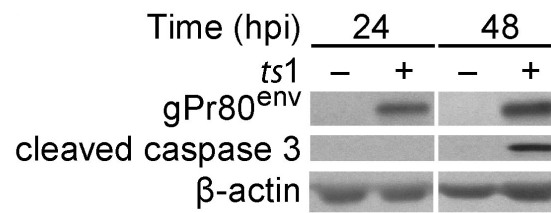


Figure 2.5. Cellular apoptosis in *ts1*-infected astrocytes. An apoptotic marker, cleaved caspase 3 appeared at 48 hpi whereas translated viral pPr80env did at 24 hpi.

2.3.3. p53 does not play an important role in *ts1*-induced apoptosis.

Previous studies showed increased p53 levels in *ts1*-infected astrocytes and in *ts1*-infected mouse brain stem (122). Due to the observation of two distinct phases of ROS upregulation in *ts1*-infected astrocytes, we asked whether *ts1*-mediated upregulation of ROS leads to p53-dependent cell death. To address this question, we injected *ts1* virus into newborn pups with different p53 genotypic backgrounds. As shown in Figure 2.6, the absence of p53 did not prevent *ts1*-mediated neuropathogenic symptoms in *ts1*-infected mice. Rather p53 knockout mice seemed to show pathological symptoms slightly earlier than wild type mice. We also cultured PACs from p53^{+/+} and p53^{-/-} mouse brains and compared cell survival after *ts1* infection. Our data demonstrated that the absence of p53 does not prevent *ts1*-induced cell death as shown in Figure 2.7. Interestingly, p53^{-/-} PACs showed higher levels of activated caspase 3 and PUMA (p53 upregulated modulator of apoptosis) expression as compared to p53^{+/+} PACs following *ts1* infection (Figure 2.8). Interestingly we noticed that PACs were much more resistant to *ts1*-mediated cell death compared to C1 cells. In *ts1*-infected C1 cells with an MOI of 5, it took 2 days to observe significant cell death, whereas in *ts1*-infected PACs with an MOI of 20 it took 6 days. Although previous studies have reported that the progression of cytopathic effects in C1 is similar to that in PAC (5, 124), the time period of such progression is much shorter in C1 compared to PAC. Currently, we do not know why C1 cells are more susceptible to *ts1*-induced cell death than PAC. It may be due to the higher proliferative property of C1 cells as a result of SV40 large T antigen expression, which is used in cell line immortalization (124). Further studies are required to investigate whether highly proliferative cells are more susceptible to retrovirus-mediated cytopathogenesis. The fast progression of the virus life cycle in cultured C1 has come to be a useful tool in the study of the early phase of the *ts1* life cycle.

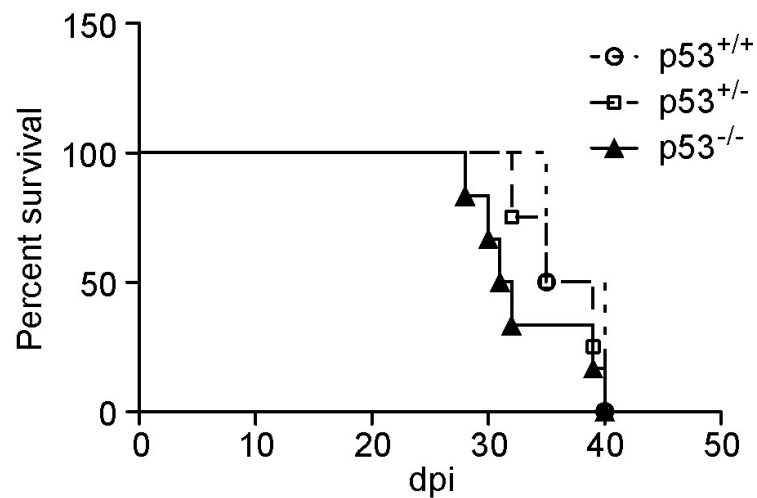


Figure 2.6. The life span of *ts1*-infected $p53^{+/+}$ and $p53^{-/-}$ mice

2-day-old mice were inoculated intraperitoneally with 50 μ l of vehicle (mock infection) or a *ts1* virus suspension containing 1×10^7 infectious units (IU)/ml of *ts1*. Survival curves for *ts1*-infected $p53^{-/-}$ mice (n=6) against survival curves for $p53^{+/+}$ (n=4) and $p53^{+/-}$ (n=12) mice. Log rank test was applied to test if the survival curves are the same. There was no significant difference between $p53^{+/+}$ and $p53^{-/-}$ mice ($p=0.496$)

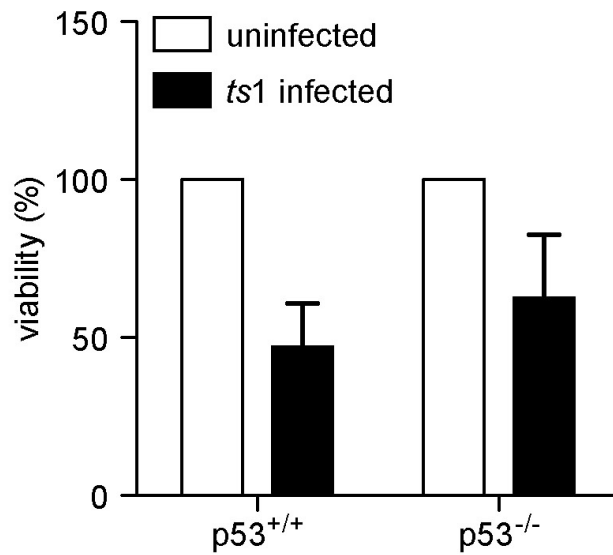


Figure 2.7. Viable cell count assay of *ts1*-infected PACs from $p53^{+/+}$ and $p53^{-/-}$ mouse

brains. PACs from $p53^{+/+}$ and $p53^{-/-}$ mouse brains were infected with *ts1* at a MOI of 20.

Viable cells were counted using the trypan blue exclusion method and the viable cell number of the *ts1*-infected group was compared to that of the uninfected in same genotype of astrocytes. Error bars represent mean \pm SEM from three independent experiments.

There was no significant difference between $p53^{+/+}$ and $p53^{-/-}$ PACs.

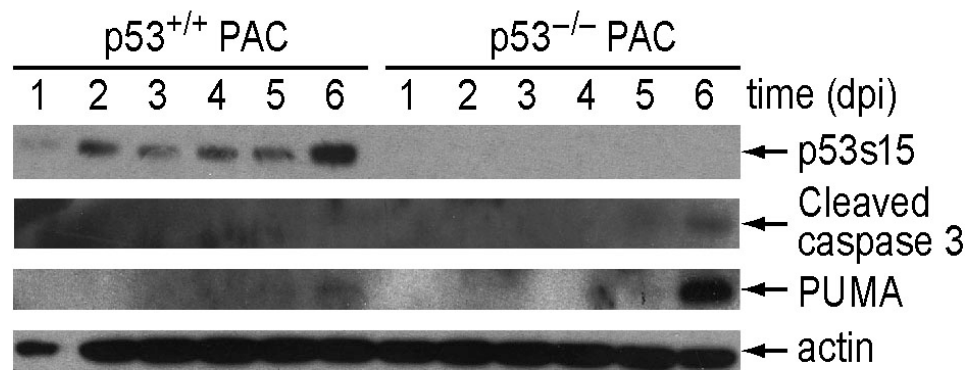


Figure 2.8. *ts1*-mediated apoptosis in PACs from *p53*^{-/-} and *p53*^{-/-} mouse brains.

After indicated time, protein lysate samples from *ts1*-infected *p53*^{-/-} and *p53*^{-/-} PACs were prepared and levels of phosphorylated p53, cleaved caspase 3, and PUMA were compared using Western blot analysis.

2.3.4. p53 is activated by ROS upregulation in the early phase of infection

In the absence of stress, p53 protein levels are kept low by the ubiquitin-mediated proteolytic pathway. When cellular stress occurs, p53 is phosphorylated and stabilized as a result (138, 139). To investigate if p53 is activated by ROS upregulation, we first examined p53 phosphorylation in response to H₂O₂-treated astrocytes. We treated C1 cells with H₂O₂, and observed p53 phosphorylation and upregulation of intracellular H₂O₂ (Figure 2.9). As shown in Figure 2.7 and Figure 2.8, *ts1*-mediated cell death occurred in a p53-independent manner. We then hypothesized that p53 may be activated as a consequence of early ROS upregulation in *ts1*-infected astrocytes. As shown in Figure 2.3, *ts1*-infected cells have higher ROS levels than uninfected cells at 4 and 8 hpi. If p53 is activated by ROS upregulation, one would expect p53 activation follows ROS upregulation, which occurs at 4-8 hpi. We observed that p53 phosphorylation was initiated at 8 hpi and reached a peak at 12 hpi. This phosphorylation appeared to increase total p53 protein level (Figure 2.10) and the levels of phosphorylated p53 persisted until cell death occurred. These results suggest that ROS upregulation induced by *ts1* infection activates p53 during the early phase of virus infection in astrocytes.

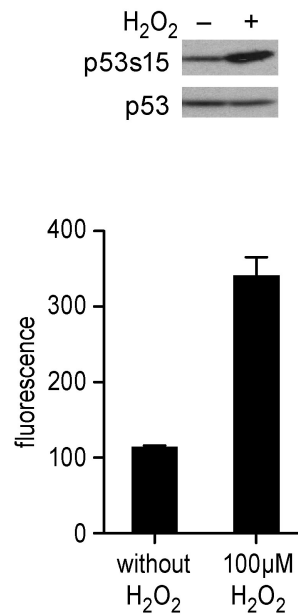


Figure 2.9. Upregulation of intracellular ROS increases p53 phosphorylation.

100μM H₂O₂ was added to C1 cells for one hour. To determine if phosphorylation of p53 is increased by ROS, both p53 phosphorylation and intracellular ROS levels were analyzed. To measure intracellular ROS, cells were loaded with CM-H₂DCFDA followed by measurement of the relative intensity of fluorescent signal. The levels of p53 phosphorylation were compared using Westernblot analysis. Total protein amounts were visualized by p53. Change in 53 levels were not detected within one hour of H₂O₂ treatment.

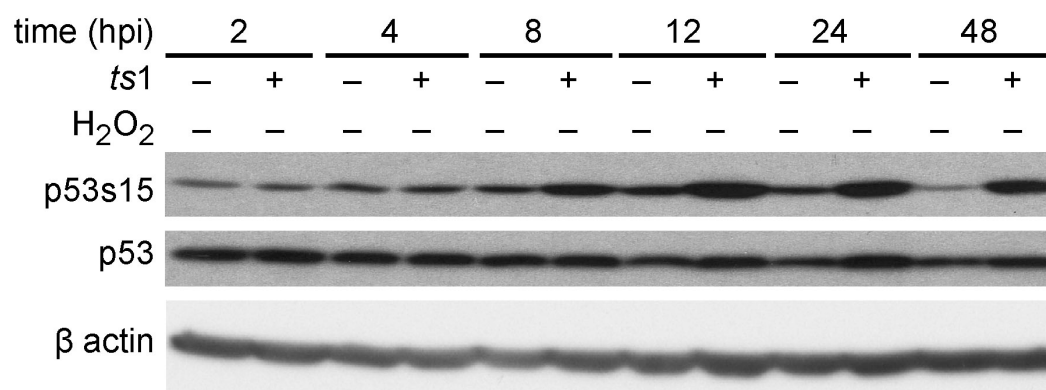


Figure 2.10. p53 phosphorylation in *ts1*-infected astrocytes

Levels of phosphorylated p53 and total p53 were compared in uninfected and *ts1*-infected samples using Western blot analysis. β-actin was probed as a protein loading control.

2.3.5. ATM phosphorylates p53 in response to ROS upregulation

ATM, the protein encoded by the ataxia-telangiectasia (A-T) mutated gene, is an upstream kinase of p53, which phosphorylates serine 15 of p53 under stressful conditions (140). In addition to its role in DNA repair, ATM also plays an important role in regulation of cellular redox status (141, 142, 143, 144, 145, 146). It is notable that ROS-induced ATM activation is a separate event from the DNA damage response (147). As shown in Figure 2.11, ATM is activated in H₂O₂-treated cells. Since *ts1* infection upregulated ROS levels during the early phase, we aimed to investigate if ATM is activated in *ts1*-infected astrocytes. Cell lysates were prepared and probed with anti-phospho ATM antibody (serine 1981). As shown in Figure 2.11, ATM activation occurred at 4 hpi, which preceded p53 phosphorylation at 8 hpi. To examine if p53 phosphorylation relies on ATM activation, we treated C1 cells with H₂O₂ and an ATM inhibitor, Ku55933. We found that this H₂O₂-induced p53 activation was inhibited by Ku55933 treatment. Furthermore, treatment of *ts1*-infected C1 with Ku55933 prevented p53 activation (Figure 2.12). Together these results suggest that ATM is a direct upstream kinase for p53 phosphorylation at the site serine 15 in response to early ROS upregulation induced by *ts1* infection.

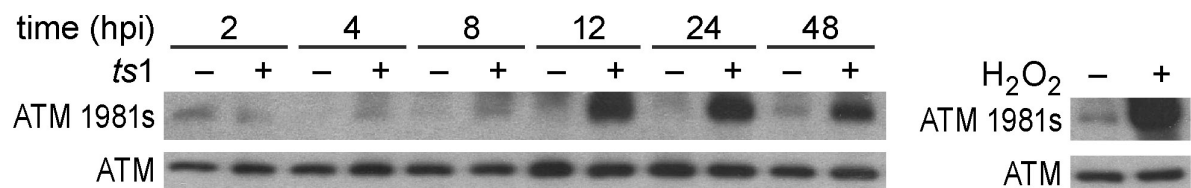


Figure 2.11. ATM activation in *ts1*-infected astrocytes and H₂O₂ treated astrocytes.

C1 cells were infected with *ts1* and harvested cell lysates at 4, 8, and 12 hours post infection were analyzed using Western blot analysis to compare the levels of phosphorylated ATM. Indicated concentration of H₂O₂ was added to C1 cells for one hour and the cells were subjected to Western blot analysis to compare phosphorylated ATM levels.

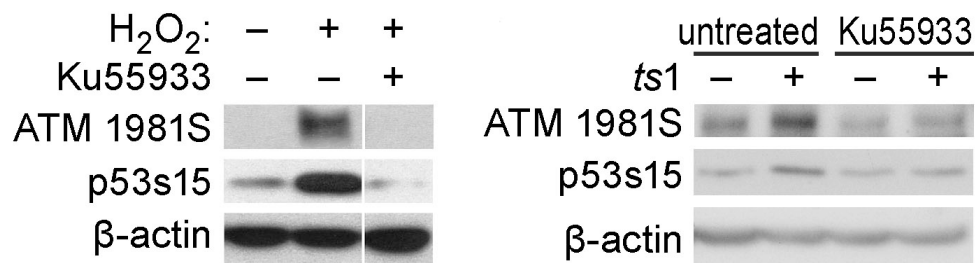


Figure 2.12. Suppression of p53 phosphorylation by inhibiting ATM activation.

C1 cells treated with 100 μ M H₂O₂ were incubated with Ku55933, an ATM inhibitor. Cell lysates were then prepared and were compared to examine the levels of phosphorylated ATM and p53. Similarly, *ts1*-infected C1 cells were treated with Ku55933 and examined the levels of phosphorylated ATM and p53.

2.3.6. p53 as an intracellular ROS modulator.

ts1 infection increases the levels of intracellular ROS in astrocytes, yet, not all *ts1*-infected astrocytes die as a result of the ROS upregulation (5). The surviving astrocytes during chronic infection with *ts1* express higher levels of GSH, suggesting that upregulation of antioxidant defenses may be a survival strategy for *ts1*-infected astrocytes (93). It has been demonstrated that expression of p53 appears to increase intracellular antioxidant (GSH and NADPH) levels (56, 57, 58). p53 has also been shown to play an important role in decreasing ROS levels in various human cancer cell lines through upregulation of antioxidant defense and metabolic enzyme gene transcription (55, 148). By the same token, lack of p53 may hamper anti-oxidant defenses in *ts1*-infected astrocytes. The next step was to determine if the absence of p53 dysregulates intracellular ROS levels in astrocytes. To address this question, we measured intrinsic intracellular ROS levels in PACs isolated from p53^{+/+} and p53^{-/-} mouse brains. Intracellular ROS levels were higher in p53^{-/-} PACs compared to those in p53^{+/+} PACs (Figure 2.13). Furthermore, when both cells were treated with the same concentration of H₂O₂, levels of intracellular ROS were more highly elevated in p53^{-/-} cells compared to in p53^{+/+} cells. This suggests that p53 is involved not only in regulating intrinsic ROS levels but also in controlling stress-mediated oxidative defenses. Since we observe ROS upregulation in the early phase of infection, viral infection appears to enhance intracellular ROS levels independently of the mitochondria. We hypothesized that this small amount of ROS upregulation is beneficial for the early viral establishment in host cells. As mentioned before, retrovirus may upregulate ROS levels leading to activation of host cells to replicate virus progeny. As shown Figure 2.14, expression of viral proteins (gPr80^{env}/gp70 and p30^{capsid}) appears earlier in p53^{+/+} cells compared to p53^{-/-} cells when they are infected in same MOI. Interestingly, expressed gPr80^{env} was processed into gp70 more efficiently in p53^{-/-} cells than in p53^{+/+} cells (Figure 2.14). It is possible that ROS upregulation may facilitate protein folding.

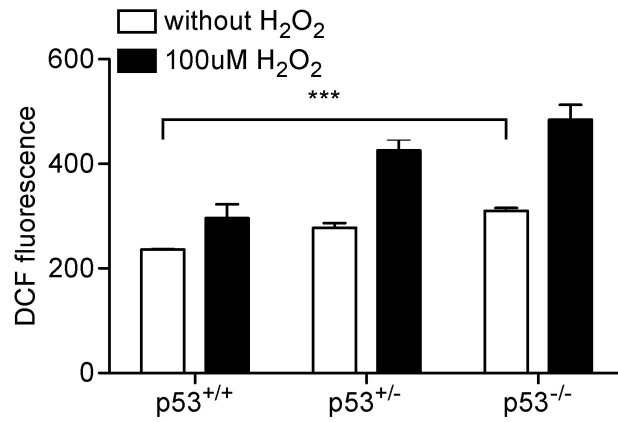


Figure 2.13. Intracellular ROS levels in PACs from p53^{+/+} and p53^{-/-} mouse brains.

p53^{+/+} and p53^{-/-} PACs were untreated or treated with H₂O₂ for 30 min. The relative ROS levels of the PACs were detected by loading with CM-H₂DCFDA, followed by measurement of the relative intensity of fluorescent signal. ****p* < 0.001 when untreated p53^{+/+} PAC compared with untreated p53^{-/-} PAC cells. ***p* < 0.01; when H₂O₂-treated p53^{+/+} PACs compared with H₂O₂-treated p53^{-/-} PACs.

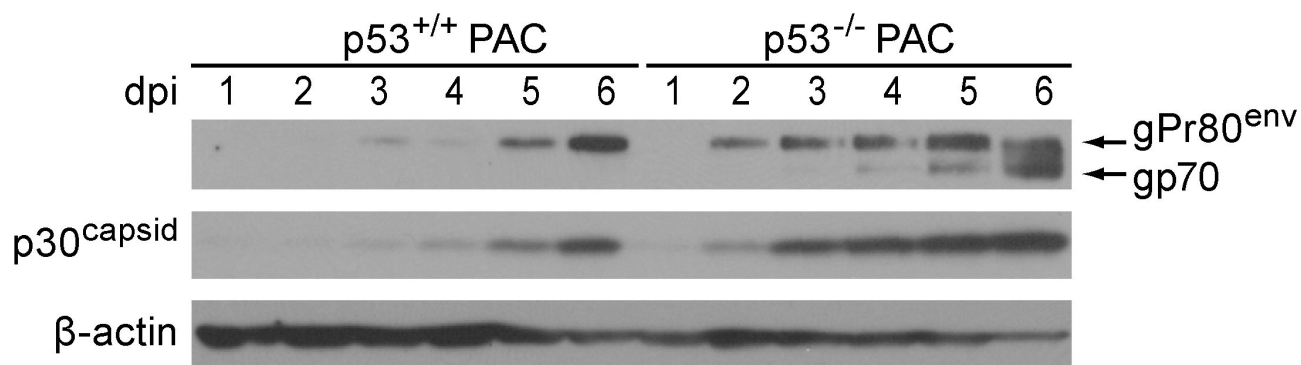


Figure 2.14. Expression of viral proteins in *ts1*-infected primary astrocytes.

PACs from *p53*^{+/+} and *p53*^{-/-} mouse brains were infected with *ts1* at the same MOI and protein lysates were prepared at 1, 2, 3, 4, 5, 6 dpi. Western blot analysis shows that expression of gPr80/70^{Env} and p30^{capsid} appears earlier in *p53*^{-/-} PAC compared to *p53*^{+/+} PAC.

We found that gp91^{phox} protein expression level is downregulated in *ts1*-infected p53^{+/+} PACs and the suppression of gp91^{phox} expression does not occur in p53^{-/-} PACs (Figure 2.15). This suggests that astrocytes may have a feedback mechanism to suppress levels of gp91^{phox} to prevent further oxidative stress and that this appeared to be mediated by p53, although we do not know whether the suppression of gp91^{phox} is regulated by p53 directly or indirectly.

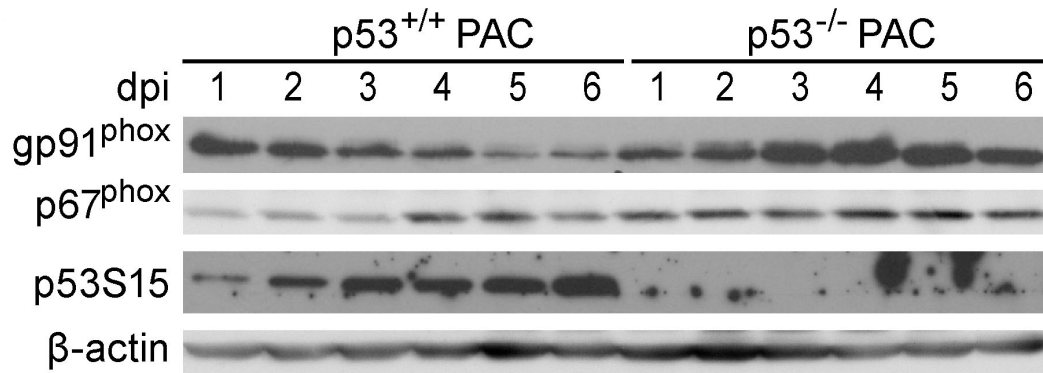


Figure 2.15. Expression of NOX subunits in *ts1*-infected PACs.

PACs from *p53*^{+/+} and *p53*^{-/-} mouse brains were infected with *ts1* at the same MOI and protein lysates were prepared at 1, 2, 3, 4, 5, 6 dpi. Western blot analysis shows the expression levels of gp91^{phox} decreased in *ts1*-infected *p53*^{+/+} PACs while the infection process continued. However, *ts1*-infected *p53*^{-/-} PACs showed increased gp91^{phox}.

2.4. Discussion

The fact that established retrovirus in the host genome hijacks the host machinery to replicate itself is well-known. The retrovirus attempts to establish its gene in the host genome and the host may try to protect its genome from viral invasion. However, until recently the early battle for cellular control between the retrovirus and the host cell has been underexplored. Recent studies suggest that the host cell status is critical for retrovirus infection (149, 150). Some retroviruses including MuLV can infect only mitotic cells (149). Even HIV cannot infect cells in the permanent resting G_0 stage, suggesting that retrovirus infection requires partially activated cells (150). We speculate that host cell status could be altered by the retrovirus in order to create the optimal environment for cellular invasion. This notion is supported by recent studies that show retroviral proteins promoting host cells transition to G1/S stages (92) to facilitate integration and replication of the retrovirus. In this study, we demonstrated at least two phases of ROS upregulation during *ts1* infection. As expected, one phase of ROS upregulation occurred during *ts1*-induced cell death (48 hpi). Surprisingly, we also detected another ROS upregulation at relatively low levels between 4-8 hpi, which is considered as the early phase of infection before expression of viral gene expression (Figure 2.16). We speculate that the increased ROS production seen here may be involved in retrovirus establishment in host cells. It has also been suggested that low levels of ROS act as an intracellular messenger to activate tyrosine kinases or to inactivate phosphatases by oxidizing cysteine residues in the active sites (62). In this study, we demonstrated that this transient early ROS upregulation is a separate event from ROS upregulation during cell death in *ts1*-infected astrocytes.

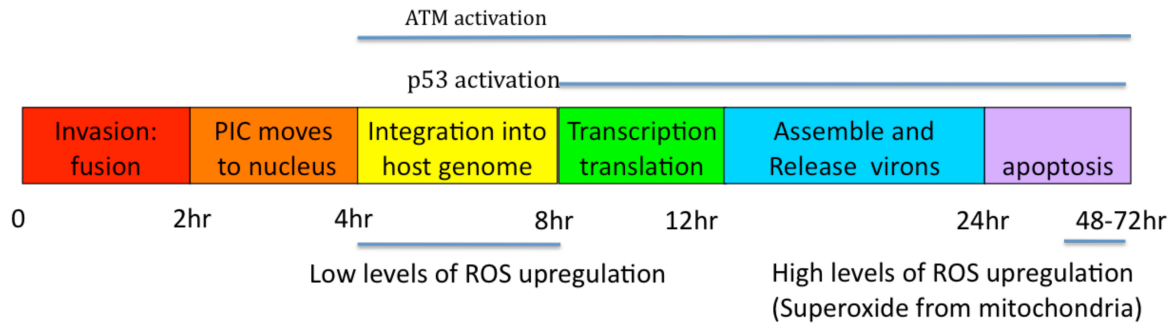


Figure 2.16. The life cycle of *ts1* and distinct ROS increases in C1 astrocytes.

After *ts1* fuses to host cell membrane (0-2 hpi), the viral PIC enclosed by capsid translocates to the host nucleus. While doing so, reverse transcriptase produces viral DNA from RNA genome in the host cytoplasm (2-4 hpi). Once viral DNA is integrated into the host genome (4-8 hpi), cells start transcription and translation from integrated viral DNA (8-12 hpi). There are two distinct phases of ROS upregulation. The first ROS increase at low levels occurs between 4-8 hpi and high levels of ROS accumulates between 48-72 hpi while cell death occurs. p53 phosphorylation is observed at 8 hpi.

Earlier observations, such as upregulation of apoptotic markers and p53 levels in *ts1*-infected astrocytes in culture, lead us to hypothesize that p53 may play a role in *ts1*-mediated cell death through promotion of pro-apoptotic gene expression (122). However, we found that cell death occurs in *ts1*-infected PACs lacking p53 expression. Wild type mice and p53 knockout mice infected with *ts1* show no significant difference in neuropathological symptoms as illustrated in Figure 2.6. These results are consistent with our previous data showing that *ts1*-infected CNS cells with high levels of p53 expression are not associated with morphologic characteristics of dying cells (122). These observations suggest that p53 does not play a critical role in *ts1*-mediated cell death. However, many studies have reported that oxidative stress accompanied by upregulation of p53 levels is a feature of several viral infections of the CNS (151, 152, 153, 154). From this, we hypothesized that the relative low levels of ROS upregulation may initiate p53 activation. In this Chapter, we demonstrated that during the early phase of *ts1*-infection the low level of ROS upregulation activated ATM, which in turn, phosphorylated p53. This result is similar to a previous study using HIV pseudoparticles in human lymphoblast cells that showed during a single cycle of HIV infection to human lymphocytes, reversely transcribed viral DNA was first detected at 4 hpi, and then disappeared (155). The exposure of cells to Vesticular stomatitis virus (VSV) enveloped-HIV pseudoparticles activates p53 at 4 hours and Ku55933 treatment inhibits p53 activation (156). The similarity between previous HIV studies and our study implicates that the process of retrovirus infection may initially trigger the activation of p53 and ATM during the early phase of infection. We further argue that ATM and p53 may be host defense elements attempting to suppress retrovirus-induced ROS induction. Thus, the absence of ATM (141) as well as p53 (Figure 2.13) exposes cells constantly to higher levels of ROS, resulting in dysregulation of normal cellular processes. Indeed, treatment of mice with anti oxidants extend the life span of cancer-prone *p53*^{-/-} and *Atm*^{-/-} mice as well as *ts1*-infected mice (55, 94, 145, 157, 158). A recent study has shown

that a mutation of a critical cysteine residue involved in disulfide bond formation specifically blocked ATM activation upon ROS treatment without interruption of ATM activation upon DNA damage, suggesting a specific role of ATM in the response to ROS (147).

Furthermore, p53 activation by ATM has been shown to protect DNA from exposure to higher ROS levels, rather than repair DNA damage in response to oxidative stress (159).

Our study raises two important questions regarding ROS upregulation during *ts1* infection. The first is; what is the source of ROS upregulation during the early phase of *ts1* infection? Although the mechanism by which retrovirus triggers ROS production is at present unclear, one of the possible candidates is NOX, which transfers electrons from NADPH to O_2 producing O_2^- . In Chapter 3, we show NOX activation during *ts1* infection. Interestingly, NOX activation also occurs in HIV infection (160, 161, 162) and overexpression of SOD, which converts O_2^- to H_2O_2 , delays neurodegeneration in the HIV mouse model (137). We speculate that ROS upregulation by NOX may be crucial for retroviral establishment in host cells. The second question is; what is the role of p53 in the response to increased ROS levels in retrovirus-infected cells? We demonstrated that lack of p53 increases intracellular ROS levels in astrocytes. We suspect that p53 may induce transcription of antioxidant genes, including GSH-generating enzyme GLS2, or NADPH-inducing enzyme TIGAR. However, we subsequently found no significant changes in GLS2 and TIGAR gene transcription in *ts1*-infected astrocytes and *ts1*-infected mouse brain (data not shown). Although SOD1 is induced by *ts1* infection during the early phase of infection, we observed that the absence of p53 does not prevent SOD1 induction (data not shown). As an alternative, we hypothesized that p53 may suppress prolonged pro-oxidant gene expression. In fact, we observed suppression of the protein levels of NOX catalytic subunit by p53 in *ts1*-infected astrocytes (Figure 2.15). We also observed earlier viral protein expression in p53-deficient astrocytes compared to wild type cells (Figure 2.14), suggesting that sustained ROS upregulation by NOX may potentiate viral gene transactivation

employed by *ts1*. Similarly it has been reported that p53 overexpression inhibits HIV-1 transcription at viral long terminal repeat (LTR), although p53 is unlikely to bind viral LTR directly (163, 164). Early treatment with NAC or upregulation of Nrf2 suppresses Tat-induced HIV-1 LTR transactivation (165). The delay in virus replication, however, was not due to cell death (166).

Temporal and spatial ROS regulation is involved in several important aspects of retrovirus-induced neuropathogenesis. Previously, ROS upregulation has been assumed to be associated with cytopathic effects. We observed that high ROS levels from the mitochondria appeared to be connected to *ts1*-induced cell death whereas low levels of ROS upregulation in the cytoplasm is associated with early viral establishment before transcription of viral gene integrated in the host genome (Figure 2.2, Figure 2.3). Therefore, suppression of the initial phase of ROS upregulation may provide an effective strategy for preventing retroviral establishment in the host genome. Furthermore, regulating the levels of ROS can be a key determinant of viral latency and replication in astrocytes. Previously *ts1* has been shown to have enhanced replication in the CNS compared to its parental MoMuLV-TB WT (43). The higher viral titer of *ts1* compared to MoMuLV-TB WT in the CNS seems to correlate with higher ROS production elicited by *ts1* infection (5) and the treatment of an antioxidant, galavit (GVT) or monosodium luminal (MSL), reduces *ts1* virus amounts in the CNS (94). In this study, we demonstrated that higher basal level of ROS due to the absence of p53 facilitates viral gene expression. Most importantly, ROS upregulation in *ts1*-infected astrocytes likely has profound effects on the microenvironment of neurons. Astrocytic support is crucial to neuronal protection from ROS damage in various neurodegenerative disease models (54, 167, 168, 169). *ts1* infection causes thiol depletion in astrocytes (5). In a previous study in our laboratory, minocycline treatment prevented death of cultured astrocytes infected by *ts1* through oxidative stress attenuation without affecting virus titers. Furthermore, minocycline prevented death of primary neurons when

cocultured with *ts1*-infected astrocytes through ROS suppression and Nrf2 promotion (126). In summary, we propose that a better understanding of the retrovirus-induced upregulation of ROS in the context of virus-host cell interaction may lead to improved treatment strategies for retrovirus-induced neurodegeneration. Effective targets for pharmacological and transgenic antioxidant therapies will require further investigation.

Chapter 3. *ts1* infection activates NOX in the early stage of virus life cycle

3.1. Introduction

In Chapter 2, we divided the *ts1* life cycle in astrocytes into the pre-integration and post-integration phases based on viral gene integration into the host genome. The integrated viral gene transcription begins at approximately 8 hpi. In the post-integration phase, the newly synthesized translated *ts1* Env protein cannot be properly folded. As a result of misfolding, it is accumulated in the ER, leading to ER stress and eventually to cell death. We observed at least two different phases of ROS upregulations in *ts1*-infected astrocyte cultures. The first one occurs during early retroviral establishment (pre-integration phase). The early ROS upregulation is relatively low compared to the ROS levels in the late phase and is unlikely to be released from the mitochondria or ER (Figure 1.4). On the contrary, the second ROS upregulation appears to be due to O_2^- released from the mitochondria while the cell death pathway is activated. We hypothesized that the first stage of ROS upregulation is caused by NOX and that the early increase in ROS may be involved in the early establishment of retrovirus in the host cells.

3.1.1. NOX in *ts1*-induced neurodegeneration

A great deal of research has focused on NOX because it was the first inducible system identified with intended ROS generation. Conversely, O_2^- production in the mitochondria is an unintended output as a byproduct of energy metabolism. Use of cell-free systems led to the discovery of the different roles for NOX subunits, $p47^{phox}$, $p67^{phox}$, Rac and $p40^{phox}$. The current working model of the NOX complex is as follows: phosphorylation of $p47^{phox}$ leads to a conformational change allowing its interaction with $p22^{phox}$, which in turn allows $p47^{phox}$ to bring $p67^{phox}$ into contact with catalytic subunit $gp91^{phox}$. When this occurs, the GTP bound

Rac interacts with the gp91^{phox}, and subsequently interacts with p67^{phox}. The complex is capable of generating O₂⁻ by transferring electrons from NADPH to O₂ (Figure 3.1) (170).

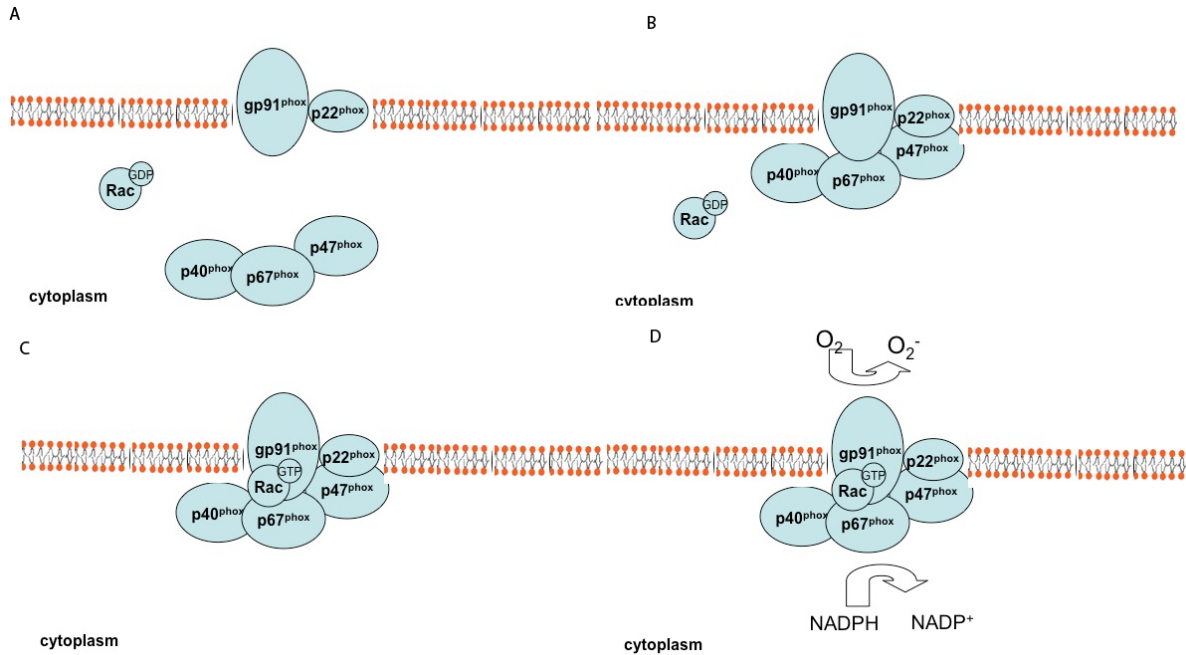


Figure 3.1. The current model of NOX complex activation in phagocytes. Upon the activation signal, the cytoplasmic subunits including p40^{phox}, p47^{phox}, p67^{phox} are translocated to transmembrane subunits (gp91^{phox} and p22^{phox}). A small GTPase protein Rac then interacts with NOX complex. Subsequently, NOX complex transfers an electron from NADPH to O₂ and generates a respiratory O₂⁻ burst in the extracellular environment.

ts1 cannot infect non-dividing neurons, however neuronal death is apparent in the *ts1*-infected CNS. There is growing evidence that ROS cause ND via non-cell autonomous mechanism (171, 172). We believe that *ts1* infection causes ROS upregulation in astrocytes. Due to that, infected astrocytes are unable to provide adequate antioxidant defenses to neurons. As a consequence, neurons may die. Previously it has been shown that antioxidant treatment prolonged *ts1*-infected mouse life span (94). Furthermore, oxidative stress caused by *ts1* infection has been established through demonstration of cysteine depletion in brain stem tissue slice culture (Lungu Gina, unpublished data) and decrease of GSH levels in *ts1*-infected astrocyte culture (5). However, until now, the source of ROS production in *ts1*-infected astrocytes was unclear. In this study we demonstrate that activation of NOX is one of the sources of ROS production in *ts1*-infected astrocytes and that NOX activation is unlikely to play a direct role in *ts1*-mediated astrocytic cell death. Furthermore, NOX appears to play an important role in viral gene integration into the host genome. Consistent with the results from *in vitro* experiments, we also observed decreased viral replication and delayed onset of neuropathological symptoms in *ts1*-infected mice when the mice were treated with NOX inhibitor.

3.2. Materials and Methods

3.2.1. NOX activity assay

To determine NADPH levels in the cytoplasm, NADPH assay kit (BioVision, CA) was used following instruction of manufacturer. Briefly, cells were trypsinized and washed with PBS following apocynin treatment. NADPH is extracted from the cell pellets (5×10^5 cells) and incubated with an enzyme mixture and colormetric developer for 1 hour at 37°C. After reaction, the reaction mixtures assayed at Abs450nm using a plate reader. NADPH (0, 20, 40, 60, 80, 100 pmol) was also incubated with an enzyme mixture and the developer to plot

the NADPH standard curve (data not shown). To measure the relative amount of O_2^- production, the same number of cells (1×10^4 cells/per well) were placed in 24-well plate and infected with *ts1*. Following infection, cells were washed with PBS and incubated with 50mM oxidized cytochrome c (Sigma Aldrich) in PBS (pH 7.4) for 1 hour at 37°C. The absorbance at OD550 was measured before and after the reaction, and the change of Abs550 was calculated. As a negative control, 5 units of purified SOD (Sigma Aldrich) were added with oxidized cytochrome c. To detect O_2^- levels in the CNS, DHE was applied to uninfected mice or 30 days post *ts1* infected mice as described (53). Briefly, two serial intraperitoneal injections of freshly prepared dihydroethidium (DHE) (Molecular Probes, Eugene, OR) (27 mg/kg) were given at 30 minute-intervals. After 18 hours, mice were perfused intracardially with cold saline followed by 4% paraformaldehyde in PBS for immunohistochemistry experiments. The whole brain is incubated in 30% sucrose solution overnight and frozen in optimal cutting temperature (OCT) embedding medium (Sakura Finetek, Inc., Torrance, CA) for frozen-section for immunohistochemistry

3.2.2. Apocynin treatment to *ts1*-infected mice.

To test the animal affect of apocynin treatment on *ts1*-mediated neuropathogenesis, mouse pups at 2 days post natal were infected with *ts1* and divided into two groups, one group receiving normal saline and the other receiving freshly prepared 100mg/kg of apocynin (Sigma Aldrich) (amount/body weight) delivered intraperitoneally for five continuous days per week, followed by two resting days. Mice from all groups were checked daily for clinical signs of disease and sacrificed when moribund and paralyzed. All animal procedures were performed according to protocols approved by The University of Texas M. D. Anderson Cancer Center Institutional Animal Care and Use Committee.

3.2.3. Tissue virus titer assay

The virus titer assay was performed as described in (94). Briefly, brainstems were removed at 30 days post infection (dpi), snap-frozen in liquid nitrogen and kept frozen until they were used. Frozen brainstem tissues were weighed and then homogenized (40 strokes) (Kontes Glass Co., Vineland, NJ) in 2 ml ice-cold basal DMEM. Cell debris was removed by filtration through a 0.45- μ m syringe filter (Pall Corporation, Ann Arbor, MI). The titers (IU/ml) of *ts1* in these lysates were determined using a modified 15F assay as described before. The titer of virus was taken as the average titer from three to six mice.

3.2.4. Immunohistochemistry and immunocytochemistry

For immunohistochemistry, frozen mouse brain tissues were sliced into 6 μ m sagittal sections encompassing the brain stem region. Brains tissue slices were washed in PBS and incubated in 5% normal donkey serum in PBS/0.1% Triton X-100 for 1 hour at room temperature. Primary antibodies (GFAP: 1: 200, NeuN: 1:1000, and p30^{capsid}: 1:500,) were diluted in 5% normal donkey serum in PBS and applied to the slices for one hour at room temperature, after which the slices are washed in PBS and incubated in a 1:500 dilution of TexasRed conjugated donkey anti-goat IgG or Fluorescein isothiocyanate (FITC)-conjugated donkey anti-mouse IgG antibodies for one hour at room temperature and mounted sequentially in glass slides using prolong antifade reagent containing 4',6-diamidino-2-phenylindole (DAPI) (Molecular Probes, Eugene, OR).

Uninfected control or *ts1*-infected C1 cells were placed on poly-L-lysine coated coverslips and fixed in 4% paraformaldehyde for 20 minutes, then washed with PBS. The fixed cells were incubated in PBS containing 0.05% Tween 20 and 5% donkey serum for 30 minutes and washed with PBS. The coverslips were then incubated with goat anti-gPr80^{env}/gp70^{env} antibody followed by anti-goat IgG secondary antibody conjugated with Texas Red (Jackson ImmunoResearch, West Grove, PA). As an immunostaining control,

mouse anti- β tubulin antibody (Sigma Aldrich) and anti-mouse IgG secondary antibody conjugated with FITC (Jackson ImmunoResearch, West Grove, PA) were used. The stained coverslips were mounted on slide with Prolong anti-fade mounting reagent (Molecular Probes, Eugene, OR) containing DAPI.

3.2.5. Genomic DNA preparation and quantitative PCR

C1 astrocytes were infected with *ts1* at a MOI of 5. The control group was not treated with any drug, and the other two groups are treated either with 10mM NAC or 1mM apocynin. mRNA was extracted using RNeasy extraction kit and Oligotex, following the manufacturer's instruction (Quiagen, Valencia, CA). Genomic DNA was purified using the genomic DNA extraction kit, following the manufacturer's instruction (Promega, Madison, WI). High Capacity cDNA Archive kit (Applied Biosystems, Foster City, CA) was used to synthesize cDNA and qPCR was subsequently performed on the ABI 7900HT Fast Real Time PCR system with primers specific to *ts1* gPr80^{env} using SYBR Green master mix (BioRad, Inc. Hercules, CA) (173). RNA levels were normalized to the endogenous house-keeping gene GAPDH. The experimental Ct was calibrated against the GAPDH control product and ddCt method was used to determine the amount PCR product relative to that of RNA or genomic DNA purified from uninfected cells

3.3. Results

3.3.1. Cellular distribution of NOX subunits in astrocytes

The current model of NOX activation is based on phagocytic cells. It is known that catalytic subunit gp91^{phox} is localized at the plasma membrane. Upon translocation of cytoplasmic subunit p47^{phox} to the membrane, its partner p67^{phox} is also translocated to the membrane and turns on the catalytic activity of p91^{phox}. We examined p67^{phox} and p47^{phox}

localization in our system to verify NOX activation after *ts1* infection. C1 cells were lysed after *ts1* infection, and fractionated into four different subcellular fractions; cytoplasmic, membrane, soluble nuclear and chromatin bound insoluble nuclear fractions. As expected, gp91^{phox} was nonetheless localized at the membrane fraction in any case and p47^{phox} existed predominantly in the cytoplasm of uninfected cells (Figure 3.2). To our surprise, we observed that p67^{phox} was primarily localized at the membrane instead of the cytoplasm regardless of the status of *ts1* infection in the astrocytes. It is noteworthy that the membrane fraction includes not only integral proteins at the plasma membrane but also proteins from membrane bound organelles, such as the ER and mitochondria. Following *ts1* infection, p47^{phox} is translocated from the cytoplasm to the membrane as shown in Figure 3.2. We also observed p47^{phox} protein band shift in western blotting analysis, suggesting posttranslational modification. This lower band of p47^{phox} only appeared when cells were infected with *ts1*. At present we do not know whether the localization of p67^{phox} at the membrane is a characteristic specific to astrocytes.

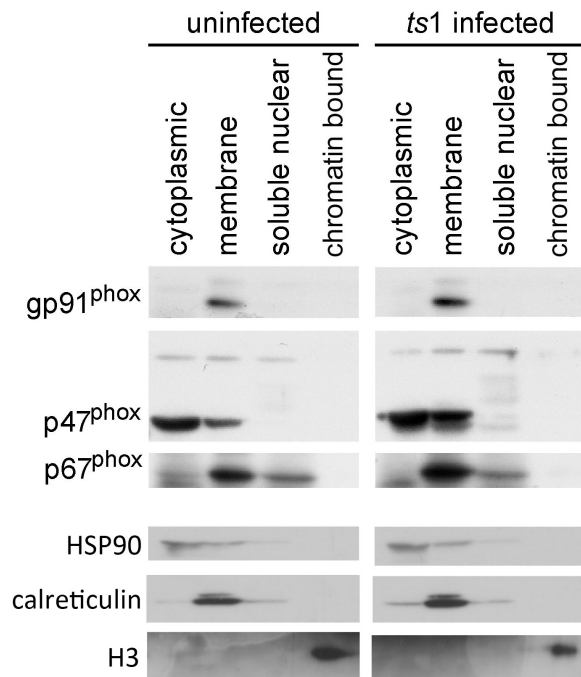


Figure 3.2. Cellular distribution of NOX subunits in C1 astrocytes.

C1 cells were lysed after *ts1* infection and fractionated into four different subcellular fractions, cytoplasm, membrane, soluble nuclear and chromatin bound insoluble nuclear fractions. gp91^{phox} and p22^{phox} are nevertheless localized at the membrane fraction. p47^{phox} exists predominantly in the cytoplasm of uninfected cells and translocates to the membrane after *ts1* infection. p67^{phox} is primarily localized at the membrane instead of the cytoplasm regardless of the status of *ts1* infection status in the astrocytes. To verify the fractionation, anti-HSP90 (cytoplasmic), calreticulin (membrane) and H3 (chromatin bound) antibodies were used followed manufacture's information.

3.3.2. NOX is activated in *ts1*-infected astrocytes

As mentioned above, p67^{phox} in astrocytes is already located at the membrane regardless of *ts1* infection. Therefore, we could not verify NOX activation by the activator of catalytic subunit gp91^{phox}, p67^{phox} translocation in *ts1*-infected astrocytes as seen during NOX activation from other systems (174). Therefore, we first needed to develop NOX enzyme activity assays. Although we observed p47^{phox} translocation, it was still not clear whether post-translational modification and translocation of p47^{phox} are directly related to NOX activation. The activated NOX complex consumes NADPH in the cytoplasm, and transfers electrons to oxygen, thereby generating O₂⁻. This sequence of events allows us to detect the change of NOX activity by measuring the substrate (NADPH) and product (O₂⁻) of NOX to determine whether *ts1* infection of astrocytes activates NOX (Figure 3.3). We compared NADPH levels in *ts1*-infected astrocytes to levels in uninfected astrocytes. As shown in Figure 3.3, the NADPH levels were decreased in *ts1*-infected astrocytes. The results showed that *ts1*-infected cells treated with NOX inhibitor, apocynin, had unchanged NADPH levels, suggesting that decreased NADPH in *ts1*-infected astrocytes is due to NOX activation. We then investigated if *ts1*-infected astrocytes change O₂⁻ production in living cells. The heme group in cytochrome c preferentially accepts singlet electron from O₂⁻. Reduced cytochrome c was measured by the increase in absorbance at 550nm. Therefore, this reaction provides a useful tool to distinguish O₂⁻ from other ROS. We added oxidized cytochrome c to uninfected and *ts1*-infected astrocytes and then measured the change of Abs550 after incubation with oxidized cytochrome c (Figure 3.3). We observed increased O₂⁻ in *ts1*-infected astrocytes compared with those in uninfected astrocytes. We added purified SOD as a control sample. We hypothesized that if *ts1* infection causes O₂⁻ production, the extracellular O₂⁻ can be immediately converted to H₂O₂ by SOD. We confirmed that there would not be singlet electron transfer to cytochrome c in the *ts1*-

infected astrocytes with SOD. Together these results suggest that NOX is activated by *ts1* infection and releases O_2^- to the extracellular microenvironment (Figure 3.3).

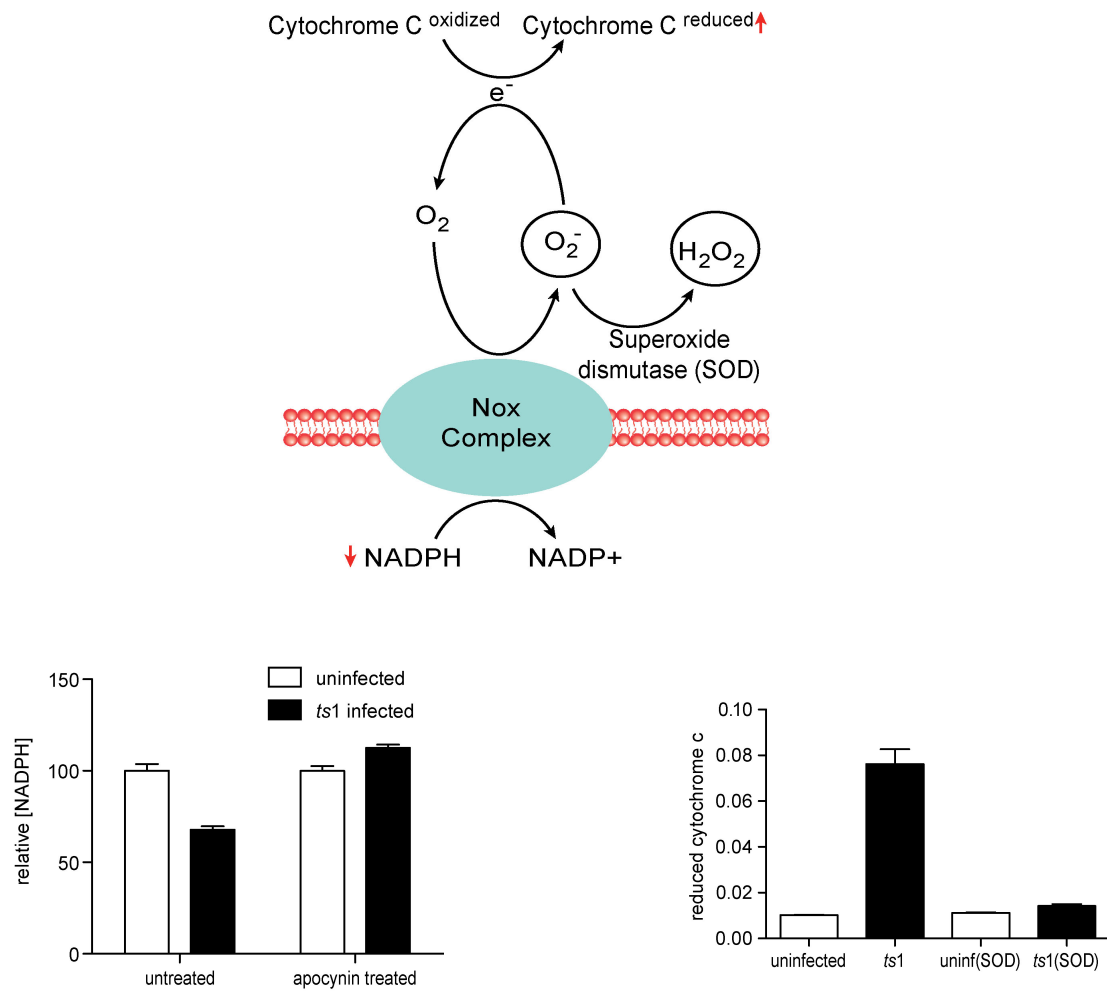


Figure 3.3. NOX activation in *ts1*-infected astrocytes.

The schematic diagram of experimental design (top). The heme group in cytochrome c preferentially accepts singlet electron from O₂⁻ and reduced cytochrome c was measured by the change in absorbance at 550nm. NADPH levels decreased in *ts1*-infected astrocytes. Apocynin treatment reverses NADPH levels. O₂⁻ production is upregulated in *ts1*-infected astrocytes compared with that in uninfected astrocytes. O₂⁻ production disappears with the addition of SOD in the medium.

3.3.3. NOX activation occurs in early phase of *ts1* infection

In Chapter 2, we observed two distinct phases of ROS upregulation in *ts1*-infected astrocytes. The first phase of ROS upregulation occurred at 4-8 hpi coinciding with early viral establishment followed by a second phase during cell death (48 hpi). Therefore, we further investigated NOX activities focusing on the phases of infection. As shown in Figure 3.4, the substrate of NOX (NADPH) was decreased at 4-24 hpi. However, O_2^- production was increased only at 24 hpi, but not at 4 hpi in the extracellular environment (Figure 3.5). Considering that H_2O_2 levels measured by DCF fluorescence were upregulated only at 4-8 hpi but not at 24 hpi (Figure 2.3), we suspected that intracellular SOD might attempt to reduce the upregulated O_2^- immediately by converting O_2^- to H_2O_2 after *ts1* infection. Indeed, we observed higher levels of SOD levels in the cytoplasm at 2 and 4 hpi (Figure 3.6). To investigate if there was any change in local distribution of SOD at 4 hours in *ts1*-infected cells, we immunostained uninfected and *ts1*-infected astrocytes using anti-SOD antibody. Upregulated SOD is accumulated in the perinuclear area at 4 hpi in *ts1*-infected astrocytes whereas SOD in uninfected cells distributes evenly throughout the cytoplasm (Figure 3.7). Corresponding to SOD redeployment, we do not observe H_2O_2 levels increase at 24 hpi following *ts1* infection (data not shown). It appears that early activation of NOX coincides with the redistribution of SOD in the early phase of infection. Once the virus establishes its presence in the host genome, SOD rearrangement did not occur any more although extracellular O_2^- production increased at 24 hours after *ts1* infection. We did not observe any changes in the levels of NADPH at 48 hpi following *ts1* infection, suggesting that NOX activation is not involved in the apoptotic process after *ts1* infection.

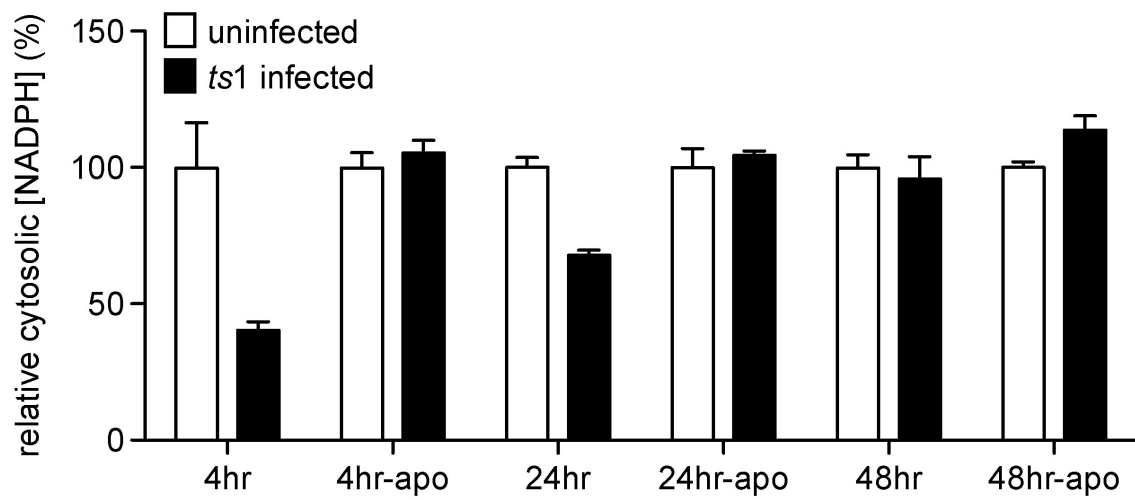


Figure 3.4. Measurement of intracellular NADPH levels during *ts1* life cycle

Cellular NADPH levels were measured from the cells collected as time indicated after *ts1* infection as described in Material and Methods. NADPH levels are decreased at 4-24 hpi, however there was no difference in 48 hpi regardless of *ts1* infection status. Treatment of apocynin reverses NADPH consumption in *ts1*-infected cells.

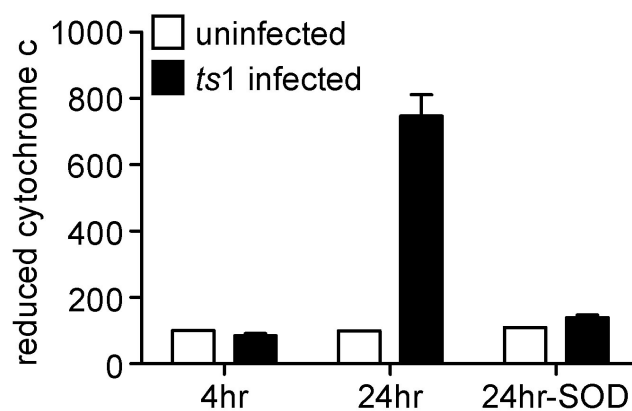


Figure 3.5. Measurement of extracellular O_2^- production during *ts1* life cycle.

Extracellular O_2^- levels were measured after *ts1* infection as described in Material and Methods. O_2^- production is increased only at 24 hpi, however no difference at 4 hpi.

Addition of SOD in the culture reverses O_2^- production.

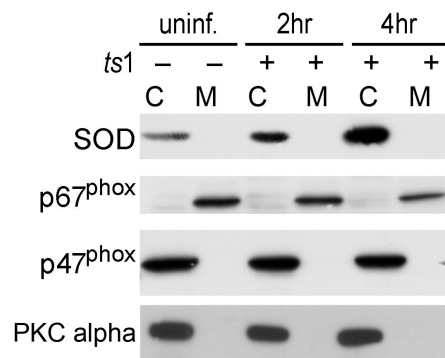


Figure 3.6. SOD upregulation in the early phase of *ts1*-infection.

The levels of intracellular SOD are increased in the cytoplasm at 2 and 4 hpi but there are no changes in levels of p47^{phox} and p67^{phox}. C and M represent cytoplasmic and membrane fractions. PKC α (cytoplasmic protein) was used for protein loading control.

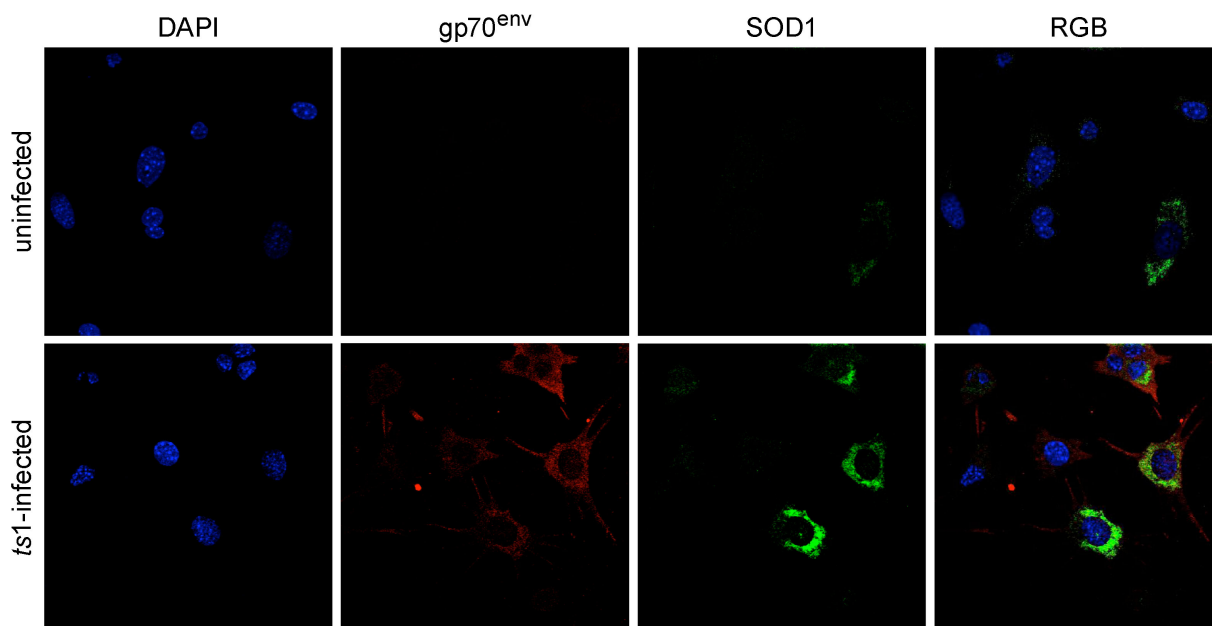


Figure 3.7. Redistribution of SOD during the early phase of *ts1* infection.

SOD was immunostained using anti-SOD antibody in uninfected and *ts1*-infected astrocytes. Upregulated SOD is accumulated in the perinuclear area at 4 hpi in *ts1*-infected astrocytes (blue, DAPI; red, gp70^{env}; green, SOD1).

3.3.4. O_2^- upregulation by NOX activation may enhance viral gene integration into host genome.

It is possible that NOX activation in the early phase of *ts1* infection may be a “priming” process to turn on intracellular signal transduction pathways that are necessary for viral establishment in the host genome. In other words, ROS upregulation by NOX activation at the membrane after initial contact with viral envelope protein may not have a completely detrimental effect on the cells in causing cell death because NOX activation is not detected in the last phase of infection. We hypothesized that NOX activation at the early phase of virus infection may facilitate the integration of viral DNA into the host genome. In Chapter 2, we observed that viral gene transcription from the integrated viral genome started approximately at 8 hpi (Figure 2.1). Along with intracellular ROS, particularly H_2O_2 , at 4-8 hpi following *ts1* infection, SOD redistribution at the perinuclear area suggests that H_2O_2 converted from O_2^- by SOD may allow viral DNA to access the host nucleus. To investigate whether ROS upregulation by NOX activation is involved in early viral establishment in the host genome, we treated *ts1*-infected C1 cells with apocynin or NAC. We then investigated viral *env* DNA from purified host genomic DNA using qPCR analysis. As shown in Figure 3.8, genomic DNA purified from apocynin or NAC-treated, *ts1*-infected cells contains significantly lower viral *env* gene compared to that from untreated *ts1*-infected cells. We also observed that apocynin-treated cells have lower *env* transcription, which further supports the concept of decreased viral gene integration into the host by inhibition of NOX.

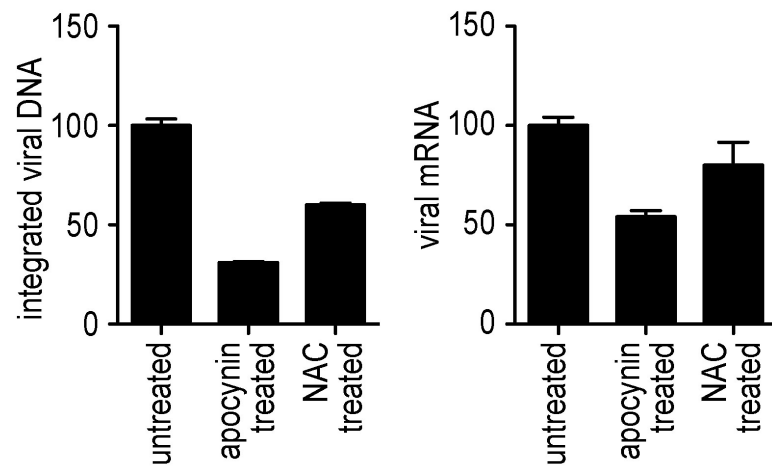


Figure 3.8. Inhibition of NOX decreased viral establishment into the host genome

ts1-infected C1 cells were treated with apocynin or NAC. Viral *env* DNA integrated into the host genomic DNA was quantified using qPCR. Genomic DNA purified from apocynin or NAC-treated cells had significantly lower viral *env* gene compared to that from untreated cells. Apocynin-treated cells shows lower *env* transcription, supporting decreased viral gene integration into the host by inhibition of NOX.

To validate that the *in vitro* result shown here correlates to the *in vivo* results from the brain, we hypothesized that inhibition of NOX may decrease viral titer in the *ts1*-infected mouse brain. We infected two groups of mice with *ts1*, one with apocynin treatment and the other without treatment. In 30 days of *ts1* infection, we dissected brain stems from untreated and apocynin treated, infected mice and performed viral titer assays. As expected, lower viral titer was observed in apocynin-treated mouse compared to untreated *ts1*-infected mouse as shown in Figure 3.9. These results suggest NOX activation is involved in early viral establishment in *ts1*-infected cells.

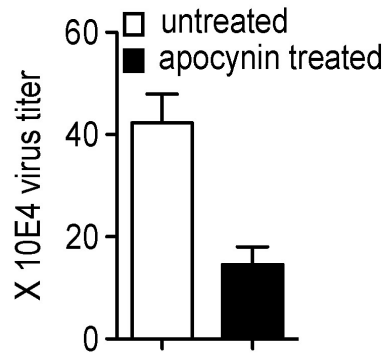


Figure 3.9. *ts1* viral titer assay in the apocynin-treated mouse CNS

Two groups of mice were inoculated with *ts1*, one with apocynin treatment and the other without treatment. After 30 days of infection, brain stems of infected mice were dissected and viral titer assays were performed using the tissues. Lower viral titer was observed in apocynin-treated mice compared to untreated *ts1*-infected mice.

3.3.5. O_2^- production increased in the *ts1*-infected mouse brain stems

To replicate retrovirus, cells must be highly proliferative. However, the quiescent environment of the CNS does not favor high viral replication. This may explain why the cytopathic effect of *ts1* infection seems much more severe *in vitro* as opposed to *in vivo*. As described above, we demonstrated that NOX is activated in *ts1*-infected astrocytes *in vitro* (Figure 3.3). However, we still do not know if NOX is activated in the *ts1*-infected mouse brain. To determine if O_2^- is increased in the *ts1*-infected brain, we injected DHE intraperitoneally into both uninfected and infected mice. DHE is a cell-permeable probe, which undergoes oxidation in the presence of O_2^- leading to the formation of fluorescent ethidium. We observed stronger DHE fluorescence in *ts1*-infected brain stems near spongiform lesions compared to normal uninfected brain stems, suggesting that O_2^- production is increased in the *ts1*-infected brain stem (Figure 3.10). Although higher DHE fluorescence was detected overall in *ts1*-infected brain stem tissues, it appeared in several distinct spots. These areas did not overlap with anti-GFAP immunostainings (Figure 3.10). To verify if DHE fluorescent cells are astrocytes (GFAP positive cells), we immunostained GFAP and labeled nuclei with DAPI. As shown in Figure 3.11, we observed that O_2^- increased in GFAP-positive cells as well as some GFAP-negative cells. Interestingly, the subcellular O_2^- detected by DHE seemed to be more concentrated in cell body near the perinuclear area where cytoskeletal GFAP was not stained (Figure 3.11). GFAP are mostly localized at the cellular periphery. GFAP-positive cells were closely localized near neurons (NeuN-positive cells) in the CNS as shown in Figure 3.12. We attempted to detect the localization of viral proteins in the *ts1*-infected mouse CNS by performing immunofluorescence using anti-p30^{capsid} antibody. GFAP-positive cells were infected by *ts1*. Viral capsids were localized in both peripheral regions and the cell body area in astrocytes (GFAP positive cells) in the *ts1*-infected mouse CNS (Figure 3.13). We also noticed that some GFAP-negative cells were infected by *ts1*. We do not know what type of cells they are

and how they contribute to the neuronal microenvironment at present.

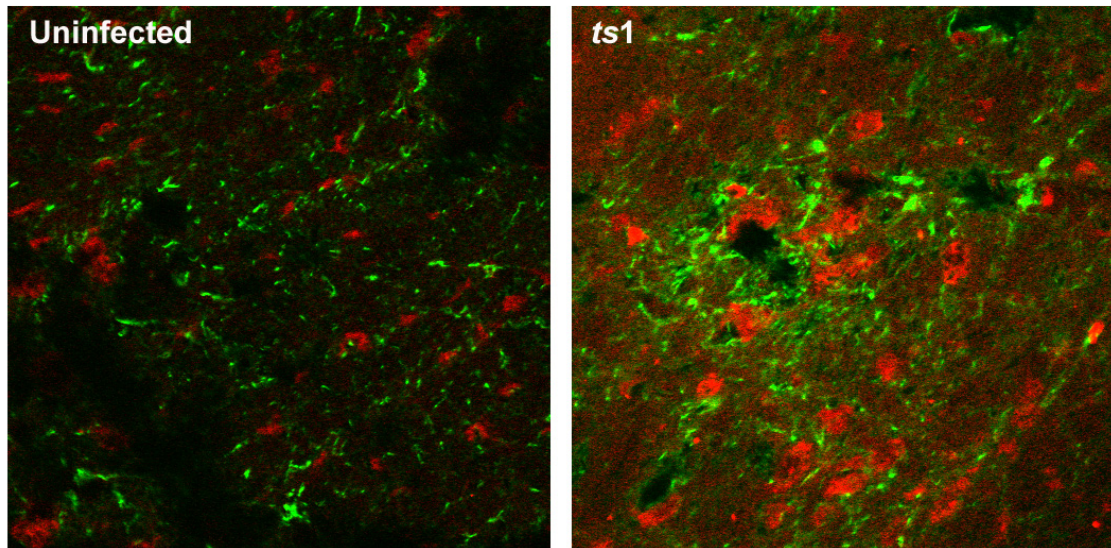


Figure 3.10. O_2^- upregulation and reactive gliosis in the *ts1*-infected CNS

Freshly prepared DHE solution was injected intravenously into both uninfected and infected mice (30 dpi). Brain stem tissue sections were fixed in paraformaldehyde and used for immunostaining using anti-GFAP (14). Stronger DHE fluorescence (red) in *ts1*-infected brain stems is shown near spongiform lesions compared to normal uninfected brain stems.

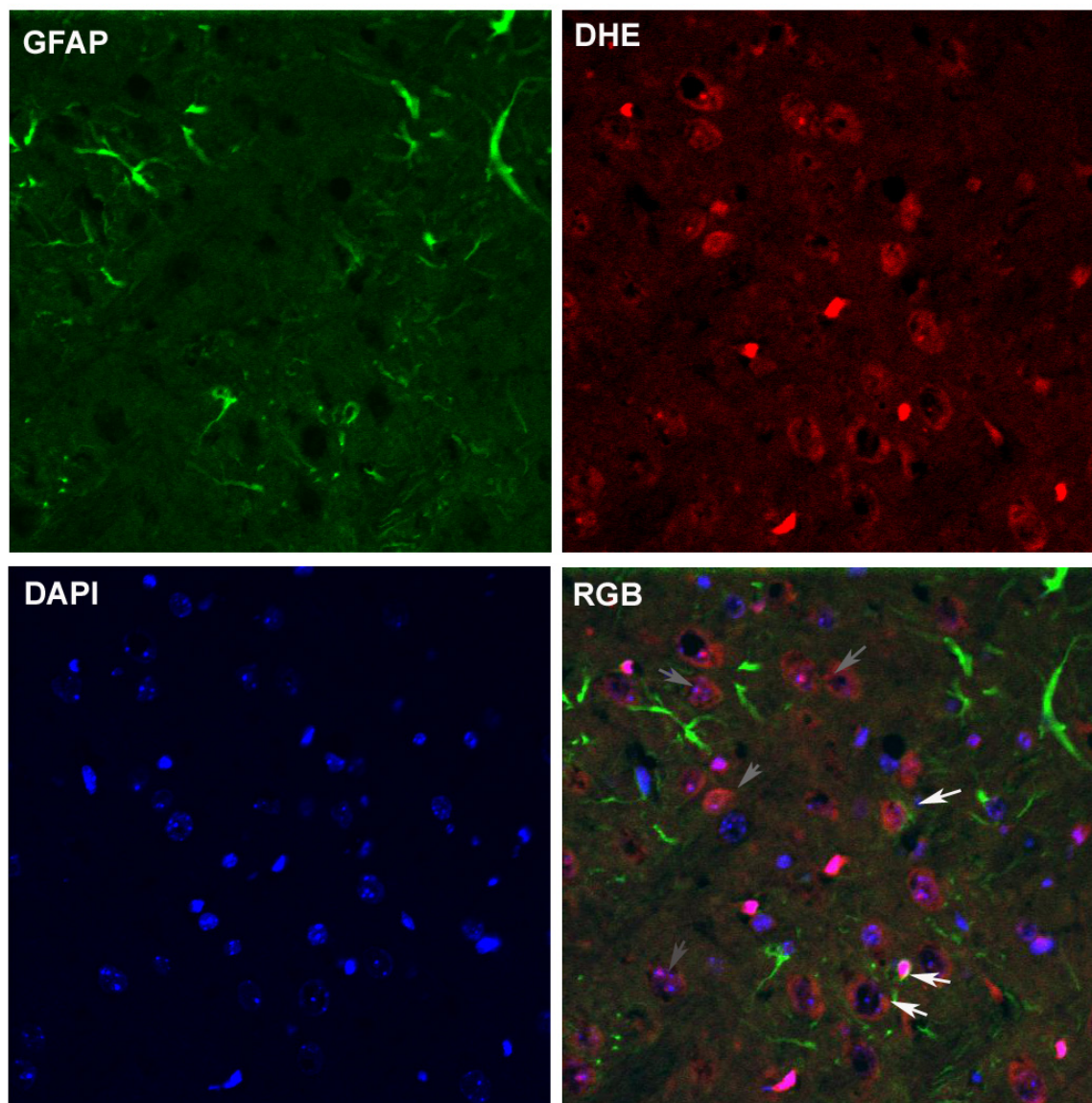


Figure 3.11. The subcellular O_2^- upregulation in the perinuclear area of the *ts1*-infected CNS cells. Brain stem tissue sections from DHE injected, *ts1*-infected mice were prepared as described in Materials and Methods, followed with immunostaining with anti-GFAP antibody. White arrows represent the GFAP positive cells with high DHE, and gray arrows represent the GFAP negative cells with high DHE. The subcellular O_2^- detected by DHE seemed to be more concentrated in cell bodies near the perinuclear area where cytoskeletal GFAP were not stained.

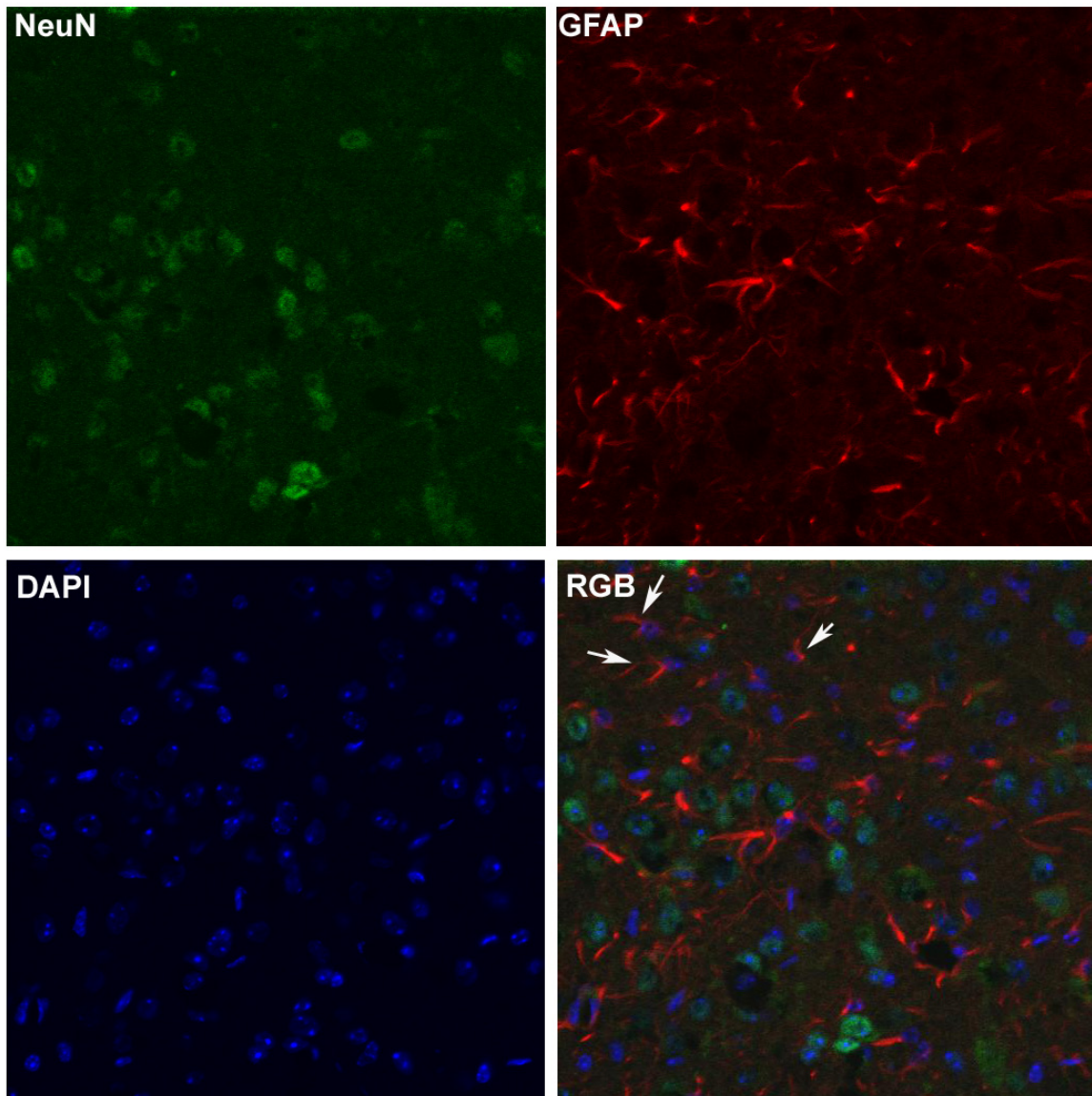


Figure 3.12. Intimate location of astrocytes and neurons in the CNS.

GFAP (red) positive astrocytes are located closely to NeuN (14) positive neurons.

Astrocytic peripheral feet stained by GFAP surrounded neurons. Blue, DAPI. The white arrows indicate astrocytes (GFAP positive, NeuN negative). The area stained with GFAP is not overlapped with DAPI stained area, indicating that GFAP is not staining perinuclear area.

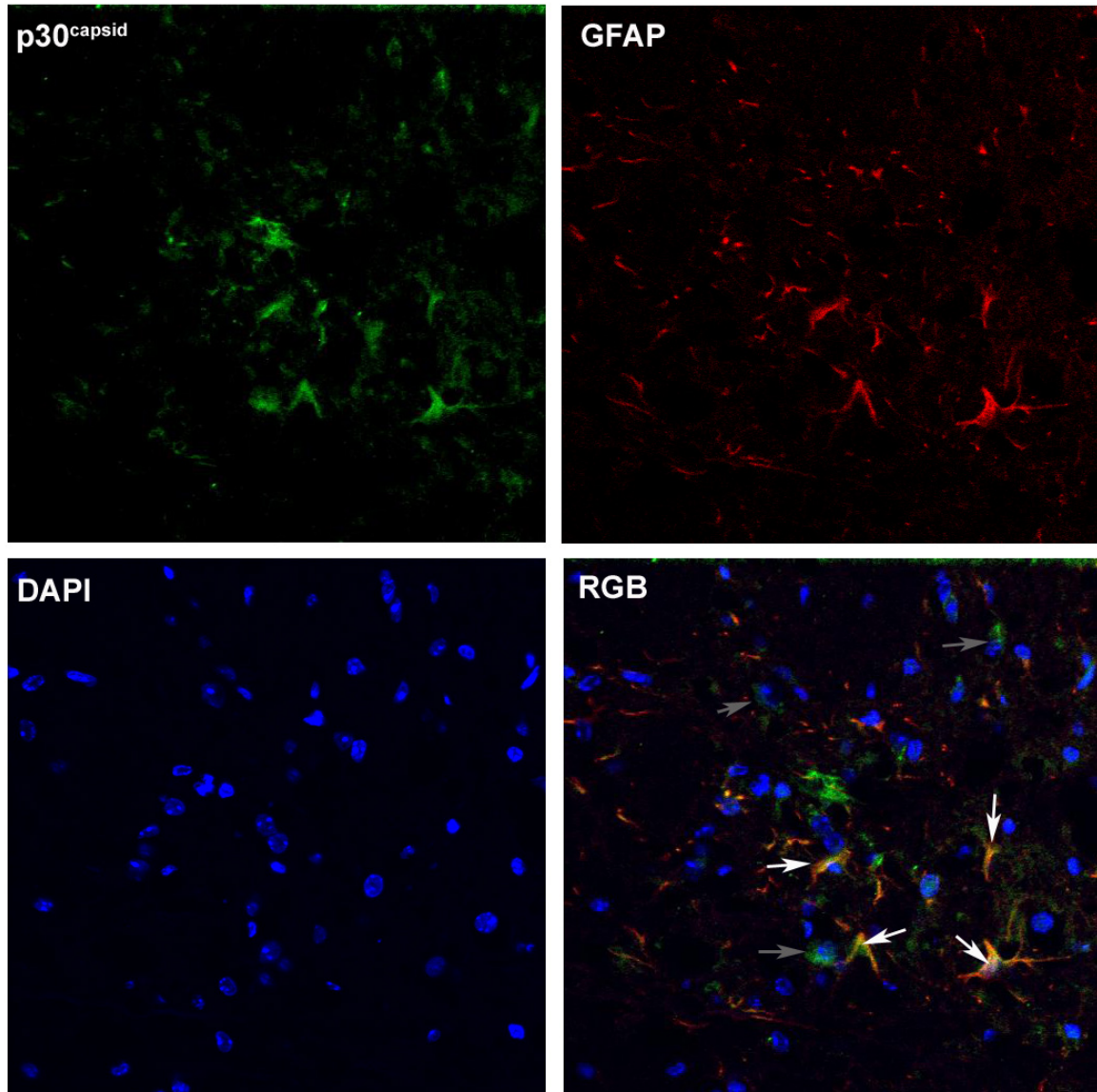


Figure 3.13. Astrocytes are infected by *ts1* in the CNS

Viral p30^{capsid} (14) were observed at both peripheral and perinuclear regions in GFAP-positive astrocytes. White arrows represent the GFAP (red) -positive cells with *ts1* infection. Gray arrows represent the GFAP-negative cells with *ts1* infection, indicating there may be either GFAP-negative astrocytes or some cell types other than astrocytes.

To verify that the O_2^- upregulation was caused by NOX activation in the *ts1*-infected brain stem, we treated the *ts1*-infected mice with apocynin. Our results showed that apocynin treatment reduced overall DHE fluorescence levels in the *ts1*-infected mouse brain stem including astrocytes (Figure 3.14). NOX was expressed in neurons and detrimental effects of NOX activation in neurons have been reported (53). To identify whether neurons have higher O_2^- levels after *ts1* infection, we immunostained brain stems of DHE-injected animals with anti-NeuN (neuronal marker) antibodies. We observed lower DHE fluorescence in NeuN positive cells in apocynin treated, *ts1*-infected mouse brain stems as compared to untreated *ts1*-infected mouse brain stems (Figure 3.15). These results suggest that NOX activation following *ts1* infection causes oxidative stress in neurons.

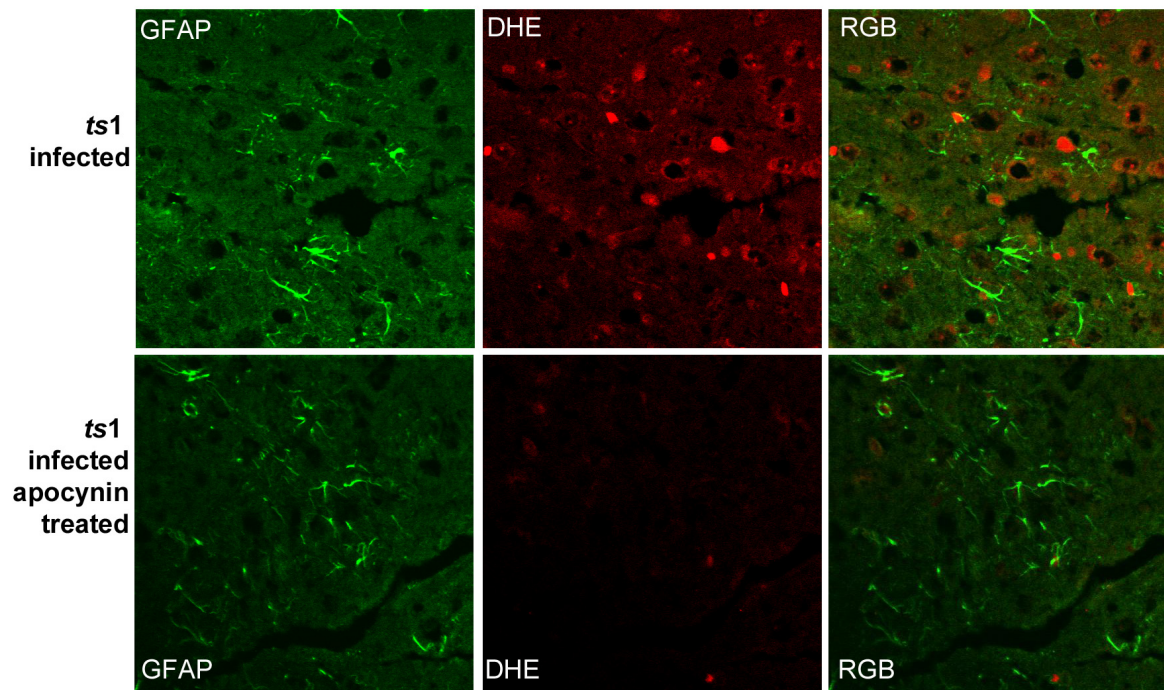


Figure 3.14. Inhibition of NOX decreased O_2^- levels in the *ts1*-infected CNS.

Freshly prepared DHE solution was injected intraperitoneally into both uninfected and infected mice. Brain stem tissue sections from the mice were prepared as described in Material and Methods followed by immunostaining using anti-GFAP (14) antibody. DHE (red) represent O_2^- and apocynin treated CNS has overall lower DHE fluorescence.

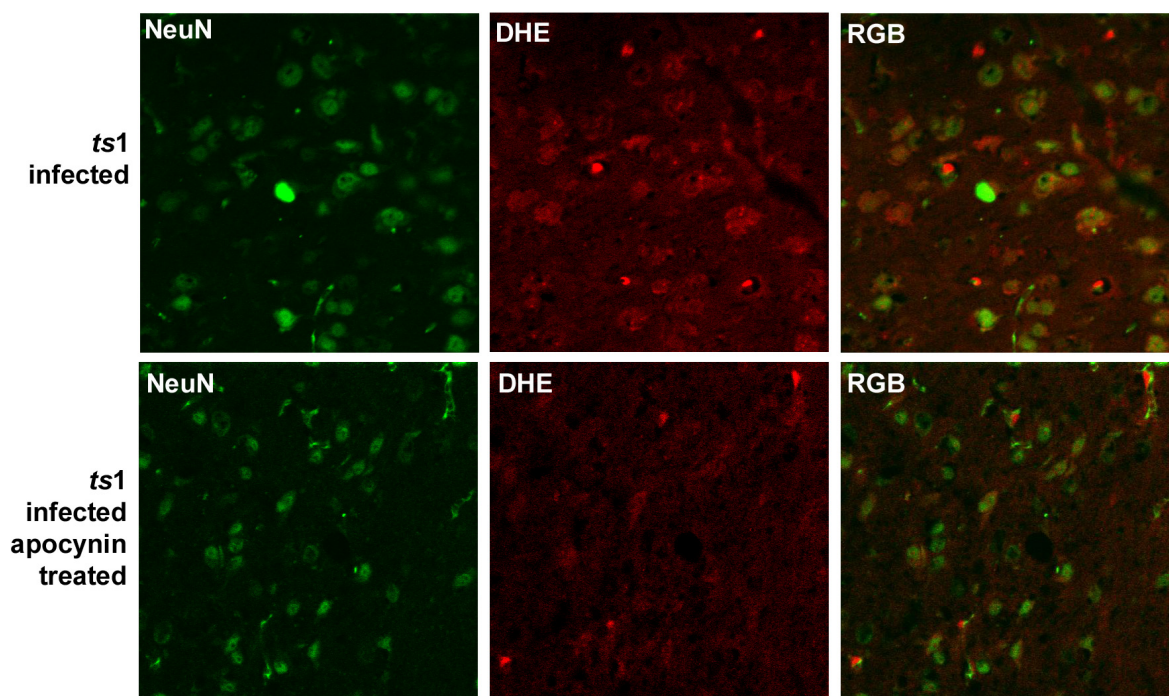


Figure 3.15. Inhibition of NOX decreased neuronal O_2^- levels in neurons of *ts1*-infected CNS. DHE injected animals were sacrificed and immunostained for NeuN (14). DHE (red) represent O_2^- and apocynin treatment decreased DHE fluorescence levels in neurons of *ts1*-infected CNS.

3.3.6. Inhibition of NOX prevents *ts1*-mediated cell death and prolongs the life span of *ts1*-infected mice

ts1 infection in astrocytes is a known cause of cell death. To investigate if the inhibition of NOX activation could prevent cell death, we treated *ts1*-infected astrocytes with apocynin. Viable cell counts of *ts1*-infected astrocytes with or without apocynin treatment confirmed that apocynin prevents *ts1*-mediated cell death significantly (Figure 3.16). Previous work from our lab has shown that *ts1* infection increases caspase-3 activation, and decreases Bcl2 levels in astrocytes (48). We questioned whether the inhibition of NOX affects cell death after *ts1* infection. To determine if NOX plays a crucial role in inducing apoptosis, we utilized pro-apoptotic and anti-apoptotic markers in *ts1* infected astrocytes cultures. Our results showed that NOX inhibition increased Bcl-2 levels, and decreased activated caspase 3 levels. These results suggest that inhibition of NOX decreases *ts1*-mediated astrocytic death. This may be due to suppression of viral replication as shown in Figure 3.9. Furthermore, inhibition of NOX with apocynin treatment extends life span of *ts1*-infected mice, as shown in Figure 3.18. *ts1* has a more potent cytopathic effect than MoMuLV-TB WT. Although MoMuLV-TB WT has a cytopathic effect on astrocytes, lesions in the WT-infected brain are much less severe when compared to those in the *ts1*-infected brain. WT virus does not cause neuropathological symptoms in mouse, such as hind limb paralysis (34). The neurovirulent effect of *ts1* is due to the accumulation of misfolded viral *env* protein in the ER resulting in UPR and resulting in cell death. To determine if NOX inhibition affects *ts1*-induced UPR, we treated *ts1*-infected astrocytes with apocynin and examined BiP as an indicator of the ER stress. Apocynin treatment did not change BiP upregulation despite low viral replication as shown in Figure 3.17 and Figure 3.8, indicating that O₂⁻ generation by NOX activation and UPR are likely to be triggered by separate signaling pathways. It is noteworthy that gPr80^{env} processing was improved in p53^{-/-} PACs (Figure 2.15). We suspect that gp91^{phox} upregulation due to the absence of p53 may facilitate protein folding.

By suppressing NOX, gPr80^{env} folding may be less efficient despite less viral replication.

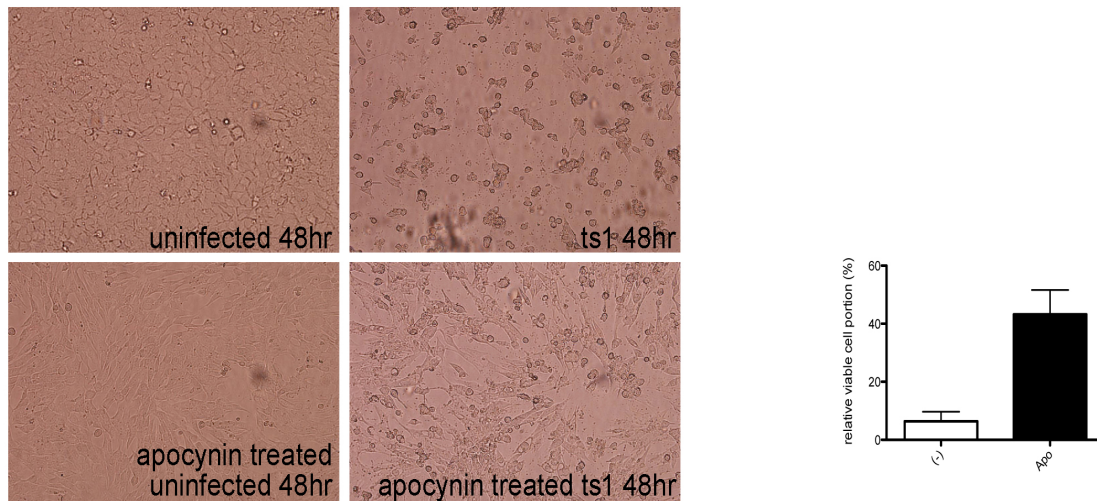


Figure 3.16. Inhibition of NOX activation prevented *ts1*-mediated astrocytic cell death.

Viable cell number was counted from *ts1*-infected astrocyte culture with or without apocynin treatment and then compared with the cell number of uninfected controls. The value of percentile of infected cells are presented. $p < 0.05$ when apocynin treated cells compared with untreated $p53^{-/-}$ PAC cells.

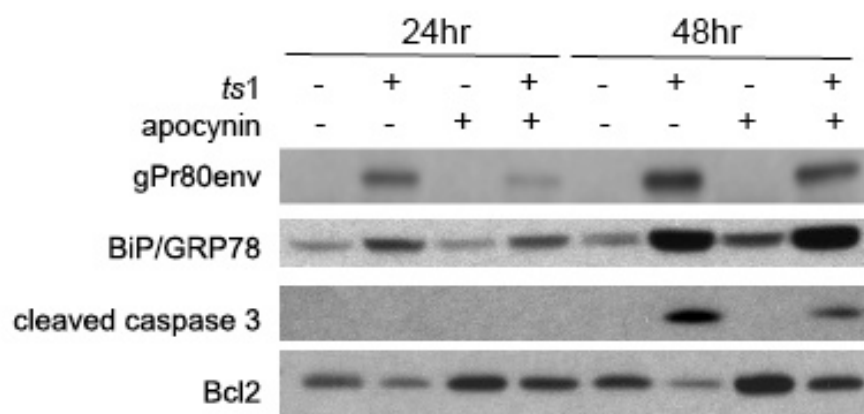


Figure 3.17. Inhibition of NOX suppressed *ts1*-mediated apoptosis, but not the ER stress. The cell lysates showed increased Bcl-2 and decreased activated caspase 3 levels in *ts1*-infected astrocytes by apocynin treatment. However apocynin treatment did not change the expression of gPr80^{env} and BiP, suggesting no difference in ER stress caused by *ts1* infection.

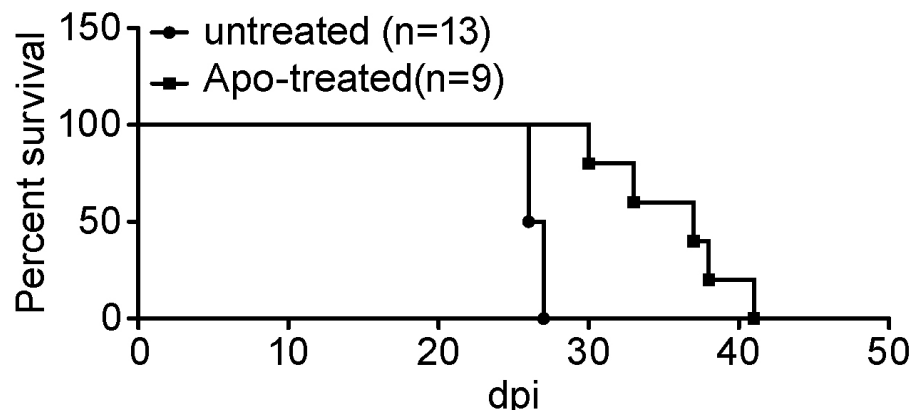


Figure 3.18. Inhibition of NOX activation extended the life span of *ts1*-infected mice.

Twenty two mice were infected with *ts1*. 2 days after birth then divided into two groups. 3 days after *ts1* inoculation, nine mice received intraperitoneal injections of 100mg/kg of apocynin, and the other thirteen mice received the same volume of normal saline.

Treatment was continued for 5 days/week (p value<0.01).

3.4. Discussion

As mentioned before, *ts1* cannot infect neurons. However, neurons die as a result of *ts1*-infection in the mouse brain. The infection of astrocytes causes neuronal cell death as evidenced by neuron-astrocyte coculture experiments (126). In Chapter 2, we observed ROS upregulation at 4-8 hpi in astrocyte culture. This occurs in the early phase of retrovirus infection and we hypothesized that this ROS upregulation was associated with retroviral establishment in the host genome. The ROS are unlikely to come from the mitochondria or ER. Instead, we suspect that early ROS upregulation is accomplished by NOX activation. In this Chapter, we investigated activation of NOX in *ts1*-infected astrocytes and attempted to correlate the phenomena to ND in *ts1*-infected mouse.

Until recently, little was known about the role of NOX in the CNS and NOX was primarily studied in immune cells. However, recent studies demonstrate that NOX components are expressed in non-immune cells including astrocytes and neurons (53, 54). Studies from Chapter 2 and 3 show that not all ROS are equivalent. The temporal (4, 24, and 48 hpi) and spatial (mitochondria, cytoplasm, extracellular microenvironment) ROS appear to be controlled by different cellular sources. We demonstrated NOX activation in *ts1*-infected astrocytes by measuring the levels of NADPH (substrate) and O_2^- (product). The data clearly indicate that NOX activation occurs between 4 to 24 hpi in *ts1*-infected astrocytes, which is independent of the *ts1*-mediated cell death process. Furthermore, distribution of cellular ROS scavenging enzymes also impacts local ROS signaling initiated by O_2^- production (47). We found that intracellular H_2O_2 upregulation at 4 hpi is likely due to upregulation of both NOX and SOD1 whereas O_2^- upregulation at the plasma membrane at 24 hpi is due solely to NOX activation.

The entry of viral envelope protein may trigger host cell changes. Most retroviruses, including HIV, penetrate host cells through fusion with the host plasma membrane by

binding to specific receptor or through endocytosis. It has been shown that CD4-independent HIV-1 entry occurs through endocytosis (175, 176). The route of entrance to the host cytoplasm appears to be cell type-dependent. For example, ecotropic MLV invades NIH 3T3 cells by endocytosis, whereas it enters rat XC cells by fusion at plasma membrane (177). In particular, endocytosis enables formation of microdomains that contain different microenvironments different from the cytoplasm. Short-lived O_2^- , which can be converted to long-lived and diffusible ROS derivatives, increases high ROS concentration in the microdomains on a low global ROS background. High levels of ROS in a specific location may activate ROS signaling pathways while global intracellular ROS concentrations remain low. It is noteworthy that at 4 hpi, intracellular NADPH levels decreased without detection of extracellular O_2^- upregulation. Recent studies also show CD4-independent HIV infection and MLV infection involving inhibition of cathepsin B in endosomes, increasing host cell susceptibility to viral infection (178, 179). Surprisingly, NOX activation specifically suppresses cysteine proteases (cathepsin B/L) via reversible oxidation of cysteine cathepsins within the phagosome (180). We presume that there may be two phases of NOX activation followed by *ts1* infection. During the pre-integration phase, viral particles penetrate the host membrane via endocytosis. In the endosomes, the first phase of NOX activation by *ts1* may inhibit cysteine proteases and this may protect the viral capsid from lysis. Interestingly, we observed that SOD localization in the perinuclear area within 4 hpi. We suspect that localization of SOD in the virus containing endosomes may be an attempt by the host cell to prevent the preintegrated viral complex access to nuclear membrane. As shown in Figure 3.8, inhibition of NOX decreased viral establishment in the host genome. SOD1 overexpression has been shown to prevent neuronal death in HIV *env* expressing mouse brain. Our study demonstrated that upregulated O_2^- was more highly detected in the cell body rather than in the periphery of cells in the *ts1*-infected brain stem.

At 24 hpi, we observed p47^{phox} translocation from the cytoplasm to the plasma membrane and O₂⁻ production in the extracellular environment without SOD redistribution toward the plasma membrane, which is the second phase of NOX activation. We hypothesized that NOX activation at the plasma membrane may be used by the virus as a mechanism to stimulate cell proliferation. Extracellular O₂⁻ may eventually be converted into a more permeable form of H₂O₂ outside of the cell. As a result, overall ROS levels in either the extracellular environment of neighboring cells or in the cytoplasm of *ts1*-infected cells may be increased. We attempted to suppress gp91^{phox} expression using shRNA containing lentivirus molecule. Unfortunately lentivirus transduction itself seemed to activate NOX and the lentivirus-transduced cells appeared to be *ts1*-resistant. In other words, for some unknown reason, these cells did not show any cytopathic effect as a result of *ts1* infection. However, we observed that cell growth was decreased in gp91^{phox} shRNA lentivirus-transduced cells compared to the control lentivirus-transduced cells (data not shown). We suspect that constant ROS production at low levels by small amounts of NOX activity may play a mitogenic role.

3.4.1. Subcellular localization of NOX subunits may determine its local activation using different subunits

gp91^{phox} and p22^{phox} are colocalized at the plasma membrane, whereas the p47^{phox} and p67^{phox} subunits are known to be distributed in the cytoplasm without stimulants. In neurons, both p47^{phox} and p67^{phox} subunits exhibit punctate staining at the membrane within 4 hours after nerve growth factor deprivation (181). Immunodepletion of p67^{phox} from aortic fibroblast particulates resulted in loss of NADPH oxidase activity, which could be restored by the addition of recombinant p67^{phox} (182). These previous studies support the current NOX activation model in which assembly of cytoplasmic p67^{phox} accompanied with its partner p47^{phox} and catalytic subunit gp91^{phox} occurs at the plasma membrane. Although

expression of NOX subunits has been reported in astrocytes, the distribution of each subunit is assumed to be similar to those in macrophages (54). However, in this study, we found that p67^{phox} is unexpectedly localized at the membrane fraction whereas p47^{phox} is at the cytoplasm without any stimulation. Thus, NOX activation may be more complicated than previously assumed. Some members of the NOX catalytic protein family do not require p47^{phox} for its activation. It is possible that NOX complex activation may be different depending on the subcellular localization of NOX subunits. For example, NOX activity at the plasma membrane is decreased by p47^{phox} mutant expression whereas intracellular NOX activity during phagocytosis exhibits no change by p47^{phox} mutant expression (183). In our study, we observed p47^{phox} translocation in astrocytes only at 24 hpi and not at 4 hours hpi. This may imply that NOX activation at 4 hpi is related to a phagocytosis-dependent process. Although NOX activation has been reported in various NDs in recent years, mechanisms for its activation or deactivation is still unclear. At least three serine phosphorylation sites on p47^{phox} by casein kinase 2 (CK2) are identified. Inhibition of CK2 has been shown to increase and prolong NOX activity, indicating that p47^{phox} phosphorylation by CK2 negatively regulates NOX activity. Inhibition of CK2 also enhances p47^{phox} translocation to membrane (184). Along with p47^{phox} translocation at 24 hpi, we also observed p47^{phox} protein mobility shifted to a lower band. Although we have not investigated whether *ts1* infection suppresses CK2 activity in reference to the p47^{phox} protein band shift, it would be interesting to study if the lower p47^{phox} band is dephosphorylated p47^{phox} via suppression of CK2 in *ts1*-infected astrocytes.

3.4.2. NOX isoforms may have distinct functions in different subcellular location.

As mentioned before, *ts1* has a cytopathic effect on astrocytes due to ER stress caused by misfolded *env* protein (32). Zhao X et al showed that the induction of apoptosis in mink epithelial cells by mink cell focus-forming (MCF)-MuLV infection results in the

accumulation of high levels of both unintegrated viral DNA and the envelope precursor, gPr80^{env} (185). Comparisons of envelope protein expression of MCF-MuLV and noncytopathic NZB-9 MuLV strains demonstrate that the accumulation of MCF13 gPr80^{env} results in ER stress and is sufficient for the induction of apoptosis (185). ER stress may be related to intracellular ROS induction in *ts1*-infected cells. Due to mutation, the precursor viral envelope protein of *ts1*, gPr80^{env} is unable to fold properly and unable to proceed to the Golgi apparatus. The UPR activates NOX, which may be localized to the ER membrane. This is notable because endothelial cells have 100 times higher NOX4 expression compared to NOX2. NOX4 in endothelial cells is predominantly expressed in the ER membrane yet not in lysosomes or mitochondria, suggesting that NOX4 may be involved in repairing *ts1*-mediated UPR in endothelial cells (186). This may explain why *ts1* is not cytopathic to endothelial cells. Increased expression of NOX4 in astrocytes may prevent neuropathic symptoms facilitated by UPR in the *ts1*-infected mouse brain.

3.4.3. The complex relationship of *ts1* infection, O₂⁻, and neuronal death

In this study, we showed that NOX is activated by *ts1* infection and NOX activation appears to be involved in early virus establishment in the host cells. In fact, little information is currently available regarding NOX in the context of retrovirus infection. There are a few important observations to be addressed in *ts1*-infected mouse brain. First, we have reported astrogliosis in *ts1*-infected mouse brain and from this study we know that all GFAP- positive cells in *ts1*-infected mouse brain are not necessarily *ts1*-infected cells. At present, we do not know whether astrocytes become active as a result of *ts1* infection, or due to migration of uninfected astrocytes to *ts1*-infected area in order to compensate for dysfunctional infected astrocytes. O₂⁻ produced by infected astrocytes may function as a chemokine to attract uninfected astrocytes. Second, we do not know if prevalent viral particles produced by infected cells cause O₂⁻ production not only in astrocytes but also in

neurons. *ts1* is not expected to invade the nucleus in neurons because neurons are not mitotic cells. NADPH levels decrease in a NOX-dependent mechanism at 4 hpi, suggesting that NOX activation occurs before viral gene integration. Some HIV viral proteins have been shown to activate NOX in neurons. O_2^- upregulation near the perinuclear area in neurons may be damaging neurons. Therefore, we cannot exclude the possibility that NOX activation in neurons by *ts1* particles without viral gene integration may cause O_2^- upregulation, leading to neuronal death in the *ts1*-infected mouse brain. Thirdly, *ts1*-infected astrocytes may not be the cells that produce viral progeny actively in the CNS. If extracellular O_2^- or other ROS from astrocytic NOX activation damages nearby neurons, *ts1*-infected neuron degeneration may be recovered by thiol supplements including GSH (5) (126).

Chapter 4. Conclusion and future direction

Throughout the history of retrovirology, paradigm shifts have been observed as new discoveries are made. The first major finding was the discovery of animal-infecting retroviruses including RSV and MuLV, second was the development of the viral assay, and third was the identification of reverse transcription. The most recent paradigm change in retrovirology followed the discovery of human retroviruses, most notably HIV. The discovery and investigation of retrovirus-induced human disease models, including the struggle against AIDS, would have been significantly delayed if not for the knowledge and tools created from years of research on animal retroviruses, which provided the basic framework for human retroviruses. Unfortunately, the research limitations for human retrovirus-induced diseases have created a challenge for investigators analyzing the mechanism of pathogenesis in the whole body system. Ethics and safety standards make studies on human subject impossible. Therefore, studies of retrovirus-mediated pathogenesis in animal models are extremely valuable. In contrast to cytopathogenesis caused by retroviruses, retrovirus-induced pathogenesis in its early and middle stages is esoteric. Incomplete understanding of viral establishment and replication in host cells, cellular susceptibility, and communication between infected cells and uninfected cells may hinder the development of effective therapeutic treatments. Therefore, establishment of retrovirus-infected animal models with pathogenic symptoms is crucial.

4.1. Conclusion

Previous studies in our laboratory demonstrated that *ts1* infection exerts different

effects upon various cell types in the CNS. While there is no significant inflammatory infiltration in the *ts1*-infected brain, there is consistent appearance of astrogliosis. Neuronal death was also evident in *ts1*-infected brain although *ts1* does not infect neurons. Additionally, it was demonstrated that *ts1* infection causes signs of oxidative stress in the brain and astrocytes in culture. For example, depletion of reduced thiols and ROS upregulation have been reported in *ts1*-infected astrocytes (5). Recently cocultures of infected astrocytes and neurons demonstrated that drastic upregulation of ROS and caspase activation occurred in neurons as a result of *ts1*-infection in astrocytes, indicating that neuronal loss may be a consequence of dysfunctional astrocytes (126). Minocycline treatment was also shown to suppress ROS upregulation significantly in both *ts1*-infected astrocytic cells alone and neurons cocultured with the infected astrocytes. Another antioxidant, MSL, also extends the life span of *ts1*-infected mice by suppressing oxidative stress and decreasing virus titer in the brain (94). However, antioxidant treatment does not function as an anti-viral agent but does decrease viral replication by suppressing ROS levels. Therefore, we hypothesized that retrovirus-induced ND may not be directly caused by neuronal infection. Instead, astrocytes acting as caretakers for neurons provide an antioxidant defense and *ts1* infection makes the astrocytes dysfunctional. This change in microenvironment appears to be the cause of neuronal death.

As noted before, *ts1* infection has a cytopathic effect on astrocytes. Previous studies have been more focused on virus-mediated oxidative stress and mitochondria-mediated cell death processes. In this study, we proposed that dual faces of ROS upregulation are involved in retrovirus-induced host cell signaling that may affect cell fates. We thus investigated the life cycle of the retrovirus *ts1* in the context of ROS upregulation. In Chapter 2, we demonstrated that *ts1* infection induces two distinctive ROS upregulations in astrocytes. The first ROS upregulation, which is relatively low level, occurred in early stage

of infection. This early ROS upregulation seems to activate host cells to facilitate viral gene integration. Despite its well-known role in apoptosis, p53 appears to play an important role in cellular anti-oxidant defense in *ts1*-infected astrocytes. As a result of ROS upregulation during the early phase of *ts1* infection, p53 activation suppresses the upregulation of NOX. In the absence of p53, expression of viral proteins in host cells occurred earlier in cells exhibiting normal p53 expression. Another important finding of our study is that NOX seems to play an important role in the early ROS production. In Chapter 3, we demonstrate that NOX is activated by *ts1* infection in the early stage of infection and inhibition of NOX decreases viral DNA integration into the host genome. The second round of ROS upregulation takes place in the late stage of infection, following *ts1* establishment and protein synthesis in the host cells. Due to a single amino acid substitution on the envelope protein, the precursor envelope protein does not fold properly and therefore accumulates in the ER, resulting in cell death. As a consequence cells die. The second ROS upregulation appears to play an important role in mitochondria-mediated apoptotic processes.

Overall this study establishes three important aspects of cellular ROS upregulation in retrovirus-infected CNS cells. First, this study shows that retrovirus infection actively adapts the changes in host intracellular environment. Earlier perspectives on ROS upregulation are mainly based on the passive relationship between retrovirus and the host cell, suggesting that retroviral infection is dependent on host cell cycle status. However, we discover that the interaction between retrovirus and the host cells is rather mutual. Until this point, the question of whether a retrovirus actively participates in changing the host intracellular environment has not been explored. It is known that various ROS levels can drive different cell fates. Low levels of ROS can induce proliferation whereas moderate levels of ROS cause growth arrest, and high levels of ROS can cause cellular death (Figure 1.5). In order to establish itself in the host cell, retrovirus may utilize the host cells' defenses to integrate viral genes into the host genome by activation of endogenous NOX. Cells that are arrested

in G1/S transition have been shown to be much less efficiently infected by MuLV and lentivirus (90). In this study, we demonstrate that retrovirus invasion increases low levels of ROS in astrocytes during the early phase of life cycle. Retroviruses may actively promote ROS levels to overcome the quiescent environment of cells in the CNS, and host cells may activate p53 in an attempt to suppress ROS upregulation as a self-defense strategy. Secondly, this study explores the importance of temporal and spatial regulation of ROS in retrovirus-infected astrocytes. As mentioned earlier, all ROS are not equal. The locations and the timing of ROS upregulation appear to be very precisely regulated in different phase of the virus life cycle. The first wave of ROS upregulation by NOX and SOD occurs in the cytoplasm before the viral gene is integrated into the host genome. After the viral gene is integrated into host genome, the second wave of ROS appears at the plasma membrane by NOX, which is not associated with ER stress. The third wave of ROS production is from the mitochondria, followed by activation of cell death. We distinguished at least three different locations and timing of ROS production and observed that each ROS upregulation does not last throughout the entire retrovirus life cycle. Most studies on ROS and their effects may use too high concentrations compared to the ROS concentrations in physiological conditions. ROS are generally unstable and react quickly with cellular molecules, which are in some cases at unintended locations. Thus, to investigate the effects of ROS on physiological conditions, a system that activates endogenous ROS production is necessary. We demonstrate that *ts1*-infected astrocytes can provide useful tools to study the effects of ROS on astrocytes. Most importantly, ROS upregulation may generate different cellular effects depending on the location and concentration. Third, tissue staining using DHE fluorescence shows that neurons as well as *ts1*-infected astrocytes in the mouse CNS are under oxidative challenge as a result of *ts1* infection (Figure 3.10). Neurons are specialized in their function. Their redox balance and metabolism are primarily supported by nearby astrocytes, more specifically by providing reduced thiols for anti

oxidant defense. In particular, the metabolism of neurons depends heavily on mitochondria. Therefore, antioxidant defense is critical for the elimination of mitochondrial respiratory byproducts. This study, as well as previous work from our lab, substantiates that *ts1* infection reduces the precursor of GSH (cysteine) and GSH levels, therefore increasing ROS levels. Furthermore, *ts1*-infected astrocytes can release O_2^- into the extracellular environment, which may directly damage neurons. Many neurodegenerative diseases are associated with oxidative stress, and thereby, ROS upregulation by dysfunctional astrocytes may also be applicable to other neurodegenerative disease models.

The regulation of intracellular or extracellular ROS levels is unlikely to be orchestrated by one simple signaling pathway, but rather by a complex signaling network. In this study, we investigated that NOX, SOD and p53 play important roles in the ROS regulation using the *ts1*-infected astrocyte system.

4.2. Proposed model and future studies.

ROS research is an inherently challenging field due to the transient nature of ROS. The concept that ROS play different roles in cellular processes at different concentrations and locations has been proposed. Moreover, cellular redox status may vary between cell types in order for the different cells to optimally perform their functions. Here we have described ROS upregulation during retrovirus infection and illustrate its complexity. As mentioned above, the timing of ROS upregulation is associated with different phases of the virus life cycle. To investigate how each ROS upregulation contributes to the retrovirus life cycle, modulation of p53, SOD and NOX are essential. Based on the observations from Chapter 2 and 3, we proposed a model of ROS upregulation in *ts1*-infected astrocytes. It may be summarized by the activation of NOX by retroviral invasion at the plasma membrane and the fusion of the viral receptor with viral envelope protein forms vesicles either as a

phagosome or an early endosome. As a first line of defense, SOD is quickly upregulated and catalyzes O_2^- to H_2O_2 . Therefore, 4-8 hpi, the H_2O_2 increase is observed. In the vesicles, retrovirus may develop a system to adapt the ROS by modulating PIC components to facilitate integration into the host genome. H_2O_2 is more membrane permeable than O_2^- , and therefore, cytoplasmic H_2O_2 may increase concomitantly with the rise of H_2O_2 in the vesicles and activation of cytoplasmic p53. Activated p53 downregulates NOX expression levels via a negative feedback mechanism. It is important to validate the sequential processes during the different phase of ROS upregulation in the life cycle of retrovirus.

Furthermore, ROS upregulation by retrovirus-infected astrocytes plays an important role in neuronal death. It is crucial to investigate which phase of ROS upregulation is associated with neuronal death to identify the most efficient therapeutic targets. Throughout this study, we demonstrated three different ROS upregulations from different sources. However, at present, we do not know whether ROS upregulation by *ts1*-infected astrocytes is associated with a direct or indirect killing mechanism of nearby neurons. The effect of ROS upregulation in the CNS can be summarized into three possibilities. First, ROS upregulation facilitates retroviral replication in the CNS. As we have shown in this study, ROS upregulation in the early phase of infection is associated with viral establishment. Targeting this step will decrease dissemination of progeny viruses and prevent further infection. Second, decreased antioxidant defense and increased ROS in the microenvironment may make neurons vulnerable, and consequently lead to cell death. We demonstrate a prevalence of O_2^- upregulation in the *ts1*-infected mouse CNS and in the extracellular environment of *ts1*-infected astrocytes in culture. Previous studies in our laboratory have shown that the depletion of reduced thiols in *ts1*-infected astrocytes cultures and decreased cysteine levels in *ts1*-infected brain slice culture (Lungu Gina, unpublished data). However, these signs of oxidative stress are not defined in the context

of the *ts1*-infected astrocytes status. Third, ROS upregulation in *ts1*-infected astrocytes may disrupt its endogenous functions, for example recycling glutamate and providing nutrients. Previously, it has been reported that ROS upregulation can change GS expression in astrocytes. An abundance of the excitatory neurotransmitter glutamate in the extracellular environment is capable of inducing neuronal cell death. Further studies exploring the direct or indirect effect of astrocytic ROS upregulation would be beneficial in the development of an effective therapeutic target and in the understanding of other neurodegenerative models associated with oxidative stress. ROS regulation at multiple levels compounds the difficulty of data interpretation. Possible overlapping of the different phases in culture adds substantial technical challenges that may affect an overall study of the role of ROS upregulation in the life cycle of the retrovirus. These studies offer new insights into the mechanisms for retrovirus-host cell interaction that facilitate or inhibit viral replication, in particular during the early phase of infection. Better understanding of the cellular ROS regulation system would lead us to opportunities for suppression of permanent retrovirus establishment in the host cells. Furthermore the knowledge gained from this study will help us to develop therapeutic strategies to influence the course and outcome of diseases caused by retrovirus-infection.

BIBLIOGRAPHY

1. Levy, J. A. 1986. The multifaceted retrovirus. *Cancer Res* 46:5457-5468.
2. Levy, J. A. 1995. *The Retroviridae*. Plenum Press, New York.
3. Yuen, P. H., D. Malehorn, C. Knupp, and P. K. Wong. 1985. A 1.6-kilobase-pair fragment in the genome of the *ts1* mutant of Moloney murine leukemia virus TB that is associated with temperature sensitivity, nonprocessing of Pr80env, and paralytogenesis. *J Virol* 54:364-373.
4. Wong, P. K. Y., Kim, S., Kim, S.J., Kuang X., Lynn W.S. . 2010. Oxidative stress-mediated neurodegeneration: a tale of two models. A. S. McNeill, editor. Nova Science Publishers, Inc. 1-44.
5. Qiang, W., J. M. Cahill, J. Liu, X. Kuang, N. Liu, V. L. Scofield, J. R. Voorhees, A. J. Reid, M. Yan, W. S. Lynn, and P. K. Wong. 2004. Activation of transcription factor Nrf-2 and its downstream targets in response to moloney murine leukemia virus *ts1*-induced thiol depletion and oxidative stress in astrocytes. *J Virol* 78:11926-11938.
6. Barreto, G. E., J. Gonzalez, Y. Torres, and L. Morales. 2011. Astrocytic-neuronal crosstalk: Implications for neuroprotection from brain injury. *Neurosci Res*.
7. Rous, P. 1911. A Sarcoma of the Fowl Transmissible by an Agent Separable from the Tumor Cells. *J Exp Med* 13:397-411.
8. Temin, H. M., and S. Mizutani. 1970. RNA-dependent DNA polymerase in virions of Rous sarcoma virus. *Nature* 226:1211-1213.
9. Baltimore, D. 1970. RNA-dependent DNA polymerase in virions of RNA tumour viruses. *Nature* 226:1209-1211.
10. Coffin, J. M., S. H. Hughes, and H. E. Varmus. 1997. *The Interactions of Retroviruses and their Hosts*.

11. Tazi, J., N. Bakkour, V. Marchand, L. Ayadi, A. Aboufirassi, and C. Branlant. 2010. Alternative splicing: regulation of HIV-1 multiplication as a target for therapeutic action. *FEBS J* 277:867-876.
12. Canivet, M., A. D. Hoffman, D. Hardy, J. Sernatinger, and J. A. Levy. 1990. Replication of HIV-1 in a wide variety of animal cells following phenotypic mixing with murine retroviruses. *Virology* 178:543-551.
13. Yamashita, M., and M. Emerman. 2006. Retroviral infection of non-dividing cells: old and new perspectives. *Virology* 344:88-93.
14. Doitsh, G., M. Cavrois, K. G. Lassen, O. Zepeda, Z. Yang, M. L. Santiago, A. M. Hebbeler, and W. C. Greene. 2010. Abortive HIV infection mediates CD4 T cell depletion and inflammation in human lymphoid tissue. *Cell* 143:789-801.
15. Finkel, T. H., G. Tudor-Williams, N. K. Banda, M. F. Cotton, T. Curiel, C. Monks, T. W. Baba, R. M. Ruprecht, and A. Kupfer. 1995. Apoptosis occurs predominantly in bystander cells and not in productively infected cells of HIV- and SIV-infected lymph nodes. *Nat Med* 1:129-134.
16. Jekle, A., O. T. Keppler, E. De Clercq, D. Schols, M. Weinstein, and M. A. Goldsmith. 2003. In vivo evolution of human immunodeficiency virus type 1 toward increased pathogenicity through CXCR4-mediated killing of uninfected CD4 T cells. *J Virol* 77:5846-5854.
17. Burrows, F. J., M. Gore, W. R. Smiley, M. Y. Kanemitsu, D. J. Jolly, S. B. Read, T. Nicholas, and C. A. Kruse. 2002. Purified herpes simplex virus thymidine kinase retroviral particles: III. Characterization of bystander killing mechanisms in transfected tumor cells. *Cancer Gene Ther* 9:87-95.
18. Yadav, A., and R. G. Collman. 2009. CNS inflammation and macrophage/microglial biology associated with HIV-1 infection. *J Neuroimmune Pharmacol* 4:430-447.

19. Lynn, W. S., and P. K. Wong. 1995. Neuroimmunodegeneration: do neurons and T cells use common pathways for cell death? *FASEB J* 9:1147-1156.
20. Antony, J. M., Y. Zhu, M. Izad, K. G. Warren, M. Vodjgani, F. Mallet, and C. Power. 2007. Comparative expression of human endogenous retrovirus-W genes in multiple sclerosis. *AIDS Res Hum Retroviruses* 23:1251-1256.
21. Lombardi, V. C., F. W. Ruscetti, J. Das Gupta, M. A. Pfof, K. S. Hagen, D. L. Peterson, S. K. Ruscetti, R. K. Bagni, C. Petrow-Sadowski, B. Gold, M. Dean, R. H. Silverman, and J. A. Mikovits. 2009. Detection of an infectious retrovirus, XMRV, in blood cells of patients with chronic fatigue syndrome. *Science* 326:585-589.
22. Georgsson, G. 1994. Neuropathologic aspects of lentiviral infections. *Ann N Y Acad Sci* 724:50-67.
23. Moses, A. V., F. E. Bloom, C. D. Pauza, and J. A. Nelson. 1993. Human immunodeficiency virus infection of human brain capillary endothelial cells occurs via a CD4/galactosylceramide-independent mechanism. *Proc Natl Acad Sci U S A* 90:10474-10478.
24. Langford, D., A. Grigorian, R. Hurford, A. Adame, R. J. Ellis, L. Hansen, and E. Masliah. 2004. Altered P-glycoprotein expression in AIDS patients with HIV encephalitis. *J Neuropathol Exp Neurol* 63:1038-1047.
25. Langford, D., J. Marquie-Beck, S. de Almeida, D. Lazzaretto, S. Letendre, I. Grant, J. A. McCutchan, E. Masliah, and R. J. Ellis. 2006. Relationship of antiretroviral treatment to postmortem brain tissue viral load in human immunodeficiency virus-infected patients. *J Neurovirol* 12:100-107.
26. Dimcheff, D. E., S. Askovic, A. H. Baker, C. Johnson-Fowler, and J. L. Portis. 2003. Endoplasmic reticulum stress is a determinant of retrovirus-induced spongiform neurodegeneration. *J Virol* 77:12617-12629.

27. Stoica, G., S. I. Tasca, and P. K. Wong. 2000. Motor neuronal loss and neurofilament-ubiquitin alteration in MoMuLV-ts1 encephalopathy. *Acta Neuropathol* 99:238-244.
28. Wong, P. K., E. Shikova, Y. C. Lin, K. Saha, P. F. Szurek, G. Stoica, R. Madden, and B. R. Brooks. 1992. Murine leukemia virus induced central nervous system diseases. *Leukemia* 6 Suppl 3:161S-165S.
29. Wong, P. K., and J. A. McCarter. 1973. Genetic studies of temperature-sensitive mutants of Moloney-murine leukemia virus. *Virology* 53:319-326.
30. Wong, P. K. 1990. Moloney murine leukemia virus temperature-sensitive mutants: a model for retrovirus-induced neurologic disorders. *Curr Top Microbiol Immunol* 160:29-60.
31. Kamps, C. A., Y. C. Lin, and P. K. Wong. 1991. Oligomerization and transport of the envelope protein of Moloney murine leukemia virus-TB and of *ts1*, a neurovirulent temperature-sensitive mutant of MoMuLV-TB. *Virology* 184:687-694.
32. Szurek, P. F., P. H. Yuen, J. K. Ball, and P. K. Wong. 1990. A Val-25-to-Ile substitution in the envelope precursor polyprotein, gPr80^{env}, is responsible for the temperature sensitivity, inefficient processing of gPr80^{env}, and neurovirulence of *ts1*, a mutant of Moloney murine leukemia virus TB. *J Virol* 64:467-475.
33. Wong, P. K., G. Prasad, J. Hansen, and P. H. Yuen. 1989. *ts1*, a mutant of Moloney murine leukemia virus-TB, causes both immunodeficiency and neurologic disorders in BALB/c mice. *Virology* 170:450-459.
34. Zachary, J. F., C. J. Knupp, and P. K. Wong. 1986. Noninflammatory spongiform polioencephalomyelopathy caused by a neurotropic temperature-sensitive mutant of Moloney murine leukemia virus TB. *Am J Pathol* 124:457-468.
35. Clark, S., J. Duggan, and J. Chakraborty. 2001. Tsl and LP-BM5: a comparison of two murine retrovirus models for HIV. *Viral Immunol* 14:95-109.

36. Saha, K., P. H. Yuen, and P. K. Wong. 1994. Murine retrovirus-induced depletion of T cells is mediated through activation-induced death by apoptosis. *J Virol* 68:2735-2740.
37. Ronaldson, P. T., and R. Bendayan. 2008. HIV-1 viral envelope glycoprotein gp120 produces oxidative stress and regulates the functional expression of multidrug resistance protein-1 (Mrp1) in glial cells. *J Neurochem* 106:1298-1313.
38. Pollicita, M., C. Muscoli, A. Sgura, A. Biasin, T. Granato, L. Masuelli, V. Mollace, C. Tanzarella, C. Del Duca, P. Rodino, C. F. Perno, and S. Aquaro. 2009. Apoptosis and telomeres shortening related to HIV-1 induced oxidative stress in an astrocytoma cell line. *BMC Neurosci* 10:51.
39. Lindl, K. A., C. Akay, Y. Wang, M. G. White, and K. L. Jordan-Sciutto. 2007. Expression of the endoplasmic reticulum stress response marker, BiP, in the central nervous system of HIV-positive individuals. *Neuropathol Appl Neurobiol* 33:658-669.
40. Sabri, F., K. Titanji, A. De Milito, and F. Chiodi. 2003. Astrocyte activation and apoptosis: their roles in the neuropathology of HIV infection. *Brain Pathol* 13:84-94.
41. Stoica, G., E. Floyd, O. Illanes, and P. K. Wong. 1992. Temporal lymphoreticular changes caused by *ts1*, a paralytogenic mutant of Moloney murine leukemia virus TB. *Lab Invest* 66:427-436.
42. Stoica, G., O. Illanes, S. I. Tasca, and P. K. Wong. 1993. Temporal central and peripheral nervous system changes induced by a paralytogenic mutant of Moloney murine leukemia virus TB. *Lab Invest* 69:724-735.
43. Wong, P. K., C. Knupp, P. H. Yuen, M. M. Soong, J. F. Zachary, and W. A. Tompkins. 1985. *ts1*, a Paralytogenic mutant of Moloney murine leukemia virus TB, has an enhanced ability to replicate in the central nervous system and primary nerve cell culture. *J Virol* 55:760-767.

44. An, S. F., M. Groves, F. Gray, and F. Scaravilli. 1999. Early entry and widespread cellular involvement of HIV-1 DNA in brains of HIV-1 positive asymptomatic individuals. *J Neuropathol Exp Neurol* 58:1156-1162.
45. Poland, S. D., G. P. Rice, and G. A. Dekaban. 1995. HIV-1 infection of human brain-derived microvascular endothelial cells in vitro. *J Acquir Immune Defic Syndr Hum Retrovirol* 8:437-445.
46. Demarex, N., and L. Scorrano. 2009. Reactive oxygen species are NOXious for neurons. *Nat Neurosci* 12:819-820.
47. Wang, W., H. Fang, L. Groom, A. Cheng, W. Zhang, J. Liu, X. Wang, K. Li, P. Han, M. Zheng, J. Yin, M. P. Mattson, J. P. Kao, E. G. Lakatta, S. S. Sheu, K. Ouyang, J. Chen, R. T. Dirksen, and H. Cheng. 2008. Superoxide flashes in single mitochondria. *Cell* 134:279-290.
48. Liu, N., X. Kuang, H. T. Kim, G. Stoica, W. Qiang, V. L. Scofield, and P. K. Wong. 2004. Possible involvement of both endoplasmic reticulum- and mitochondria-dependent pathways in MoMuLV-ts1-induced apoptosis in astrocytes. *J Neurovirol* 10:189-198.
49. Riemer, J., N. Bulleid, and J. M. Herrmann. 2009. Disulfide formation in the ER and mitochondria: two solutions to a common process. *Science* 324:1284-1287.
50. Liu, N., V. L. Scofield, W. Qiang, M. Yan, X. Kuang, and P. K. Wong. 2006. Interaction between endoplasmic reticulum stress and caspase 8 activation in retrovirus MoMuLV-ts1-infected astrocytes. *Virology* 348:398-405.
51. Santos, C. X., L. Y. Tanaka, J. Wosniak, and F. R. Laurindo. 2009. Mechanisms and implications of reactive oxygen species generation during the unfolded protein response: roles of endoplasmic reticulum oxidoreductases, mitochondrial electron transport, and NADPH oxidase. *Antioxid Redox Signal* 11:2409-2427.

52. Behe, P., and A. W. Segal. 2007. The function of the NADPH oxidase of phagocytes, and its relationship to other NOXs. *Biochem Soc Trans* 35:1100-1103.
53. Brennan, A. M., S. W. Suh, S. J. Won, P. Narasimhan, T. M. Kauppinen, H. Lee, Y. Edling, P. H. Chan, and R. A. Swanson. 2009. NADPH oxidase is the primary source of superoxide induced by NMDA receptor activation. *Nat Neurosci* 12:857-863.
54. Abramov, A. Y., J. Jacobson, F. Wientjes, J. Hothersall, L. Canevari, and M. R. Duchen. 2005. Expression and modulation of an NADPH oxidase in mammalian astrocytes. *J Neurosci* 25:9176-9184.
55. Sablina, A. A., A. V. Budanov, G. V. Ilyinskaya, L. S. Agapova, J. E. Kravchenko, and P. M. Chumakov. 2005. The antioxidant function of the p53 tumor suppressor. *Nat Med* 11:1306-1313.
56. Bensaad, K., A. Tsuruta, M. A. Selak, M. N. Vidal, K. Nakano, R. Bartrons, E. Gottlieb, and K. H. Vousden. 2006. TIGAR, a p53-inducible regulator of glycolysis and apoptosis. *Cell* 126:107-120.
57. Suzuki, S., T. Tanaka, M. V. Poyurovsky, H. Nagano, T. Mayama, S. Ohkubo, M. Lokshin, H. Hosokawa, T. Nakayama, Y. Suzuki, S. Sugano, E. Sato, T. Nagao, K. Yokote, I. Tatsuno, and C. Prives. 2010. Phosphate-activated glutaminase (GLS2), a p53-inducible regulator of glutamine metabolism and reactive oxygen species. *Proc Natl Acad Sci U S A* 107:7461-7466.
58. Hu, W., C. Zhang, R. Wu, Y. Sun, A. Levine, and Z. Feng. 2010. Glutaminase 2, a novel p53 target gene regulating energy metabolism and antioxidant function. *Proc Natl Acad Sci U S A* 107:7455-7460.
59. Budanov, A. V., A. A. Sablina, E. Feinstein, E. V. Koonin, and P. M. Chumakov. 2004. Regeneration of peroxiredoxins by p53-regulated sestrins, homologs of bacterial AhpD. *Science* 304:596-600.

60. Lambeth, J. D. 2004. NOX enzymes and the biology of reactive oxygen. *Nat Rev Immunol* 4:181-189.
61. Mahadev, K., H. Motoshima, X. Wu, J. M. Ruddy, R. S. Arnold, G. Cheng, J. D. Lambeth, and B. J. Goldstein. 2004. The NAD(P)H oxidase homolog Nox4 modulates insulin-stimulated generation of H₂O₂ and plays an integral role in insulin signal transduction. *Mol Cell Biol* 24:1844-1854.
62. Rhee, S. G. 2006. Cell signaling. H₂O₂, a necessary evil for cell signaling. *Science* 312:1882-1883.
63. Juarez, J. C., M. Manuia, M. E. Burnett, O. Betancourt, B. Boivin, D. E. Shaw, N. K. Tonks, A. P. Mazar, and F. Donate. 2008. Superoxide dismutase 1 (SOD1) is essential for H₂O₂-mediated oxidation and inactivation of phosphatases in growth factor signaling. *Proc Natl Acad Sci U S A* 105:7147-7152.
64. Immenschuh, S., E. Baumgart-Vogt, M. Tan, S. Iwahara, G. Ramadori, and H. D. Fahimi. 2003. Differential cellular and subcellular localization of heme-binding protein 23/peroxiredoxin I and heme oxygenase-1 in rat liver. *J Histochem Cytochem* 51:1621-1631.
65. Li, Q., M. M. Harraz, W. Zhou, L. N. Zhang, W. Ding, Y. Zhang, T. Eggleston, C. Yeaman, B. Banfi, and J. F. Engelhardt. 2006. Nox2 and Rac1 regulate H₂O₂-dependent recruitment of TRAF6 to endosomal interleukin-1 receptor complexes. *Mol Cell Biol* 26:140-154.
66. Miller, F. J., Jr., M. Filali, G. J. Huss, B. Stanic, A. Chamseddine, T. J. Barna, and F. S. Lamb. 2007. Cytokine activation of nuclear factor kappa B in vascular smooth muscle cells requires signaling endosomes containing Nox1 and CIC-3. *Circ Res* 101:663-671.
67. Oakley, F. D., R. L. Smith, and J. F. Engelhardt. 2009. Lipid rafts and caveolin-1 coordinate interleukin-1beta (IL-1beta)-dependent activation of NFkappaB by

- controlling endocytosis of Nox2 and IL-1 β receptor 1 from the plasma membrane. *J Biol Chem* 284:33255-33264.
68. Lamb, F. S., J. G. Moreland, and F. J. Miller, Jr. 2009. Electrophysiology of reactive oxygen production in signaling endosomes. *Antioxid Redox Signal* 11:1335-1347.
 69. Jha, N. K., O. Latinovic, E. Martin, G. Novitskiy, M. Marin, K. Miyauchi, J. Naughton, J. A. Young, and G. B. Melikyan. 2011. Imaging single retrovirus entry through alternative receptor isoforms and intermediates of virus-endosome fusion. *PLoS Pathog* 7:e1001260.
 70. Goff, S. P. 2004. Retrovirus restriction factors. *Mol Cell* 16:849-859.
 71. Yan, M., W. Qiang, N. Liu, J. Shen, W. S. Lynn, and P. K. Wong. 2001. The ataxia-telangiectasia gene product may modulate DNA turnover and control cell fate by regulating cellular redox in lymphocytes. *FASEB J* 15:1132-1138.
 72. Trkola, A. 2004. HIV-host interactions: vital to the virus and key to its inhibition. *Curr Opin Microbiol* 7:555-559.
 73. Gorry, P. R., C. Ong, J. Thorpe, S. Bannwarth, K. A. Thompson, A. Gatignol, S. L. Vesselingh, and D. F. Purcell. 2003. Astrocyte infection by HIV-1: mechanisms of restricted virus replication, and role in the pathogenesis of HIV-1-associated dementia. *Curr HIV Res* 1:463-473.
 74. Ghafouri, M., S. Amini, K. Khalili, and B. E. Sawaya. 2006. HIV-1 associated dementia: symptoms and causes. *Retrovirology* 3:28.
 75. Sabri, F., E. Tresoldi, M. Di Stefano, S. Polo, M. C. Monaco, A. Verani, J. R. Fiore, P. Lusso, E. Major, F. Chiodi, and G. Scarlatti. 1999. Nonproductive human immunodeficiency virus type 1 infection of human fetal astrocytes: independence from CD4 and major chemokine receptors. *Virology* 264:370-384.
 76. Brack-Werner, R. 1999. Astrocytes: HIV cellular reservoirs and important participants in neuropathogenesis. *AIDS* 13:1-22.

77. Thannickal, V. J., and B. L. Fanburg. 2000. Reactive oxygen species in cell signaling. *Am J Physiol Lung Cell Mol Physiol* 279:L1005-1028.
78. Szatrowski, T. P., and C. F. Nathan. 1991. Production of large amounts of hydrogen peroxide by human tumor cells. *Cancer Res* 51:794-798.
79. Burdon, R. H. 1995. Superoxide and hydrogen peroxide in relation to mammalian cell proliferation. *Free Radic Biol Med* 18:775-794.
80. Nose, K., M. Shibamura, K. Kikuchi, H. Kageyama, S. Sakiyama, and T. Kuroki. 1991. Transcriptional activation of early-response genes by hydrogen peroxide in a mouse osteoblastic cell line. *Eur J Biochem* 201:99-106.
81. Huo, Y., W. Y. Qiu, Q. Pan, Y. F. Yao, K. Xing, and M. F. Lou. 2009. Reactive oxygen species (ROS) are essential mediators in epidermal growth factor (EGF)-stimulated corneal epithelial cell proliferation, adhesion, migration, and wound healing. *Exp Eye Res* 89:876-886.
82. Ranjan, P., V. Anathy, P. M. Burch, K. Weirather, J. D. Lambeth, and N. H. Heintz. 2006. Redox-dependent expression of cyclin D1 and cell proliferation by Nox1 in mouse lung epithelial cells. *Antioxid Redox Signal* 8:1447-1459.
83. Havens, C. G., A. Ho, N. Yoshioka, and S. F. Dowdy. 2006. Regulation of late G1/S phase transition and APC Cdh1 by reactive oxygen species. *Mol Cell Biol* 26:4701-4711.
84. Sattler, M., T. Winkler, S. Verma, C. H. Byrne, G. Shrikhande, R. Salgia, and J. D. Griffin. 1999. Hematopoietic growth factors signal through the formation of reactive oxygen species. *Blood* 93:2928-2935.
85. Deng, X., F. Gao, and W. S. May, Jr. 2003. Bcl2 retards G1/S cell cycle transition by regulating intracellular ROS. *Blood* 102:3179-3185.

86. Iiyama, M., K. Kakihana, T. Kurosu, and O. Miura. 2006. Reactive oxygen species generated by hematopoietic cytokines play roles in activation of receptor-mediated signaling and in cell cycle progression. *Cell Signal* 18:174-182.
87. Honore, S., H. Kovacic, V. Pichard, C. Briand, and J. B. Rognoni. 2003. Alpha2beta1-integrin signaling by itself controls G1/S transition in a human adenocarcinoma cell line (Caco-2): implication of NADPH oxidase-dependent production of ROS. *Exp Cell Res* 285:59-71.
88. McCrann, D. J., A. Eliades, M. Makitalo, K. Matsuno, and K. Ravid. 2009. Differential expression of NADPH oxidases in megakaryocytes and their role in polyploidy. *Blood* 114:1243-1249.
89. Foli, A., M. A. Maiocchi, J. Lisziewicz, and F. Lori. 2007. A checkpoint in the cell cycle progression as a therapeutic target to inhibit HIV replication. *J Infect Dis* 196:1409-1415.
90. Emerman, M. 2000. Learning from lentiviruses. *Nat Genet* 24:8-9.
91. de la Fuente, C., A. Maddukuri, K. Kehn, S. Y. Baylor, L. Deng, A. Pumfery, and F. Kashanchi. 2003. Pharmacological cyclin-dependent kinase inhibitors as HIV-1 antiviral therapeutics. *Curr HIV Res* 1:131-152.
92. Wang, J., E. L. Reuschel, J. M. Shackelford, L. Jeang, D. K. Shivers, J. A. Diehl, X. F. Yu, and T. H. Finkel. 2011. HIV-1 Vif promotes the G- to S-phase cell-cycle transition. *Blood* 117:1260-1269.
93. Qiang, W., X. Kuang, J. Liu, N. Liu, V. L. Scofield, A. J. Reid, Y. Jiang, G. Stoica, W. S. Lynn, and P. K. Wong. 2006. Astrocytes survive chronic infection and cytopathic effects of the *ts1* mutant of the retrovirus Moloney murine leukemia virus by upregulation of antioxidant defenses. *J Virol* 80:3273-3284.
94. Jiang, Y., V. L. Scofield, M. Yan, W. Qiang, N. Liu, A. J. Reid, W. S. Lynn, and P. K. Wong. 2006. Retrovirus-induced oxidative stress with neuroimmunodegeneration is

- suppressed by antioxidant treatment with a refined monosodium alpha-luminol (Galavit). *J Virol* 80:4557-4569.
95. Bensaad, K., and K. H. Vousden. 2005. Savior and slayer: the two faces of p53. *Nat Med* 11:1278-1279.
 96. Masuda, M., M. P. Remington, P. M. Hoffman, and S. K. Ruscetti. 1992. Molecular characterization of a neuropathogenic and nonerythroleukemogenic variant of Friend murine leukemia virus PVC-211. *J Virol* 66:2798-2806.
 97. Webster, H., and K. E. Astrom. 2009. Gliogenesis: historical perspectives, 1839-1985. *Adv Anat Embryol Cell Biol* 202:1-109.
 98. Wong, P. K., and P. H. Yuen. 1994. Cell types in the central nervous system infected by murine retroviruses: implications for the mechanisms of neurodegeneration. *Histol Histopathol* 9:845-858.
 99. Bergmann, C. C., T. E. Lane, and S. A. Stohlman. 2006. Coronavirus infection of the central nervous system: host-virus stand-off. *Nat Rev Microbiol* 4:121-132.
 100. Li, Y. 2008. Defineing murin retroviral components and viral life cycle events required for inducing spongiform motor neuron degeneration. Kent state university.
 101. Cheng-Mayer, C., J. T. Rutka, M. L. Rosenblum, T. McHugh, D. P. Stites, and J. A. Levy. 1987. Human immunodeficiency virus can productively infect cultured human glial cells. *Proc Natl Acad Sci U S A* 84:3526-3530.
 102. Chiodi, F., S. Fuerstenberg, M. Gidlund, B. Asjo, and E. M. Fenyo. 1987. Infection of brain-derived cells with the human immunodeficiency virus. *J Virol* 61:1244-1247.
 103. Dewhurst, S., J. Bresser, M. Stevenson, K. Sakai, M. J. Evinger-Hodges, and D. J. Volsky. 1987. Susceptibility of human glial cells to infection with human immunodeficiency virus (HIV). *FEBS Lett* 213:138-143.
 104. Brack-Werner, R., A. Kleinschmidt, A. Ludvigsen, W. Mellert, M. Neumann, R. Herrmann, M. C. Khim, A. Burny, N. Muller-Lantzsch, D. Stavrou, and et al. 1992.

- Infection of human brain cells by HIV-1: restricted virus production in chronically infected human glial cell lines. *AIDS* 6:273-285.
105. Toggas, S. M., E. Masliah, E. M. Rockenstein, G. F. Rall, C. R. Abraham, and L. Mucke. 1994. Central nervous system damage produced by expression of the HIV-1 coat protein gp120 in transgenic mice. *Nature* 367:188-193.
 106. Nedergaard, M., B. Ransom, and S. A. Goldman. 2003. New roles for astrocytes: redefining the functional architecture of the brain. *Trends Neurosci* 26:523-530.
 107. Salmina, A. B. 2009. Neuron-glia interactions as therapeutic targets in neurodegeneration. *J Alzheimers Dis* 16:485-502.
 108. Miralles, V. J., I. Martinez-Lopez, R. Zaragoza, E. Borrás, C. Garcia, F. V. Pallardo, and J. R. Vina. 2001. Na⁺ dependent glutamate transporters (EAAT1, EAAT2, and EAAT3) in primary astrocyte cultures: effect of oxidative stress. *Brain Res* 922:21-29.
 109. Wang, T., N. Gong, J. Liu, I. Kadiu, S. D. Kraft-Terry, R. L. Mosley, D. J. Volsky, P. Ciborowski, and H. E. Gendelman. 2008. Proteomic modeling for HIV-1 infected microglia-astrocyte crosstalk. *PLoS One* 3:e2507.
 110. Visalli, V., C. Muscoli, I. Sacco, F. Sculco, E. Palma, N. Costa, C. Colica, D. Rotiroti, and V. Mollace. 2007. N-acetylcysteine prevents HIV gp 120-related damage of human cultured astrocytes: correlation with glutamine synthase dysfunction. *BMC Neurosci* 8:106.
 111. Churchill, M. J., S. L. Wesselingh, D. Cowley, C. A. Pardo, J. C. McArthur, B. J. Brew, and P. R. Gorry. 2009. Extensive astrocyte infection is prominent in human immunodeficiency virus-associated dementia. *Ann Neurol* 66:253-258.
 112. Castegna, A., L. Palmieri, I. Spera, V. Porcelli, F. Palmieri, M. J. Fabis-Pedrini, R. B. Kean, D. A. Barkhouse, M. T. Curtis, and D. C. Hooper. 2011. Oxidative stress and

- reduced glutamine synthetase activity in the absence of inflammation in the cortex of mice with experimental allergic encephalomyelitis. *Neuroscience* 185:97-105.
113. Di Giorgio, F. P., M. A. Carrasco, M. C. Siao, T. Maniatis, and K. Eggan. 2007. Non-cell autonomous effect of glia on motor neurons in an embryonic stem cell-based ALS model. *Nat Neurosci* 10:608-614.
 114. Pocernich, C. B., R. Sultana, H. Mohammad-Abdul, A. Nath, and D. A. Butterfield. 2005. HIV-dementia, Tat-induced oxidative stress, and antioxidant therapeutic considerations. *Brain Res Brain Res Rev* 50:14-26.
 115. Suresh, D. R., V. Annam, K. Pratibha, and B. V. Prasad. 2009. Total antioxidant capacity--a novel early bio-chemical marker of oxidative stress in HIV infected individuals. *J Biomed Sci* 16:61.
 116. Shih, A. Y., D. A. Johnson, G. Wong, A. D. Kraft, L. Jiang, H. Erb, J. A. Johnson, and T. H. Murphy. 2003. Coordinate regulation of glutathione biosynthesis and release by Nrf2-expressing glia potently protects neurons from oxidative stress. *J Neurosci* 23:3394-3406.
 117. Moi, P., K. Chan, I. Asunis, A. Cao, and Y. W. Kan. 1994. Isolation of NF-E2-related factor 2 (Nrf2), a NF-E2-like basic leucine zipper transcriptional activator that binds to the tandem NF-E2/AP1 repeat of the beta-globin locus control region. *Proc Natl Acad Sci U S A* 91:9926-9930.
 118. Li, P. F., R. Dietz, and R. von Harsdorf. 1999. p53 regulates mitochondrial membrane potential through reactive oxygen species and induces cytochrome c-independent apoptosis blocked by Bcl-2. *EMBO J* 18:6027-6036.
 119. Garden, G. A., W. Guo, S. Jayadev, C. Tun, S. Balcaitis, J. Choi, T. J. Montine, T. Moller, and R. S. Morrison. 2004. HIV associated neurodegeneration requires p53 in neurons and microglia. *FASEB J* 18:1141-1143.

120. Jones, G. J., N. L. Barsby, E. A. Cohen, J. Holden, K. Harris, P. Dickie, J. Jhamandas, and C. Power. 2007. HIV-1 Vpr causes neuronal apoptosis and in vivo neurodegeneration. *J Neurosci* 27:3703-3711.
121. Nardacci, R., A. Antinori, L. M. Larocca, V. Arena, A. Amendola, J. L. Perfettini, G. Kroemer, and M. Piacentini. 2005. Characterization of cell death pathways in human immunodeficiency virus-associated encephalitis. *Am J Pathol* 167:695-704.
122. Kim, H. T., S. Tasca, W. Qiang, P. K. Wong, and G. Stoica. 2002. Induction of p53 accumulation by Moloney murine leukemia virus-ts1 infection in astrocytes via activation of extracellular signal-regulated kinases 1/2. *Lab Invest* 82:693-702.
123. Ding, B., S. G. Chi, S. H. Kim, S. Kang, J. H. Cho, D. S. Kim, and N. H. Cho. 2007. Role of p53 in antioxidant defense of HPV-positive cervical carcinoma cells following H₂O₂ exposure. *J Cell Sci* 120:2284-2294.
124. Lin, Y. C., C. W. Chow, P. H. Yuen, and P. K. Wong. 1997. Establishment and characterization of conditionally immortalized astrocytes to study their interaction with *ts1*, a neuropathogenic mutant of Moloney murine leukemia virus. *J Neurovirol* 3:28-37.
125. Shikova, E., Y. C. Lin, K. Saha, B. R. Brooks, and P. K. Wong. 1993. Correlation of specific virus-astrocyte interactions and cytopathic effects induced by *ts1*, a neurovirulent mutant of Moloney murine leukemia virus. *J Virol* 67:1137-1147.
126. Kuang, X., V. L. Scofield, M. Yan, G. Stoica, N. Liu, and P. K. Wong. 2009. Attenuation of oxidative stress, inflammation and apoptosis by minocycline prevents retrovirus-induced neurodegeneration in mice. *Brain Res* 1286:174-184.
127. Aksenov, M. Y., U. Hasselrot, A. K. Bansal, G. Wu, A. Nath, C. Anderson, C. F. Mactutus, and R. M. Booze. 2001. Oxidative damage induced by the injection of HIV-1 Tat protein in the rat striatum. *Neurosci Lett* 305:5-8.

128. Nisole, S., and A. Saib. 2004. Early steps of retrovirus replicative cycle. *Retrovirology* 1:9.
129. Albanese, A., D. Arosio, M. Terreni, and A. Cereseto. 2008. HIV-1 pre-integration complexes selectively target decondensed chromatin in the nuclear periphery. *PLoS One* 3:e2413.
130. Ardavin, C., F. Luthi, M. Andersson, L. Scarpellino, P. Martin, H. Diggelmann, and H. Acha-Orbea. 1997. Retrovirus-induced target cell activation in the early phases of infection: the mouse mammary tumor virus model. *J Virol* 71:7295-7299.
131. Boven, L. A., L. Gomes, C. Hery, F. Gray, J. Verhoef, P. Portegies, M. Tardieu, and H. S. Nottet. 1999. Increased peroxynitrite activity in AIDS dementia complex: implications for the neuropathogenesis of HIV-1 infection. *J Immunol* 162:4319-4327.
132. Wilt, S. G., N. V. Dugger, N. D. Hitt, and P. M. Hoffman. 2000. Evidence for oxidative damage in a murine leukemia virus-induced neurodegeneration. *J Neurosci Res* 62:440-450.
133. Viviani, B., E. Corsini, M. Binaglia, C. L. Galli, and M. Marinovich. 2001. Reactive oxygen species generated by glia are responsible for neuron death induced by human immunodeficiency virus-glycoprotein 120 in vitro. *Neuroscience* 107:51-58.
134. Liu, N., W. Qiang, X. Kuang, P. Thuillier, W. S. Lynn, and P. K. Wong. 2002. The peroxisome proliferator phenylbutyric acid (PBA) protects astrocytes from *ts1* MoMuLV-induced oxidative cell death. *J Neurovirol* 8:318-325.
135. Turchan, J., C. B. Pocernich, C. Gairola, A. Chauhan, G. Schifitto, D. A. Butterfield, S. Buch, O. Narayan, A. Sinai, J. Geiger, J. R. Berger, H. Elford, and A. Nath. 2003. Oxidative stress in HIV demented patients and protection ex vivo with novel antioxidants. *Neurology* 60:307-314.

136. Fischer-Smith, T., and J. Rappaport. 2005. Evolving paradigms in the pathogenesis of HIV-1-associated dementia. *Expert Rev Mol Med* 7:1-26.
137. Louboutin, J. P., L. Agrawal, B. A. Reyes, E. J. Van Bockstaele, and D. S. Strayer. 2007. Protecting neurons from HIV-1 gp120-induced oxidant stress using both localized intracerebral and generalized intraventricular administration of antioxidant enzymes delivered by SV40-derived vectors. *Gene Ther* 14:1650-1661.
138. Kubbutat, M. H., S. N. Jones, and K. H. Vousden. 1997. Regulation of p53 stability by Mdm2. *Nature* 387:299-303.
139. Maki, C. G., J. M. Huibregtse, and P. M. Howley. 1996. In vivo ubiquitination and proteasome-mediated degradation of p53(1). *Cancer Res* 56:2649-2654.
140. Canman, C. E., D. S. Lim, K. A. Cimprich, Y. Taya, K. Tamai, K. Sakaguchi, E. Appella, M. B. Kastan, and J. D. Siliciano. 1998. Activation of the ATM kinase by ionizing radiation and phosphorylation of p53. *Science* 281:1677-1679.
141. Kim, J., and P. K. Wong. 2009. Oxidative stress is linked to ERK1/2-p16 signaling-mediated growth defect in ATM-deficient astrocytes. *J Biol Chem* 284:14396-14404.
142. Kim, J., and P. K. Wong. 2009. Loss of ATM impairs proliferation of neural stem cells through oxidative stress-mediated p38 MAPK signaling. *Stem Cells* 27:1987-1998.
143. Bagley, J., G. Singh, and J. Iacomini. 2007. Regulation of oxidative stress responses by ataxia-telangiectasia mutated is required for T cell proliferation. *J Immunol* 178:4757-4763.
144. Quick, K. L., and L. L. Dugan. 2001. Superoxide stress identifies neurons at risk in a model of ataxia-telangiectasia. *Ann Neurol* 49:627-635.
145. Schubert, R., L. Erker, C. Barlow, H. Yakushiji, D. Larson, A. Russo, J. B. Mitchell, and A. Wynshaw-Boris. 2004. Cancer chemoprevention by the antioxidant tempol in Atm-deficient mice. *Hum Mol Genet* 13:1793-1802.

146. Barlow, C., P. A. Dennery, M. K. Shigenaga, M. A. Smith, J. D. Morrow, L. J. Roberts, 2nd, A. Wynshaw-Boris, and R. L. Levine. 1999. Loss of the ataxia-telangiectasia gene product causes oxidative damage in target organs. *Proc Natl Acad Sci U S A* 96:9915-9919.
147. Guo, Z., S. Kozlov, M. F. Lavin, M. D. Person, and T. T. Paull. 2010. ATM activation by oxidative stress. *Science* 330:517-521.
148. Matoba, S., J. G. Kang, W. D. Patino, A. Wragg, M. Boehm, O. Gavrilova, P. J. Hurley, F. Bunz, and P. M. Hwang. 2006. p53 regulates mitochondrial respiration. *Science* 312:1650-1653.
149. Roe, T., T. C. Reynolds, G. Yu, and P. O. Brown. 1993. Integration of murine leukemia virus DNA depends on mitosis. *EMBO J* 12:2099-2108.
150. Tang, S., B. Patterson, and J. A. Levy. 1995. Highly purified quiescent human peripheral blood CD4+ T cells are infectible by human immunodeficiency virus but do not release virus after activation. *J Virol* 69:5659-5665.
151. Jayadev, S., B. Yun, H. Nguyen, H. Yokoo, R. S. Morrison, and G. A. Garden. 2007. The glial response to CNS HIV infection includes p53 activation and increased expression of p53 target genes. *J Neuroimmune Pharmacol* 2:359-370.
152. Watanabe, D., T. Honda, K. Nishio, Y. Tomita, Y. Sugiura, and Y. Nishiyama. 2000. Corneal infection of herpes simplex virus type 2--induced neuronal apoptosis in the brain stem of mice with expression of tumor suppressor gene (p53) and transcription factors. *Acta Neuropathol* 100:647-653.
153. Ehsan, A., H. Fan, P. A. Eagan, H. A. Siddiqui, and M. L. Gulley. 2000. Accumulation of p53 in infectious mononucleosis tissues. *Hum Pathol* 31:1397-1403.

154. Jordan-Sciutto, K. L., G. Wang, M. Murphy-Corb, and C. A. Wiley. 2000. Induction of cell-cycle regulators in simian immunodeficiency virus encephalitis. *Am J Pathol* 157:497-507.
155. Kim, S. Y., R. Byrn, J. Groopman, and D. Baltimore. 1989. Temporal aspects of DNA and RNA synthesis during human immunodeficiency virus infection: evidence for differential gene expression. *J Virol* 63:3708-3713.
156. Lau, A., K. M. Swinbank, P. S. Ahmed, D. L. Taylor, S. P. Jackson, G. C. Smith, and M. J. O'Connor. 2005. Suppression of HIV-1 infection by a small molecule inhibitor of the ATM kinase. *Nat Cell Biol* 7:493-500.
157. Reliene, R., and R. H. Schiestl. 2006. Antioxidant N-acetyl cysteine reduces incidence and multiplicity of lymphoma in Atm deficient mice. *DNA Repair (Amst)* 5:852-859.
158. Reliene, R., and R. H. Schiestl. 2007. Antioxidants suppress lymphoma and increase longevity in Atm-deficient mice. *J Nutr* 137:229S-232S.
159. Chen, Q. M., J. C. Bartholomew, J. Campisi, M. Acosta, J. D. Reagan, and B. N. Ames. 1998. Molecular analysis of H₂O₂-induced senescent-like growth arrest in normal human fibroblasts: p53 and Rb control G1 arrest but not cell replication. *Biochem J* 332 (Pt 1):43-50.
160. Salmen, S., M. Colmenares, D. L. Peterson, E. Reyes, J. D. Rosales, and L. Berrueta. 2010. HIV-1 Nef associates with p22-phox, a component of the NADPH oxidase protein complex. *Cell Immunol* 263:166-171.
161. Olivetta, E., C. Mallozzi, V. Ruggieri, D. Pietraforte, M. Federico, and M. Sanchez. 2009. HIV-1 Nef induces p47(phox) phosphorylation leading to a rapid superoxide anion release from the U937 human monoblastic cell line. *J Cell Biochem* 106:812-822.

162. Olivetta, E., D. Pietraforte, I. Schiavoni, M. Minetti, M. Federico, and M. Sanchez. 2005. HIV-1 Nef regulates the release of superoxide anions from human macrophages. *Biochem J* 390:591-602.
163. Duan, L., I. Ozaki, J. W. Oakes, J. P. Taylor, K. Khalili, and R. J. Pomerantz. 1994. The tumor suppressor protein p53 strongly alters human immunodeficiency virus type 1 replication. *J Virol* 68:4302-4313.
164. Coley, W., K. Kehn-Hall, R. Van Duyne, and F. Kashanchi. 2009. Novel HIV-1 therapeutics through targeting altered host cell pathways. *Expert Opin Biol Ther* 9:1369-1382.
165. Zhang, H. S., H. Y. Li, Y. Zhou, M. R. Wu, and H. S. Zhou. 2009. Nrf2 is involved in inhibiting Tat-induced HIV-1 long terminal repeat transactivation. *Free Radic Biol Med* 47:261-268.
166. Sawaya, B. E., K. Khalili, W. E. Mercer, L. Denisova, and S. Amini. 1998. Cooperative actions of HIV-1 Vpr and p53 modulate viral gene transcription. *J Biol Chem* 273:20052-20057.
167. Lynn, W. S., and P. K. Wong. 1997. Possible control of cell death pathways in ataxia telangiectasia. A case report. *Neuroimmunomodulation* 4:277-284.
168. Marchetto, M. C., A. R. Muotri, Y. Mu, A. M. Smith, G. G. Cezar, and F. H. Gage. 2008. Non-cell-autonomous effect of human SOD1 G37R astrocytes on motor neurons derived from human embryonic stem cells. *Cell Stem Cell* 3:649-657.
169. Lucius, R., and J. Sievers. 1996. Postnatal retinal ganglion cells in vitro: protection against reactive oxygen species (ROS)-induced axonal degeneration by cocultured astrocytes. *Brain Res* 743:56-62.
170. Bedard, K., and K. H. Krause. 2007. The NOX family of ROS-generating NADPH oxidases: physiology and pathophysiology. *Physiol Rev* 87:245-313.

171. Wu, D. C., D. B. Re, M. Nagai, H. Ischiropoulos, and S. Przedborski. 2006. The inflammatory NADPH oxidase enzyme modulates motor neuron degeneration in amyotrophic lateral sclerosis mice. *Proc Natl Acad Sci U S A* 103:12132-12137.
172. Marden, J. J., M. M. Harraz, A. J. Williams, K. Nelson, M. Luo, H. Paulson, and J. F. Engelhardt. 2007. Redox modifier genes in amyotrophic lateral sclerosis in mice. *J Clin Invest* 117:2913-2919.
173. Kuang, X., W. Hu, M. Yan, and P. K. Wong. 2010. Phenylbutyric acid suppresses protein accumulation-mediated ER stress in retrovirus-infected astrocytes and delays onset of paralysis in infected mice. *Neurochem Int* 57:738-748.
174. Nitti, M., A. L. Furfaro, C. Cevasco, N. Traverso, U. M. Marinari, M. A. Pronzato, and C. Domenicotti. 2010. PKC delta and NADPH oxidase in retinoic acid-induced neuroblastoma cell differentiation. *Cell Signal* 22:828-835.
175. Miyauchi, K., M. M. Kozlov, and G. B. Melikyan. 2009. Early steps of HIV-1 fusion define the sensitivity to inhibitory peptides that block 6-helix bundle formation. *PLoS Pathog* 5:e1000585.
176. Miyauchi, K., Y. Kim, O. Latinovic, V. Morozov, and G. B. Melikyan. 2009. HIV enters cells via endocytosis and dynamin-dependent fusion with endosomes. *Cell* 137:433-444.
177. Kizhatil, K., and L. M. Albritton. 1997. Requirements for different components of the host cell cytoskeleton distinguish ecotropic murine leukemia virus entry via endocytosis from entry via surface fusion. *J Virol* 71:7145-7156.
178. Yoshii, H., H. Kamiyama, K. Goto, K. Oishi, N. Katunuma, Y. Tanaka, H. Hayashi, T. Matsuyama, H. Sato, N. Yamamoto, and Y. Kubo. 2011. CD4-independent human immunodeficiency virus infection involves participation of endocytosis and cathepsin B. *PLoS One* 6:e19352.

179. Yoshii, H., H. Kamiyama, K. Minematsu, K. Goto, T. Mizota, K. Oishi, N. Katunuma, N. Yamamoto, and Y. Kubo. 2009. Cathepsin L is required for ecotropic murine leukemia virus infection in NIH3T3 cells. *Virology* 394:227-234.
180. Rybicka, J. M., D. R. Balce, M. F. Khan, R. M. Krohn, and R. M. Yates. 2010. NADPH oxidase activity controls phagosomal proteolysis in macrophages through modulation of the luminal redox environment of phagosomes. *Proc Natl Acad Sci U S A* 107:10496-10501.
181. Hilburger, E. W., E. J. Conte, D. W. McGee, and S. P. Tammariello. 2005. Localization of NADPH oxidase subunits in neonatal sympathetic neurons. *Neurosci Lett* 377:16-19.
182. Pagano, P. J., J. K. Clark, M. E. Cifuentes-Pagano, S. M. Clark, G. M. Callis, and M. T. Quinn. 1997. Localization of a constitutively active, phagocyte-like NADPH oxidase in rabbit aortic adventitia: enhancement by angiotensin II. *Proc Natl Acad Sci U S A* 94:14483-14488.
183. Li, X. J., C. C. Marchal, N. D. Stull, R. V. Stahelin, and M. C. Dinauer. 2010. p47phox Phox homology domain regulates plasma membrane but not phagosome neutrophil NADPH oxidase activation. *J Biol Chem* 285:35169-35179.
184. Park, H. S., S. M. Lee, J. H. Lee, Y. S. Kim, Y. S. Bae, and J. W. Park. 2001. Phosphorylation of the leucocyte NADPH oxidase subunit p47(phox) by casein kinase 2: conformation-dependent phosphorylation and modulation of oxidase activity. *Biochem J* 358:783-790.
185. Zhao, X., and F. K. Yoshimura. 2008. Expression of murine leukemia virus envelope protein is sufficient for the induction of apoptosis. *J Virol* 82:2586-2589.
186. Van Buul, J. D., M. Fernandez-Borja, E. C. Anthony, and P. L. Hordijk. 2005. Expression and localization of NOX2 and NOX4 in primary human endothelial cells. *Antioxid Redox Signal* 7:308-317.

VITA

Soo Jin Kim was born on October 25, 1973 in a small town, Sungju, Republic of Korea to a daughter of Suk-Gon Kim and Yun-duk Kim. After completing her high school work at Eun-Kwang Women's high school in Seoul, she entered the Seoul Women's University in 1992, where she received the Bachelor degree of Science in 1996. During the following year, she worked in the Clinical Research Center at Seoul National University Medical Center. In March 1997, she entered the graduate school at Seoul National University College of Medicine and received a Master of Science degree in Biochemistry and Molecular Biology in February 1998. In August 2000, she came in United States and joined the graduate program in Molecular Biology at The University of Texas at Austin. She received a Mater of Art Degree in Molecular Biology in December 2005. During the following year, she continued research in M.D. Anderson Cancer Center-Science Park-Research Division. In May 2006, she entered graduate school at the University of Texas M.D. Anderson Cancer center. She currently resides in Austin, TX.